Remotely Sensed Impact of Flow Alteration on Swiss Floodplains

Dissertation

zur

Erlangung der naturwissenschaftlichen Doktorwürde
(Dr. sc. nat.)

vorgelegt der

Mathematisch-naturwissenschaftlichen Fakultät

der

Universität Zürich

von

Gillian Milani

von

Porrentruy JU

Promotionskommission

Prof. Dr. Michael E. Schaepman (Vorsitz)

Dr. Mathias Kneubühler (Leitung der Dissertation)

Dr. Michael Doering

Prof. Dr. Jan Seibert

Zürich, 2020

"The student, as the river, follows the same dream: following its course without running out of its bed."

Anonymous

Abstract

Floodplains, though covering a very small fraction of the land, offer key ecosystem services to our society. Floodplains play an active role in the maintenance of river water quality, in the protection of floods, in supporting a unique biodiversity and in many other ecosystem services. In Switzerland, pristine floodplains have lost 90% of their occupied area since 1850. This work was undertaken within the framework of NRP-70, with the aim of reconciling the increase in hydropower production with support for natural biodiversity, which seems to lead to a difficult compromise in the current situation.

Airborne and spaceborne remote sensing offer unique capabilities to observe and monitor river systems and floodplains through various technologies. The current dissertation presents the use of remote sensing for observations and monitoring of floodplains and their dynamics, specifically to observe the impact of water flow alteration on the riparian ecosystems. Three complementary aspects of Swiss floodplains are considered throughout the dissertation. The work carried out in the frame of this dissertation is focused mainly on a few sections of a restricted number of river reaches. A robust methodology for riverine habitat dynamics quantification is developed, based on land cover classification produced on high-resolution imagery. Standard and infrared cameras were used to acquire images over five consecutive seasons along three river reaches. The quantification method provides recommendations for monitoring floodplains in Switzerland using unmanned aerial systems. A second method was developed to observe the resource allocation strategies of riparian vegetation at the individual level based on imaging spectroscopy. This method allowed the comparison of the distribution of strategies located along different reaches. Four imaging spectroscopy datasets acquired during two consecutive years, as well as leaf samples from two field campaigns, were used to extract plant traits from alluvial willows. Individuals located along river reaches affected by water flow alteration show a shift towards more competitive strategies. A third method was developed to observe trends in riparian vegetation over the last decades using inter-annual satellite acquisitions. The channel extent was semi-automatically detected using spectral mixture analysis. Acquisitions from Landsat missions 4, 5, 7, and 8 covering the years 1988 to 2016 over four reaches were used to extract trends and correlations with discharge data from hydrometric stations. Correlations between floods and changes in vegetation indices were found only in the case of the natural, sub-mountainous river, while no correlation was found in the case of the two reaches affected by hydropower infrastructure and the mountainous reach.

The description of vegetation development through resource allocation strategies offers a new point of view on the consequence of water flow alteration and fits with usual observation, namely the oft-observed channel narrowing. The results suggest that the processes shaping the plant characteristics of riparian vegetation operate over a relatively long period of time. In the different works undertaken, I also showed that the specificity of the riverine land cover allows for a robust description of the river landscape, such as the spatio-temporal relationships between water, gravel and vegetation cover. This thesis contributes to the discussion of impact of water flow alteration on riparian ecosystems and the possibility of management for a close future. The interactions between the flow regime, the sediment regime, riparian vegetation and other components of the floodplains are still lacking some understanding, but recent research is on the way to produce the required recommendations to implement environmental flows. Though river science is advancing from day to day, the most critical constraints to protect floodplains in Switzerland remain on the political level.

Zusammenfassung

Auengebiete bieten unserer Gesellschaft wichtige Ökosystemdienstleistungen, obwohl sie nur einen sehr kleinen Teil des Landes bedecken. Auengebiete spielen eine aktive Rolle bei der Erhaltung der Wasserqualität von Flüssen, beim Schutz vor Überschwemmungen, bei der Unterstützung einer einzigartigen Biodiversität und bei vielen anderen Ökosystemdienstleistungen. In der Schweiz haben unberührte Auen seit 1850 90% ihrer Bedeckungsfläche verloren. Diese vorliegende Arbeit wurde im Rahmen des NRP-70 durchgeführt, mit dem Ziel, den Anstieg der Wasserkraftproduktion mit der Förderung der natürlichen Biodiversität im Einklang zu bringen. Dies scheint in der gegenwärtigen Situation aber zu einem schwierigen Kompromiss zu führen.

Die luft- und weltraumgestützte Fernerkundung bietet einzigartige Möglichkeiten zur Beobachtung und Überwachung von Flusssystemen und Auengebieten durch verschiedene Technologien. Die vorliegende Dissertation stellt den Einsatz der Fernerkundung für die Beobachtung und Überwachung von Auengebieten und deren Dynamik vor, insbesondere für die Beobachtung der Auswirkungen von Wasserführungsveränderung auf die Uferökosysteme. Drei komplementäre Aspekte der Schweizer Auengebiete werden in der Dissertation berücksichtigt. Die im Rahmen dieser Dissertation durchgeführten Arbeiten fokussieren sich hauptsächlich auf wenige Abschnitte einer begrenzten Anzahl von Flüssen. Eine robuste Methodik zur Quantifizierung der Flusslebensraumdynamik wird entwickelt, die auf der Klassifizierung der Landbedeckung basiert. Diese Landbedeckung wurde auf hochauflösenden Bildern erstellt. Standard- und Infrarotkameras wurden verwendet, um während fünf aufeinanderfolgenden Jahreszeiten Bilder entlang dreier Flussabschnitte aufzunehmen. Die Quantifizierungsmethode liefert Ratschläge für die Überwachung von Auen in der Schweiz mit unbemannten Flugsystemen. Eine zweite Methode wurde entwickelt, um die Ressourcenallokationsstrategien der Ufervegetation auf individueller Ebene mit abbildender Spektroskopie zu beobachten. Diese Methode ermöglichte es, die Häufigkeitsverteilung der Strategien zu vergleichen, die sich entlang verschiedener Flussabschnitte befinden. Vier abbildende Spektroskopie-Datensätze, die während zwei aufeinander folgender Jahre aufgenommen wurden, und Blattproben aus zwei Messkampagnen wurden verwendet, um Pflanzenmerkmale aus Alluvialweiden zu erhalten. Pflanzen, die sich entlang von Flussabschnitten befinden, die von einer Veränderung der Wasserführung betroffen sind, weisen einen Wandel zu wettbewerbsfähigeren Strategien auf. Eine dritte Methode wurde entwickelt, um

Trends in der Ufervegetation in den letzten Jahrzehnten durch zwischenjährliche Satellitenaufnahmen zu beobachten. Der Flussbettumfang wurde halbautomatisch mittels Spektralmischungsanalyse ermittelt. Aufnahmen von Landsat 4, 5, 7 und 8 für die Jahre 1988 bis 2016 über vier Abschnitte hinweg wurden ausgewählt, um Trends und Korrelationen mit den Abflussdaten von hydrometrischen Stationen zu extrahieren. Ein Zusammenhang zwischen Überschwemmungen und Vegetationsindexveränderungen wurde nur für den natürlichen, präalpinen Fluss festgestellt, während für die beiden von der Wasserkraftinfrastruktur und den gebirgigen Charakter betroffenen Abschnitte kein Zusammenhang festgestellt wurde.

Die Beschreibung der Vegetationsentwicklung durch Ressourcenallokationsstrategien bietet einen neuen Blickwinkel auf die Folgen der Wasserführungsveränderung und entspricht den bekannten Beobachtungen im Zusammenhang mit Flussbettverengung. Die Ergebnisse deuten darauf hin, dass die Prozesse, die die Pflanzeneigenschaften der Ufervegetation prägen, über einen relativ langen Zeitraum laufen. In den verschiedenen Artikeln haben wir auch gezeigt, dass die Eigenschaften der Augengebiete eine robuste Beschreibung der Flusslandschaft ermöglichen, wie beispielsweise die räumlich-zeitlichen Beziehungen zwischen Wasser, Kies und Vegetationsdecke. Die vorliegende Arbeit trägt zur Diskussion über die Auswirkungen der Wasserführungsänderung auf die Uferökosysteme und die Möglichkeit von zukünftigem Management bei. Die Wechselwirkungen zwischen Abflussregime, Sedimentregime, Ufervegetation sowie anderen Komponenten der Auengebiete sind noch nicht vollständig verstanden, aber die Forschung ist auf dem Weg, die erforderlichen Empfehlungen zur Umsetzung von ökologischem Wassermanagement zu erarbeiten. Obwohl die Wissenschaft zu Auengebieten wichtige Fortschritte macht, scheinen die kritischsten Einschränkungen zum Schutz von Auen in der Schweiz auf politischer Ebene zu liegen.

Contents

This thesis is dedicated to Adrien Gaudard, with whom I got the chance to share the most memorable part of my life, leading the way to the present PhD.

Chapter 1

Introduction

1.1 Context

The research carried out within the framework of this thesis is largely motivated by the constraints in place due to Switzerland's current environmental and political situation. While the methods developed and the knowledge gathered throughout the research are intended to be universal, the motivations that led to this research are concrete and specific. In addition, the specific aspects of Swiss river management policy are important because the studies carried out are intrinsically linked to the fact that the research focuses mainly on objects found in situ, which would not be the case for more theoretical studies or studies based more on environmental modelling, for example. The local context, both in space and time, is therefore crucial in defining the need and scope of the following chapters.

1.1.1 Recent History of Floodplains in Switzerland

Since the beginning of human history, freshwater bodies have proved to be a prime location for the establishment of civilizations. In the past, riverside settlement benefited mainly from food and commercial services, thanks to the supply of fresh water, the fertility of the surrounding land and the use of the river system as a means of transport. The advantages of proximity to watercourses are also paradoxical with the natural hazards that can occur there. To this day, large rivers have aroused fears of being subjected to devastating water flow forces. In order to control the dynamic and dangerous environment of the river landscape and protect the land from flooding, hydraulic installations have been built for several centuries. The most important constructions were built in the 19th century and had an impact on floodplain ecosystems throughout Switzerland. The history of river ecosystem change in Switzerland continued with the construction of large hydropower installations in the 20th century. These modifications led to a drastic reduction in the area of pristine floodplains by 90% between 1850 and 2004 for Switzerland [1].

Until recently, riparian ecosystems were virtually unprotected. In 2011, an amendment to the Water Protection Act reversed past floodplain management strategies: the new Act requires and supports river modifications to achieve a natural state that should tend to be similar to the state before modification. The new law was initiated

and encouraged by a popular initiative called “Living Water" (*Lebendiges Wasser*), tabled in the Federal Parliament in 2006. Although a policy decision on the protection of rivers and floodplains has only recently been taken, the implementation of engineering techniques to control water flow in conjunction with sustainable river ecosystem management was in place more than a decade before the law was passed. For example, the major works started in 1997 between Brig and St-Gingolf in Valais were described as "sustainable", "environmentally friendly" and "friendly". In 2015, the Swiss Confederation set itself the objective of re-naturalising 4’000 km throughout the country in 80 years.

1.1.2 Energy Strategy 2050

Following the nuclear accident of 11 March 2011 in Fukushima, the Swiss Federal Department of the Environment, Transport, Energy and Communications (DETEC) received the task to revise the energy strategy plan, namely the Energy Perspectives for 2035. After multiple technical and political discussions, the Swiss people voted in favour of the Energy Act proposed on 21th May 2017, leading to an entry into force on 1 January 2018. In brief, the Energy Act aims to reduce the energy consumption per inhabitant, increase energy efficiency and develop renewable energies. Beyond that, the act prohibits any construction of new nuclear power plants. As a temporary measure, support is given to large-scale hydropower plants facing a sharp decrease in electricity market price. An increase of 10% of the electricity production is expected, increasing the pressure on floodplain ecosystems. The new production capacity is planned to be shared equally between the adaptation of current installations, the building of new large power plants and the increase of run-of-river installations.

1.1.3 Future Evolution — a Fragile Compromise?

Following relatively recent political decisions, the current watercourse re-naturalisation plan is in opposition to the increasing pressure imposed by the hydropower production required by the Energy Strategy 2050. A difficult compromise should therefore be driven by these different forces (Figure 1.1). In addition, glacier retreat, climate change and land use planning are further altering river ecosystems while increasing pressure on hydropower production. In this context, it is therefore crucial to seek a solution that adapts to all the current constraints and to discover new ways to best reconcile the use of water for electricity production and flow management in order to promote the return to (natural) riparian ecosystems. The government is targeting two main areas to achieve these objectives: (i) revitalisation of the river, by removing obstacles and work on the structural and dynamic elements of the river, and (ii) reducing the negative effects of hydropower facilities on the river ecosystem. For both axes, a thorough understanding of the processes taking place within the hydrographic network is required at multiple scales.

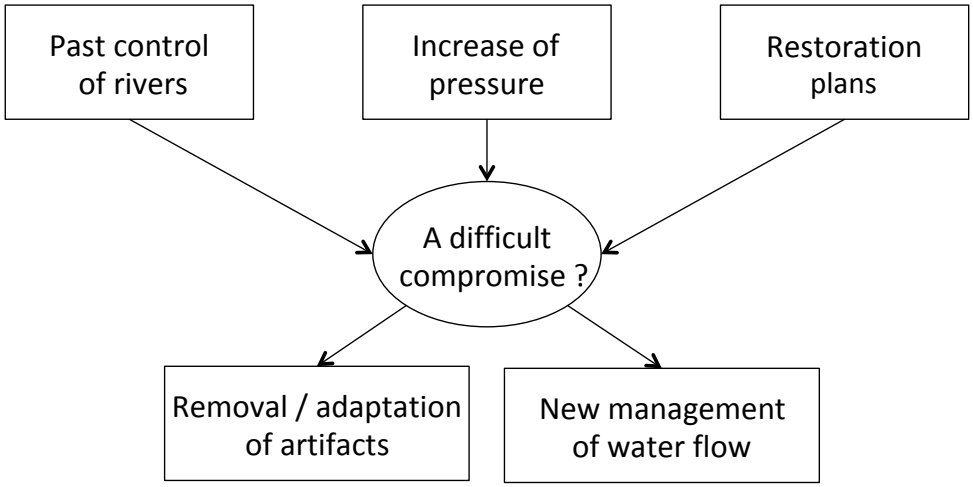

FIGURE 1.1: Schematic representation in a simplistic and abstract way of the various elements to be taken into account for the management of floodplains in Switzerland in the near future. The various solutions to this compromise can be divided into two groups: work to remove obstacles and artefacts found along the river and how to manage water and sediment flows in the river.

1.2 Floodplains: Description and Functioning

The river landscape is shaped by the variation in water flow and the flow of sediment and rocks carried by the current. Woody debris, organic matter and other components are transported by water flow and play an important role in river system processes. The transition area between the aquatic ecosystem and the terrestrial ecosystem forms the riparian ecotone. Although a clear delineation of the riparian zone is rarely possible, its extent is often perceived as the part of the land that interacts directly with the terrestrial and aquatic environments. The following definition of riparian zones has been given by Ilhardt et al. [2]:

> *"Riparian areas are the three-dimensional ecotones of interaction that include terrestrial and aquatic ecosystems, that extend down into the groundwater, up above the canopy, outward across the floodplain, up the near-slopes that drain to the water, laterally into the terrestrial ecosystem, and along the water course at a variable width."*

1.2.1 Role and Importance

The riparian corridor provides multiple ecosystem services to our society. Floodplains and riparian areas are described as providing a disproportionate number of services with respect to the fraction of the territory occupied by these ecosystems. The list of services provided spans a large variety of functions, such as climate regulation, water supply, soil formation, energy transfer and many others [3]. Worldwide, the most important services are linked to water quality regulation, flood control, erosion control of the river banks and habitat for the wildlife. Other examples

include the use of the broader riverine landscape for leisure activities, such as fishery, kayaking or swimming. Riparian vegetation and the related landforms play also a role as flood control, notably by dissipating the energy of the water flow.

In Switzerland specifically, floodplains play an important role in the wildlife habitat and hold a substantial part of the biodiversity while they cover only 0.55% of the territory. According to Tockner (2002) [4], 10% of animal species (of selected groups, including mammals, birds, amphibians and reptiles and some insects) exclusively live in their extents, while 28% are frequently found within their extents and an additional 44% are occasionally found in the same floodplains. This number sums to a total of $\sim$80% of the animal species of Switzerland that can be found in floodplains. Moreover, 50% of vegetal species found in Switzerland can be found in the floodplains.

1.2.2 Structure and Dynamics

Floodplains can be seen as a constantly changing mosaic of habitats, in a steady state under ideal conditions. This model is known as the *Shifting Mosaic Steady-state model* and abstracts some important components in a simple manner. The steady-state part describes the fact that the total area covered by each type of habitat should be relatively constant in time. In such systems, disturbances impact habitats at any successional stage. At the same time, maturation of habitats balance the loss due to disturbances. The system reaches a steady-state if the maturation and the loss due to disturbances are balanced for each type of habitat. The mosaic of habitats found in floodplains includes in-stream habitats, such as pools or riffles or in-stream woody debris, and riparian habitats, such as open gravel bars, bushes or alluvial forests. In floodplains, the disruptive element is flooding, which erodes the banks and destroys young and mature vegetation, while pioneer species are the drivers of habitat maturation, creating a first layer of soil that will later host higher vascular plants up to the creation of a riparian forest. While the heterogeneous nature of the habitat mosaic is a typical trait of natural floodplains, this habitat heterogeneity seems to fail at supporting a sufficient ecological state [5]. This fact is found at the basis of considering dynamic processes as drivers of the ecological state of floodplains.

1.2.3 Alteration of the River Course by Dam and Hydropower Plants

The main impacts of the construction of dams and hydropower plants along rivers are briefly presented here. Alteration of downstream ecosystems is induced by two main components of the river system, namely water flow and sediment flow. In the Swiss Alps, hydropower plants are often located far from the water storage site. This spatial organisation creates sections of rivers with different types of impacts: the section between the dam and the hydropower plant generally maintains a low and constant water flow, while the section immediately after the hydropower plant is subject to rapid and significant variation in water flow, creating peak flows. While the

first type of reach is called 'residual reach', the second type is called 'hydropeaking reach'. However, any type of reach downstream of a dam is affected by a decrease of sediment load. Hydropeaking as well as residual flow decreases the dynamics of floodplains. These similarities lead therefore to often comparable alterations for both kind of water flow.

The main and most frequent downstream changes following the installation of a dam are bed incision, bank stabilisation and reduction of the floodplain area [6]. The sediment load is considerably reduced by the presence of the dam, which retains all the sediment in the reservoir. This problem has been studied from a technical point of view, since the accumulation of sediments reduces the volume of the reservoir. The magnitude of the downstream effect of dams appears to be controlled by sediment loading, flooding large enough to displace sediment and local geology [7, 8]. The study of the impact of anthropogenic alteration in river systems focused mainly on the fish habitat perspective. Although the downstream effects of dams have been studied for several decades, researchers are also focusing on the effect of dam removal. Since 1970, hundreds of dams have been dismantled along American rivers, improving ecosystem functions [9]. Removal of a dam can release large amounts of sediment into the river, but stabilisation of the system has often been observed after only a few years [10].

The presentation of the effects of altered water flow on riparian vegetation requires first of all an introduction of the interactions between water flow and vegetation. The following section is therefore devoted to these interactions, including details on the effects of a changing water flow.

1.2.4 Interactions of the Water Flow with Riparian Vegetation

The flow regime affects the composition, distribution and characteristics of riparian vegetation. The effect of water flow on riparian vegetation can be summarised in six main factors [11]. The flow of water itself, especially during floods, can partially or totally destroy vegetation or scour the substrate on which it is located. Floods, in addition to their direct mechanistic power, can lead to asphyxiation by prolonged flooding. Sedimentation processes can create a new environment for colonisation and modify the texture of the riverbed, which influences the availability of water and nutrients. Variations in water flow directly influence the rise and fall of groundwater levels, which also results in differences in water availability. Water flow also has an important role in seed dispersal for riparian species. Finally, water flow and composition influence soil chemistry. These factors shape riparian vegetation in such a way that species exhibit particular and varied characteristics. For example, riparian species may have resprouting capacities, seeds that float on the water, flexible stems, a specific time to release the seeds, etc. The total amount of vegetation is in general increased following alteration of the water flow, while a decrease is observed for typical riparian vegetation [12]. Properties of the river that potentially

impact the riparian vegetation include the scouring of roots from flood, the rise and drop of the water table. The channel migration has also been described in the past has having a large impact on the composition of riparian communities [13]. Different river morphology have been observed to lead to different evolution of riparian vegetation downstream of a dam [14]. The effect of dam on the downstream riparian vegetation is overall complex and hard to predict still today [15].

Riparian vegetation also has a major influence on the geomorphology of the river [16]. During floods, riparian vegetation affects flow velocity, which modifies the impacts of water and sediment flow on geomorphology. The living plant structure and woody debris disperse flow energy, while the root system constrains the banks, increasing resistance to erosion. Large woody debris has also been described as having an important role in the channel due to many characteristics and processes, such as island formation, basin spacing or sediment storage. The presence of vegetation is also suspected to have an important role in the transformation of braided river to single-thread channels [17].

The loop created by the bi-direction path of interactions between the water flow and the riparian vegetation is commonly referred as 'feedback', which must be described by recursive models and leads to a complex representation of the river system. It is therefore not surprising that an alteration of the water flow makes changes in the riparian vegetation difficult to predict. However, uncertainties about the downstream effects of dams on riparian vegetation do not preclude their anticipation to some extent, as mentioned in the preceding section.

1.3 Remote Sensing Technology to Study Floodplains

Before addressing the research questions, an introduction to remote sensing technology is first presented. Understanding remote sensing technologies and their respective characteristics is crucial to their effective use. In addition, the development of a methodological aspect should be motivated by the need to answer an applied research question. The rationale for using remote sensing to study the river landscape is presented later in the section 1.4.

Remote sensing of the river environment encompasses a wide variety of targets, objectives and technologies. For example, remote sensing can be used to measure the bathymetry of the river or certain physico-chemical properties of the canal. LIDAR technology can be used to map the geomorphology and respective changes in landforms over time. Thermal remote sensing is used for multiple application over floodplains, given that temperature is an important property driving many ecological processes.

In this thesis, I use spectral remote sensing to study habitat dynamics and vegetation properties influenced by water flow. In the following paragraphs, the different types of remote sensing systems used in the thesis are briefly presented, followed by

a description of their capabilities to study floodplain habitats and more specifically riparian vegetation.

1.3.1 Optical Remote Sensing

The sun, located 1.5e11m from Earth, emits continuous electromagnetic radiation with an irradiance peak in the visible light range at a wavelength of 483nm. Although a significant fraction of the radiation never reaches the Earth's surface, a large part of it does and interacts with matter. Once in contact with the ground, the radiation is partially absorbed and partially reflected in a diffuse manner. Spectral remote sensing aims to record the fraction of light reflected by an object to obtain information on the properties of the object's surface. The recording of this information can be done in different ways, with advantages and disadvantages depending on the approach chosen. This compromise has led to the existence of multiple coexisting remote sensing platforms, each with its own characteristics, capabilities and limitations. Many sources of variations in the propagation of light to the object and from the object to the sensor, especially through atmospheric interactions, prevent easy use of the raw recording made at the sensor.

The categories of remote sensing platforms presented below are not clearly distinctive, since systems regrouping multiple characteristics can exist, though are very rare and often represent a compromise between the various technologies. For example, cameras recording 16 bands can be mounted on UAS, but do not offer the spatial resolution of standard a RGB camera, and do not offer the spectral resolution of an imaging spectrometer found in airborne systems.

UAS Remote Sensing

Unmanned Areal System (UAS) is the latest type of remote sensing platform currently available considered in this study. The central substance of UAS remote sensing is the use of image texture, i.e. the use of relationships between neighbouring pixels. An important product of UAS remote sensing is also the 3D model of the mapped terrain, generated as a necessary by-product for the ortho-rectification process. UAS systems can also be equipped with infrared or multispectral cameras, which can record images on a larger number of channels than standard cameras.

UAS is not the only system that can make extensive use of texture to gain information on the land cover. The UltraCam Eagle system from Vexcel Imaging released in 2011 could already produce images at a ground resolution of 5cm from an altitude of 2'000m above ground. Sub-meter images are also acquired by commercial satellites. IKONOS, launched in 2011 has recorded images at a 0.8m ground resolution up to 2015. The Worldview constellation forms today an important segment of the acquisitions of very high-resolution by satellites. However, the generation of 3D models from photogrammetry is in general not feasible with airborne or satellite high-resolution imagery.

Multispectral Imaging Systems

Multispectral imagers include instruments capable of recording energetic illumination in the visible and infrared domains of the electromagnetic spectrum with a number of bands ranging from $\sim$4 to a few tens. The spectral resolution of multispectral imagers allows information to be extracted from the image using only the spectral dimension. In other words, multispectral imagers make it possible to study objects of dimensions close to the ground resolution of the pixels of a single image. This capability opens the door to the use of remotely sensed image acquisition with coarse (500m) and medium (30m) resolution, which leads to a higher frequency of acquisition of global images. This feature allows you to use time series analysis based on satellite images. The acquisition of coarse resolution images has made it possible to build up an archive of Earth observation data for several decades now, for example by the AVHRR imager, MODIS instruments or the more recent VIIRS sensor. With a higher spatial resolution, but a lower temporal resolution, Landsat satellite constellations offer a unique archive of Earth observation data. The uniqueness of the Landsat constellation lies in its quality and consistency over time. Although improvements have been made, relatively few changes were designed from the Landsat 4 to the latest Landsat 8 mission.

Imaging Spectroscopy

Imaging spectrometers are a family of instruments that record the irradiance reaching the sensor with a very high spectral resolution. An optical spectrometer, in general terms, is often based on the principle of light disperion (i.e. the wavelength-dependent refraction) or based on diffraction gratings (i.e. the wavelength-dependent diffraction) to be able to record independently quantities of energy with different wavelengths. Imaging spectrometer are based on the same physical principles, but augment the system to be able to record spectroscopic measurement in a sweeping or scanning manner to form images. Imaging spectroscopic data provide unique descriptions of the Earth's surface, compared to other remote sensing platforms, by informing about subtle changes in the reflectance properties of observed objects. The typical wavelength sensitivity range of each detector is in the order of a few nanometers. Such a small range allows to capture small variations in reflectance. Therefore, special methods have been developed to process these data and use their specificity, such as presence absorption characteristics

The first imaging spectrometer designed for airborne remote sensing applications, the Airborne Imaging Spectrometer (AIS) [18], was completed in 1984. Since then, multiple airborne imaging spectrometers have been used worldwide, while their use and access remain relatively limited today. In a short future, a range of high-resolution imaging spectrometers onboard satellites will be available for global applications, including the Environmental Mapping and Analysis Program

(EnMAP) from the German Aerospace Center (DLR), the Sentinel-5 instrument from ESA, the Hyperspectral Infrared Imager (HyspIRI) from NASA, and many others.

1.3.2 Remote Observation of the River System

Due to the particular characteristics of the river system, remote sensing has not been widely used to observe it until recently, although this type of system has not been completely forgotten. The increase in the availability of high-resolution remote sensing data in recent years has contributed significantly to the diffusion of technology to river applications. The development of geographic information systems (GIS), as well as their adoption, is also a factor that has contributed to the specific characteristics of the river system, including its extent, form and structure. The hydrographic network, characterised by its extent, shape and structure, does not offer a form of choice for remote sensing applications. In addition, river systems occupy a small fraction of the total land available, making them easily observable for small countries such as Switzerland. For such objects, the wall-to-wall characteristics of remote sensing data are of no use. The linear shape of rivers prevents the use of coarse-resolution satellite images due to the very narrow width of the targeted objects. As noted above, natural river ecosystems are often organised into a mosaic of habitats, creating great heterogeneity in the river landscape. This heterogeneity also hinders the use of remote sensing data in the context of floodplains.

Although relatively few remote sensing applications have been carried out in floodplains compared to other ecosystems, some important applications can be highlighted.

River bathymetry is a crucial measure for describing river morphology, which is a necessary element for understanding the respective river forms and processes that shape the river system. The estimation of bathymetry by aerial remote sensing has been studied using multiple types of systems [19, 20, 21]. Estimation of river bathymetry is difficult due to the mixed and variable effect of suspended solids, riverbed and liquid phase absorption. Other properties of the aqueous phase that have been observed by remote sensing include flow rate, water surface elevation, water body delineation, temperature and various ice properties, algal concentration and turbidity.

Spatial temperature variations are particularly important in riparian areas. Due to the difference between the processes in the terrestrial and aquatic part of the floodplains, a difference of more than 10 degrees can easily be observed over a few tens of metres in the floodplain [22]. In the aquatic portion of floodplains, temperature is a critical element in determining the suitability of habitats for fish and other aquatic animals. Thermal remote sensing has been well developed for monitoring river water temperature. Some considerations and constraints in the use of thermal imaging arise from the specific characteristics of the river landscape [23].

Due to the relatively frequent morphological changes occurring in the river landscape, the terrestrial laser scanner and Lidar instruments have also been widely used in floodplains, particularly on braided rivers. Green beams were used to allow the lidar to penetrate deeper into water bodies to map the underwater topography at small-scale.

Monitoring major floods has also been an important objective for the use of remote sensing systems. Remote sensing is now integrated into emergency procedures in the event of a disaster. Flood monitoring and forecasting is actually one of the successes of remote sensing [24, 25].

1.3.3 Remote Sensing the Riparian Vegetation

Airborne films and digital cameras have been used for decades to map riparian vegetation buffers and wetlands. For example, in Switzerland, floodplains have been delimited since 1993 on infrared images acquired by airborne instruments [26]. The use of aerial or spatial remote sensing has been almost exclusively limited to delimitation and classification tasks when examining riparian vegetation [27, 28]. It is only recently that some applications of remote sensing to describe the properties of riparian vegetation have been developed [29, 30, 31, 32]. More detailed information is provided in the thesis on the specific use of remote sensing for riparian vegetation in the respective chapters.

1.4 Motivation for Research

1.4.1 Understanding Shifts in Floodplains and Riparian Vegetation

As presented in the previous section, interactions between riparian vegetation and water flow are complex and depend on many external factors, such as geology, land use or local climate. Although these interactions are now partly understood, the modification of these processes and related structural parameters by hydropower production or external factors is still poorly described. For example, the changes observed in riparian vegetation following the implementation of a dam showed different responses, without a clear explanation. Riparian ecosystems have been described as responding very quickly to changes in local climate. These ecosystems could be (or are already) among the first ecosystems in which climate change has substantial effects. In addition, the river ecosystem will respond to changes that have not previously been observable, i.e. changes that are not due to direct anthropogenic alteration of water flow, such as changes in snowfall patterns and melting of ice storage at high elevations. The lack of a description of the processes that occur in floodplains as a result of altered water flow and their high dependence on site-specific conditions demonstrate the need for research in this area for Swiss rivers.

1.4.2 Capabilities of Remote Sensing Systems

In recent years, remote sensing has been seen has an increasing source of information to monitor and understand the riverine landscape. The final report of the REstoring rivers FOR effective catchment Management (REFORM) project provides a brief and exhaustive summary of the potential and capabilities of remote sensing for supporting the observation of riverine landscape:

> *"Remote sensing data has large potential to support hydromorphological assessment and monitoring of European rivers. Hydromorphological characterisations based on remote sensing are objective, repeatable through time and support large scale planning according to the WFD [note: Water Framework Directive]. [...] Remote sensing data are integrative and do not substitute traditional river surveys based on expert interpretations, field surveys and historical analysis. Remote sensing data will support conclusions drawn from these sources providing objective, repeatable and comparable information."*

In this context, two main lines of research are widely open and complementary. The first is the study of the remote sensing system itself, which can be described as methodological research on technology. This type of research is necessary to know and understand what information can be extracted by remote sensing systems, with what accuracy and how to interpret it. The second type of research study relies on remote sensing acquisition to draw ecological or geographical inferences.

In general, the focus is set on remote sensing systems and their uses to:

1. give useful recommendation for today's challenges faced in Swiss rivers given the specificity of floodplains, namely the small-scale heterogeneity and the relatively high dynamics of habitats;
2. study spatial relations and spatial patterns in the floodplains;
3. use time series of earth observation satellites to discover how the riparian vegetation is impacted by long-term processes.

These objectives can be achieved using remote sensing, which requires research on the methodological extraction of information from remote sensing data. A second part of the thesis, in addition to research on ecohydrology and riparian vegetation, therefore consists of developing an approach for extracting relevant and valuable information from remote sensing acquisitions of floodplain ecosystems.

1.5 Research Outline

This dissertation was written in the framework of the project *Hydroecology and Floodplain Sustainability in Application - HyApp NRP70*. The main project, National Research Project 70 - Energy Turnaround (NRP70), aims to contribute to a sustainable

energy policy for Switzerland. It is expected that the scientific knowledge acquired through the programme will be put into practice as soon as possible. The HyApp sub-project focuses on the development and validation of methods and indicators to predict and quantify the impact of changing water flow. The objective of the HyApp project is to support sustainable development that reconciles the use of hydropower with the ecosystem services of the floodplains.

In this context, this thesis develops interdisciplinary research between remote sensing, ecohydrology and plant ecology. The objective of this work is to contribute to these areas by building new knowledge and creating new perspectives based on the heterogeneous heritage offered by contrasting approaches. In the different chapters of the thesis, I therefore explore new areas that can be found far from each other in terms of the development of the different areas that have occurred in the past. However, the collection of new knowledge from the different contributions will be summarised and linked to each other in the synthesis, thus creating a new and unique perspective on the studies conducted. We will see that, despite the differences in many aspects, the three main chapters shows the rise of common outcomes.

In a way, these objectives go back to an earlier focus of river research, which is more centred on describing patterns than on understanding processes. Thanks to the development of ecological models, statistical models and remote sensing, new perspectives are opening up for the study of the river landscape. For example, the development and accumulation of data from the Landsat satellite mission provides a data archive to study changes in riparian environments over the past decades. A first step in using these new tools is to extract valuable information from the data. The use of these tools to examine processes and understand how the river environment works can also be achieved if the previous step is done properly.

The main research questions addressed in this dissertation are:

1. Which features of airborne and spaceborne imagery allow a robust description of the riverine landscape and its dynamics?

2. Which impact does an alteration of the water flow have on riparian vegetation?

3. What characteristics of the water flow are necessary to support floodplains functioning?

The search for answers to these objectives resulted in the construction of the present thesis, and detailed aspect of these questions, presented further, led to three distinct chapters forming the core of the dissertation. The specific research questions which each chapter answers in more detail are presented in the following paragraphs.

Robust quantification of the riverine dynamics Quantifying land cover dynamics is based on mapping land cover evolution from data acquired at two time stages.

Change detection can be done in a single step or based on an intermediate classification step. The second case is more precisely called post-classification change detection. This case is more popular for the main reason that change detection is done in a more 'natural' way, i.e. the underlying information for change detection is the classification map, not the raw data, which makes the change easier to interpret. In addition, change mapping is often carried out as an additional step in a process for which the classification map itself is the main product. Since most change mapping products are based on change detection after classification, the focus is set on extracting a robust estimate of habitat dynamics from this approach.

The problem with mapping post-classification changes is the error rate that is (more or less) the product of classification maps. For example, a change map based on two 97% accuracy classifications, for which 6% of the land cover actually changes, produces a change map with a $\sim$50% error rate. The aim here is therefore not to search for greater classification accuracy, but to find features in the mapping of changes that are constantly mapped with very high accuracy, thus producing a precise quantification of dynamics, without relying on the wall-to-wall classification map. The accuracy of the quantification must be sufficient under variations of seasons, sensors, shadows and valid on different types of rivers. The independence of the quantification is then referred as the search for a 'robust quantification'. To discriminate the characteristics of classification maps that can provide a robust estimate of dynamics, I adopted an approach presented by Olofsson, (2013) [33].

The research questions for this chapter are therefore:

1. Which habitats of the riverine landscape exhibit the largest changes between seasons?

2. Which components of the riverine landscape best represent the riverine habitats dynamics?

3. Which characteristics of high-resolution imagery are the most important to map riverine habitats?

The study sites examined in this study are found along the Sarine river and the Sense river in the region of Fribourg, Switzerland. The data is comprised of UAS imagery acquired between 2015 and 2016 with three types of camera. The use of images acquired under snow conditions and the mapping of relatively small woody debris, as well as the co-registration of multi-modal UAS imagery are carried out in this study. These tasks have been rarely realised until now and can be useful for today's operational monitoring of river systems.

Impact of water flow alteration on plant traits Various approaches can be used to study plants and their relationships with biotic and abiotic factors of their ecosystems. The quantification of plant trait is a way to describe and compare plants. In nature, a lot of plant traits are often observed as being correlated with each other in

their magnitude or their occurrence, such as canopy height and seed mass or leaf thickness and leaf size (negative correlation) [34]. This fact has led to classifications of plant traits, among which Grime's universal adaptive strategy (also called CSR classification) is one of multiple classifications. Classifications are, of course, models of reality that do not capture all existing variations, but provide an abstract understanding of the observed state, like any model. By using such a classification, the aim is therefore to simplify the description of the processes occurring at the study sites, without assuming that the model is a perfect representation of reality. In this chapter, the impact of the alteration of water flow on plants is considered through the description of plant by the CSR strategies. As previously introduced, water flow interacts in a complex way with riparian vegetation, including feedback loops. The CSR classification here helps to abstract the complex network of interactions to focus on the general trends in plant characteristic changes triggered by altered water flow.

The research questions tackled in the second chapter are:

1. Can we map resource allocation strategies at the individual level using imaging spectroscopy?
2. Is there a difference between the resource allocation strategies found along the different reaches considered?
3. What are the processes shaping the plant traits of floodplain vegetation following a flow alteration?

The data consist of imaging spectroscopy acquired by APEX in the summer of 2015 and 2016 and samples collected in the summer of 2016. One of the particularities of this research is the mapping of resource allocation strategies at the individual level. To carry out this task, I used the quantification of CSR strategies proposed by Pierce (2017) [35].

Inter-annual dynamics of vegetation status A large Earth observation archive is now available, covering most of the Earth's surface over the past few decades and growing daily. However, few Earth observations are available at high resolution and most of them are not free, which hinders their use for time series analysis, as a generally large data set is required. In this context, the use of medium resolution imagery provided by the Landsat mission offers a free and viable alternative between temporal, spectral and spatial resolution for floodplain observation.

However, its use on the river landscape is slowed down by the small size of the object under study compared to the available spatial resolution. The idea here is therefore to use information per pixel and aggregate data per river section. Although the ground size of the Landsat product is of the same magnitude as the object of interest (i.e. the width of the river), spectral mixture analysis can be used to acquire some knowledge about the system.

The research questions examined in the third chapter are as follows:

1. How can we extract information from medium-resolution satellite data archives on relatively small rivers?
2. Which characteristics of the flood events sequence impact the vegetation status retrieved by remote sensing?
3. Does the vegetation of Swiss alpine sub-mountainous braided rivers exhibit a trend over recent decades, and what are the most likely drivers of the trend?

In this chapter, we focus on the period from 1988 to 2016, covering several floods and providing a sufficiently long period to observe the dynamics of vegetation structure. In particular, the Sense flood of 1990, which is a particularly rare event, is part of the time series. To describe the effect of water flow on the vegetation dynamics, I couple Earth satellite observation with high-resolution recorded gauge data. Two hundred hydrometric stations record, among other things, water flows and levels over the entire Swiss hydrological network. Systematic measurements have been carried out since the mid-19th century and most of the current stations have been operational for almost a century, providing a unique opportunity for river research.

1.6 Structure of the Dissertation

Chapter 1 provides the current context of the thesis, important for understanding research needs in the river system. The structure and dynamics of floodplains are presented. The remote sensing technology used in the thesis is presented as well as its capabilities in the study of river systems. Finally, the research questions are presented with a brief description of the main chapter, published in the form of peer-reviewed articles, presented in Chapters 2 to 4.

Chapter 2 is the first peer-reviewed article published in *Remote Sensing of the Environment* [36]. It provides recommendations for quantifying river habitat dynamics using high-resolution images. The results are useful for current river floodplain monitoring, restoration projects and water flow management.

Chapter 3 is the second peer-reviewed article published in *Journal of geophysical research: biogeosciences* [37]. The mapping of resource allocation strategies defined by the universal adaptive Grime theory is presented. By taking into account three reaches of watercourses under different states of alteration of water flow, we can deduce the impact of the alteration of water flow on the plant traits. The results, limited in particular by the number and sites considered, do not provide solid evidence of understanding the shaping of plant traits by water flow, but provide valuable information and open up multiple questions and opportunities for further research.

Chapter 4 is the third peer-reviewed article submitted in *IEEE Journal of Selected Topics in Applied Earth Observations and Remote Sensing* [38] to date. Satellite acquisition time series are taken into account and linked to flow data recorded by hydrometric stations. To conduct this study, I developed an approach to using medium-resolution imagery for relatively small rivers. The results are consistent with other

detailed studies conducted on the sections under consideration and therefore suggest that satellite imagery can be used to monitor changes in riparian vegetation in remote areas or where other types of data are lacking.

Chapter 5 expands on the previous chapters to synthesise the results found at the intersection of the studies conducted. These results are examined in the context of ongoing research on river systems. Finally, additional research avenues are presented and conclude the thesis.

Chapter 2

Robust Quantification of Riverine Land Cover Dynamics by High-Resolution Remote Sensing

Milani, G., Volpi, M., Tonolla, D., Doering, M., Robinson, C., Kneubühler, M., & Schaepman, M. E.

This chapter is based on the peer-reviewed article:
Remote sensing of environment, 2018, 217, 491-505
DOI: doi.org/10.1016/j.rse.2018.08.035
and has been modified to list all cited references in the Bibliography Chapter.
The layout has been adapted to uniform the current thesis.

The reprint has been made with permission from Elsevier.

G. Milani, M. Doering, C. Robinson and M. E. Schaepman conceptualized the study. G. Milani, M. Kneubühler, D. Tonolla and M. Doering elaborated the methodology. G. Milani, M. Volpi and M. Kneubühler performed the investigation. G. Milani, M. Volpi, M. Kneubühler, D. Tonolla, M. Doering, M. E. Schaepman performed the formal analysis. G. Milani wrote the first draft of the manuscript. G. Milani, M. Volpi, M. Kneubühler, D. Tonolla, M. Doering, C. Robinson, and M. E. Schaepman participated in the writing and editing of the final manuscript.

2.1 Abstract

Floodplain areas belong to the most diverse, dynamic and complex ecological habitats of the terrestrial portion of the Earth. Spatial and temporal quantification of floodplain dynamics is needed for assessing the impacts of hydromorphological controls on river ecosystems. However, estimation of land cover dynamics in a post-classification setting is hindered by a high contribution of classification errors. A possible solution relies on the selection of specific information of the change map, instead of increasing the overall classification accuracy. In this study, we analyze the capabilities of Unmanned Aerial Systems (UAS), the associated classification processes and their respective accuracies to extract a robust estimate of floodplain dynamics. We show that an estimation of dynamics should be built on specific land cover interfaces to be robust against classification errors and should include specific features depending on the season-sensor coupling. We use five different sets of features and determine the optimal combination to use information largely based on blue and infrared bands with the support of texture and point cloud metrics at leaf-off conditions. In this post-classification setting, the best observation of dynamics can be achieved by focusing on the gravel - water interface. The semi-supervised approach generated error of 10% of observed changes along highly dynamic reaches using these two land cover classes. The results show that a robust quantification of floodplain land cover dynamics can be achieved by high-resolution remote sensing.

2.2 Introduction

Floodplain areas are among the most important ecosystems in terms of biodiversity, despite their low terrestrial coverage [39]. A recent report [40] indicates that 40% of European rivers are affected by hydropower production, navigation, agriculture, flood protection or urban development, which disturb water flow, inundation, erosion and sedimentation processes that directly impact hydromorphological properties. In the last years, the concept of *habitat dynamics* has become even more relevant than *habitat heterogeneity* for supporting biodiversity in riparian areas [41, 42, 43]. The dynamics of the riverine environment have been studied by focusing on the water channel, of both short [44] and long time periods, mostly using historical photography [45] or by focusing on riparian areas [46, 47]. Moreover, several models of landscape evolution have been developed to provide temporal simulations of riverine environments [48, 49, 50, 51, 52].

The riverscape is unique in its structure, creating a heterogeneous image composition not commonly seen in remote sensing applications. The composition of the riverscape may change strongly depending on the distance from the water channel in active floodplains [53]. Closer to the water, the land cover is very heterogeneous, representing a transitional environment that consists of, e.g., drying dead

arms, gravel and sand bars, decomposing woody debris and riverine shrubs. Further from the river, the land cover exhibits more homogeneous patterns composed of riparian vegetation, floodplain to upland forest and grassland. While an ecological study would focus on so-called floodplain dynamics, i.e., the dynamics of ecological habitats, we use here the proxy of land cover dynamics for our study, i.e., the dynamics of land cover classes detected by remote sensing.

In a riverscape context, remote sensing technologies offer a unique point of view on the floodplain dynamics, allowing researchers to sample data at regular temporal intervals and cover large areas with less effort than traditional ground sampling approaches. Riverscape remote sensing embraces aspects of light propagation in the water body [54, 55], large woody debris detection [56, 57], species classification [58], sandbar relocation [59] and modeling of floodplain vegetation [60] or hydrology [61, 62, 63]. Riverscape remote sensing deploys a suite of technologies ranging from high-resolution to imaging spectrometry sensors.

Unmanned Aerial Systems (UAS) technologies are nowadays used for many applications requiring very high-resolution imagery. The efficiency and advantages of UAS for remote sensing purposes have been demonstrated in general [64] and for specific uses such as segmentation of tree crowns in forested ecosystems [65], civil engineering structures [66] or urban vegetation mapping [67]. Specific aspects of riverscape remote sensing using UAS have been validated, including immersed topography [68], submerged aquatic vegetation [69], hydraulic fish habitat [70] and hydromorphological effects of flooding [71].

Recent developments in UAS technologies offer a new perspective on the land cover component of the riverscape. Land cover classification algorithms have been successfully developed for high-resolution imagery in various environments [72, 73, 74], including GEOBIA approaches [75]. Moreover, land cover change mapping by remote sensing has been developed and applied for many years in various environments [76, 77, 78]. However, few applications in the context of a riverine landscape can be found today [79, 80, 81]. The main processes triggering the dynamics of riverscape habitats include fluvial geomorphic processes and ecological processes of succession, recruitment and dispersal [82, 83]. Various classification systems are used to discriminate habitats of the riverscape [59, 84, 85]. The current study is restricted to a coarse classification of habitats including the most important land cover types, namely water, gravel, vegetation and woody debris, to ensure that the method could be applied on different sites. Finally, the chosen land cover types relate to the main geomorphic macro-units in ecological terms composed by (i) open water, (ii) bare sediment and (iii) vegetation (e.g. vegetated sediment, vegetated islands, forest).

For observing land cover dynamics in the riverscape, post-classification change mapping is suitable because of its ability to interpret changes. In general, post-classification approaches remain more popular than pre-classification change detection [86]. Furthermore, processing images independently allows us to understand

the underlying factors of variations by modeling statistically sensor selection, seasonality, extracted covariates (or *features*), platform design and data processing to the final land cover map at each time step. However, the error rate of a change map is linked to the product of the individual error rate of the classification maps, hindering the usability of change mapping when the error rate is higher than the actual land cover changes [87]. Methods to improve the general accuracy of post-classification change mapping have been proposed to solve these issues. A direct approach consists of reducing the impact of classification errors by detecting changes before the classification step [88]. Another approach consists of using the confusion matrix of classification maps to correct the estimates of dynamics [89]. Here, we focus on the second kind of approach to determine a robust dynamics estimate with respect to the classification errors.

In this study, we analyze the capabilities of UAS technologies and their associated classification processing chain to observe post-classification dynamics in the specific case of the riverscape. We aim to determine the best observer specifications and landscape features for achieving a robust quantification of riverscape dynamics. Hence, the final aim is not an improvement of raw classification accuracy, but a robust extraction of dynamics information that takes into account potential classification errors. Robustness is here understood as a stability of the quantification against classification errors due to image acquisition, image processing, vegetation status and seasonal influences. We assess the use and importance of different types of information extracted from the acquired high-resolution imagery by studying the link between classification accuracy, features used in the machine learning algorithms, the acquisition and camera parameters, and the corresponding change maps. Finally, we assess the accuracy of the whole processing chain to carry out post-classification change mapping, including a post-analysis error-adjustment (c.f. Olofsson et al., 2013).

2.3 Materials & Methods

2.3.1 Study sites

The test area consisted of three hydromorphologically different reaches of two Swiss rivers in the pre-Alpine region, i.e., the Sarine (46°45'N 7°7'W) and the Sense (46°44'N 7°18'W) (Figure 2.1). Both rivers are located in the region of Fribourg, in western Switzerland, and share similar climatic conditions. Hydropower considerably impacts the hydrological regime of the Sarine River, while the Sense River, near Plaffeien, is one of the last Swiss rivers with almost no anthropogenic control of the hydrological regime. The reaches represented three different land cover dynamics, i.e., a residual reach along the Sarine (almost no flow changes), a hydropeaking reach along the Sarine (frequent hourly and daily flow changes), and a natural reach along the Sense (irregular natural flow changes). The regular and frequent flow changes

observed in the hydropeaking reach are due to the operation of a hydropower plant upstream of the reach. The extent of the covered areas was based on the federal inventory of floodplains of national importance (updated on 01 July 2007) issued by the Swiss Federal Office for the Environment (FOEN).

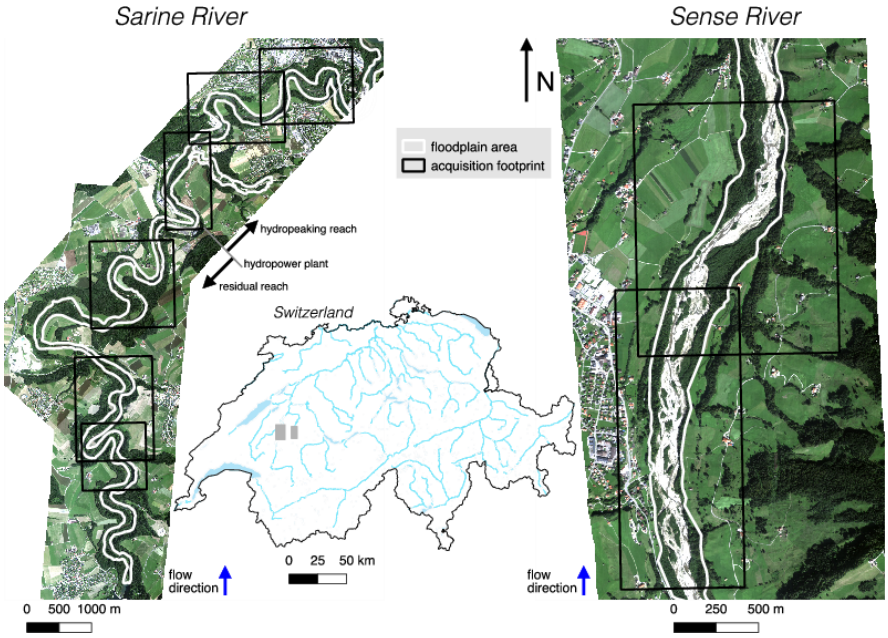

FIGURE 2.1: Sections of the Sarine and Sense Rivers along which the UAS image data were acquired. Left: the Sarine River was divided into two reaches, separated by the hydropower plant of Hauterive. Middle: the gray rectangles show the location of the reaches in Switzerland. Right: the natural reach along the Sense River.

2.3.2 Data acquisition

We collected the UAS image data using three different cameras, each with different spectral capabilities (Table 2.1). The RGB camera was a standard camera Canon IXUS 125HS [90] acquiring three wavelength bands centered at 450nm, 520nm and 660nm. The red edge camera (ReGB) was a modified version of the same camera containing three bands centered at 450nm, 500nm and 715nm. The red edge band of the camera was enforced by altering the red filter to a near-infrared filter. The multispectral camera [91] consisted of four bands centered at 550nm (R), 660nm (G), 735nm (NIR1) and 790nm (NIR2), out of which the R, G and NIR2 were used. The NIR1 band was not used because of its extremely high correlation to the NIR2 band, not providing any additional information for our land cover classes. In the case of the multispectral camera, an irradiance sensor was located on the top of the camera, which enabled the conversion of recorded radiation to reflectance quantities. While the multispectral camera was calibrated before each flight, no pre-flight or post-flight calibration was performed on the RGB and ReGB cameras. Datasets used in this study were regularly acquired throughout the year resulting in trees with leaf-on

TABLE 2.1: UAS data collection consisting of six datasets taken in different seasons. The camera type refers to the standard color (RGB), the Near-infrared – Red – Green (NirRG) and the Red edge – Green – Blue (ReGB) cameras. The classified area corresponded to the intersection of the acquired images with the floodplain delineation defined by the Swiss Federal Office for the Environment.

Dataset	Date	Image Footprint [ha]	Classified Area [ha]	Reference Area [ha]	Training Area [ha]	Acquisition Resolution [cm]
RGB Leaf-On	27.06.15	460	185	71	0.73	8
RGB Leaf-Off	16.11.15	486	169	112	1.04	8
ReGB Leaf-On	25.05.16	756	258	99	1.38	8
ReGB Leaf-Off	18.03.16	560	176	28	1.28	8
ReGB Snow	24.02.16	192	82	16	0.64	8
NirRG Leaf-On	20.08.15	595	206	97	0.78	16

and leaf-off states. The ReGB Snow and ReGB Leaf-Off datasets corresponded to the winter acquisitions over the Sense and Sarine Rivers, respectively.

In our study, four main land cover classes were investigated, i.e., water, vegetation, gravel (gravel and sand bars) and woody debris, each presenting intra-class variability, justifying statistical classification approaches. They represented around 12%, 30%, 54% and 4% of the land cover along the natural reach. Along the residual reach and the hydropeaking reach, woody debris covered less than 0.1% of the total area, hindering the use of statistical methods to predict their presence. Consequently, the woody debris class was not included in the classification of these reaches, leading to an absence of woody debris mapped automatically in the ReGB Leaf-Off scene. However, the rare woody debris patches present were injected into the classification maps used for change mapping analysis by a post-classification manual delineation that involved in our case a maximal amount of 1 hour of work per dataset.

Classification and Post-Classification Change Mapping

The image datasets acquired with the UAS were processed with the software Pix4D Mapper [92]. The software relied on automatic feature detection and matching algorithms to retrieve the internal and external orientation of oblique images. Photogrammetric processing subsequently provided dense point clouds, digital elevation models (DEM) and orthoimages. Each dataset was co-registered to a reference dataset based on orthoimages to avoid errors in the change detection pipeline due to global misregistrations.

Orthoimage-to-orthoimage registration involved co-registration of high-resolution images taken by different sensors under variable environmental and seasonal conditions. We performed the registration by using the python library SimpleITK [93] maximazing the Mattes mutual information [94], which helped to overcome the

problems of seasonal changes, sensor differences and shadow shifts. Here, we empirically modeled the image distribution by a 24-bin histogram. Specifically, to compute the deformation to align images, we estimated a 2D Euler transformation on couples of orthoimages optimized by gradient descent in a 4-level multi-resolution (hierarchical) approach.

The x-y shifts resulting from the co-registration averaged to 1.42m. The quality assessment of the co-registration was two-fold. We visually controlled the accuracy of the global registration for all pairs of orthoimages to avoid potentially large impacts on the dynamics accuracy assessment by failure of the co-registration. Then we quantified the remaining misregistrations using ground control points that were manually digitalized on a subset of six pairs of orthoimages. Remaining misregistrations varied among the datasets, with a mean ranging from 0.4m to 2.6m (Appendix B.1). In the end, the range of remaining misregistrations did not hinder the dynamics estimation, also robust to such inaccuracies of the pre-processing.

The method we developed for classification of riverscape land cover made extensive use of local features combining spectral information, texture and 3D point clouds. Detailed information on the classification can be found in Appendix 2.8.1. We extracted three main groups of features, namely spectral, textural and point cloud-based. Then, we combined these groups into five feature sets on which we trained a classifier: i) spectral (S), ii) spectral + textural (ST), iii) spectral + point cloud (SP), iv) spectral + textural + point cloud (STP), and v) spectral + textural + point cloud with semi-supervision (SemiSup).

The results of the semi-supervised approach, which is detailed in Appendix 2.8.1, were used for change mapping analysis. The complete scheme of the change mapping analysis consisted of several steps, specifically feature extraction, segmentation, semi-supervised classification, change mapping and stratified estimation (Figure 2.2). The classification scheme relies on segmentation as spatial support to account for the mosaic structure of the riverine environment. The extraction of indicators of accuracies and dynamics quantification are detailed in the next sections. To further improve classification accuracy and reduce potential false changes, we carried out a post-classification correction procedure in a GIS requiring a few hours of work, which would be a reasonable amount of time required by a monitoring project in its operational phase. The corrections applied consisted of manual adjustments of segment labels based on photo-interpretation. The change mapping was subsequently performed by differentiating co-registered consecutive classification maps. Since the classification maps differed slightly in their areal extent due to different data acquisition plans, only areas present in both classification maps were retained in the change analysis.

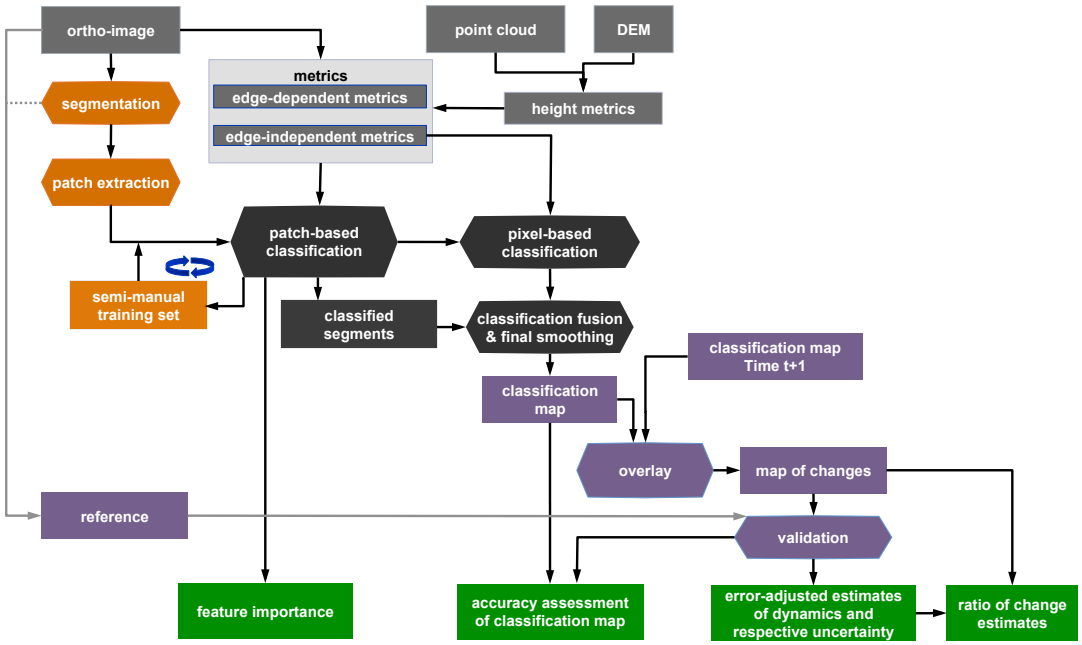

FIGURE 2.2: Visual summary of the processing scheme: input data and extracted metrics (gray), object-based classification of segments including active learning (orange), classification (black), resulting maps and extracted dynamics (purple) and an indicators of dynamics and relative accuracy (green). The final indicators correspond to the following tables and figures, from left to right: Figure 2.5, Table 2.2, Figure 2.4

and Table 2.3.

2.3.3 Accuracy assessment & Reference dataset

In order to assess a true accuracy of dynamics, the classification maps were assumed to represent the physical land cover reality, rather than the image reality. For example, a river patch covered by a leaning tree would intrinsically be defined as water from a land cover point of view. However, the leaning tree could unambiguously be considered as vegetation land cover in the image reality. To implement this concept, we defined validation areas by investigating multiple consecutive images, providing the required information about land cover dynamics.

The reference dataset was built on the change maps by extracting initial and final states corresponding to single image acquisitions. By building the reference dataset using consecutive images, the accuracy assessment was representative of the complete classification procedure. The unclassified segmented polygons were used as a starting point for delineating the reference areas. Reference polygons of homogeneous land cover were randomly chosen, stratified among change pathways, to form the reference set. We selected a total area of 50 to 60% of each land cover change pathway. To reach the given selection percentage, several iterations of classification have been performed. The proportional selection of area among each land cover change pathway (including pathway of no changes) ensured a proportionality between the size of each pathway and the weight on the accuracy metric (Appendix B.2). The extensive reference dataset ensured to account for commissions of change. In order to account for most of the omissions of change, an expert carefully inspected the orthoimages to include the areas containing substantial land cover changes in the reference dataset.

Based on the land cover change reference dataset, we extracted a reference layer for each classification map to compare the accuracy reached by the different feature sets. We compared the different classification approaches on the basis of two complementary metrics: the total disagreement statistic [95] and the multi-class recall defined as the mean producer accuracy:

$$recall = \frac{1}{J} \sum_{j=1}^{J} \frac{C_{jj}}{C_{\cdot j}} \tag{2.1}$$

for J classes, where C_{jj} is the total area labeled as j simultaneously in the classification map and in the reference dataset and where $C_{\cdot j}$ is the total area of class j in the reference dataset.

The total disagreement represents both the mismatch in predicted class proportion (quantity disagreement) and the mismatch of detected classes over the space (allocation disagreement). On the one hand, the comparison of total disagreement between datasets revealed the influence of sensor selection and seasonality on land cover type discrimination, while the comparison of the different approaches revealed the discrimination power of the respective features. The recall, on the other hand, gives equal importance to every class, independently of the proportion of the

classes. Therefore, the recall reveals the power of the classifier to discriminate among the classes rather than the actual accuracy of the classification map.

To robustly quantify the accuracy of the change maps, we applied the procedure of area estimation adjustment and uncertainty quantification [96]. This method allowed adjusting the estimation of the number of detected changes based on their spatial relation. Two independent quality measures were extracted from the results: the difference between the raw change estimates (the classification outputs) and the error-adjusted change estimates, and the uncertainty of the error-adjusted change estimates. A derivation of the expressions can be found in Card, 1982 [97] by transposing the point-based to an area-based confusion matrix consisting of all the possible change pathways. $\hat{A}_j$, the error-adjusted estimate of the total area of class j, is given by:

$$\hat{A}_j = \sum_{i=1}^{J} A_i \frac{C_{ij}}{C_{i\cdot}} \tag{2.2}$$

where A_i is the area of class i in the classified map, C_{ij} is the total area labeled as j in the reference dataset and as i in the classification map, and $C_{i\cdot}$ is the total area classified as i intersecting any of the reference polygons. The coefficient of variation is calculated by dividing the estimated standard deviation [97] (equation 24) by the error-adjusted estimate. CV_j, the respective coefficient of variation of the error-adjusted estimate of class j, is given by:

$$CV_j = \frac{S(\hat{A}_j)}{\hat{A}_j} = \frac{1}{\hat{A}_j} \sqrt{\sum_{i=1}^{J} A_i^2 \frac{\frac{C_{ij}}{C_{i\cdot}} \left(1 - \frac{C_{ij}}{C_{i\cdot}}\right)}{C_{i\cdot} - 1}} \tag{2.3}$$

While these two quantities do not present a spatial component, they are class-dependent and depend on the classification accuracy of consecutive datasets. Hence, candidates for being robust estimates of the dynamics are those changes exhibiting a ratio of raw change to error-adjusted change estimate close to 1 with a low uncertainty in the error-adjusted change estimate. Given the high coverage of the reference dataset, the error-adjusted estimates are here considered as observed dynamics. The accuracy of the raw change estimates is therefore defined by the relative difference to the error-adjusted estimates.

2.3.4 Feature Importance

Feature importance informs the user about which features are more discriminating for the land cover classification task at hand. We used such measures to understand the links between image acquisition characteristics (sensor, seasonality) and corresponding classification accuracies. The feature importance was expected to be related to the differences in accuracies between the different approaches. The use of more informative feature sets should consequently increase the final accuracy.

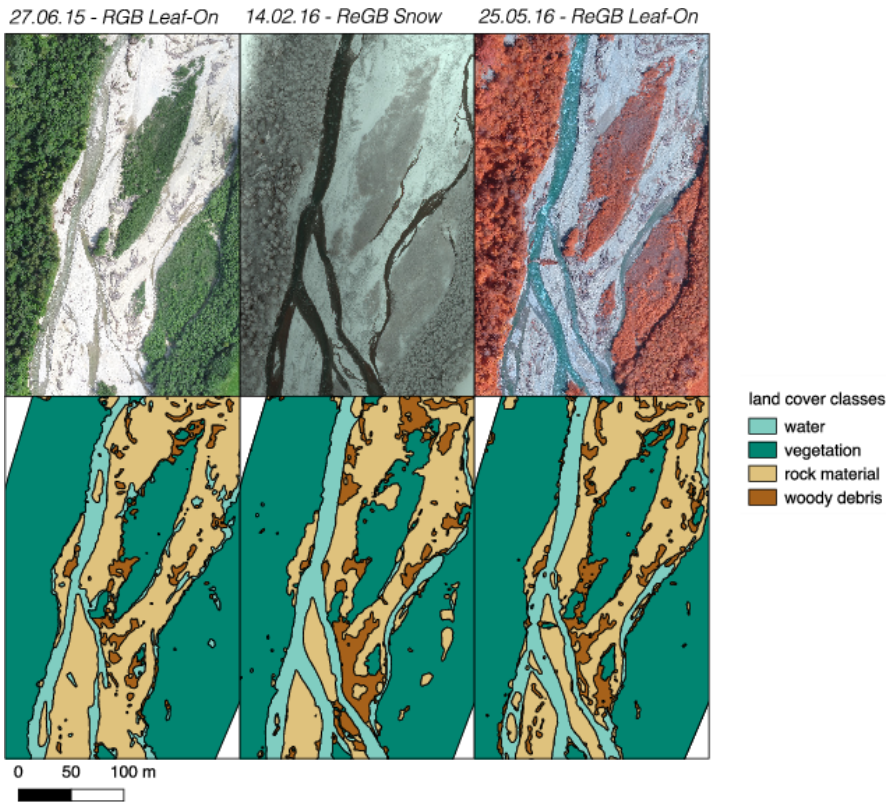

FIGURE 2.3: Subsets of land cover classifications with RGB and infrared cameras along a small section of the Sense River from different dates. The classification errors depend on the land cover type, the sensor and the environmental conditions. Images acquisition date and corresponding dataset from left to right: 27.06.15 (RGB Leaf-On), 14.02.16 (ReGB Snow), 25.05.16 (ReGB Leaf-On).

In our implementation, we used random forest by constructing node splits maximizing the Gini purity index. [98, 99]. We employed the model trained on the STP feature set, which contained all the features, also used by the SemiSup approach. The Gini coefficients were recomputed to get the feature importance by class by aggregating *a posteriori* the samples into two groups, corresponding to target and non-target classes. We grouped feature importance values according to the respective feature set to provide a comprehensive overview.

2.4 Results

The proposed methodology was applied to the five acquired UAS datasets along the three reaches previously described (Table 2.1). The subsequent assessments of classification accuracies and the feature importance summarize the results along the three reaches. Subsets of the land cover classifications performed by the SemiSup approach are visualized in Figure 2.3.

TABLE 2.2: Total disagreement and recall for all datasets and all approaches, i.e., spectral (S) spectral + textural (ST), spectral + point cloud (SP), spectral + textural + point cloud (STP) and spectral + textural + point cloud with semi-supervision (SemiSup). The accuracy assessment is polygon-based, using intersecting areas between the reference dataset (Table 2.1) and the classification maps. Since no woody debris was mapped in the ReGB Leaf-Off dataset, its accuracy cannot be directly compared. The low total disagreement and the high recall values are represented darker for easier readability.

Total disagreement	RGB Leaf-On	RGB Leaf-Off	ReGB Leaf-On	RGB Leaf-Off	ReGB Snow	NirGB Leaf-Off
S	0.058	0.067	0.054	0.053	0.084	0.054
ST	0.058	0.075	0.055	0.052	0.119	0.052
SP	0.060	0.047	0.055	0.042	0.088	0.047
STP	0.055	0.052	0.055	0.036	0.088	0.044
SemiSup	0.040	0.045	0.052	0.029	0.070	0.035
Recall						
S	0.85	0.81	0.85	0.92	0.79	0.88
ST	0.88	0.86	0.87	0.93	0.81	0.89
SP	0.88	0.86	0.86	0.94	0.84	0.89
STP	0.89	0.89	0.87	0.94	0.85	0.90
SemiSup	0.89	0.91	0.88	0.94	0.89	0.92

2.4.1 Classification Accuracy

The accuracy metrics showed a dependence both on the dataset and on the approach applied (Table 2.2). The complete results for the user and producers accuracies are presented in appendices B.3 and B.4. As expected, the disagreement was in general lower when more features were present and was always the lowest when employing the SemiSup approach. The least influence of the SemiSup approach was observed for the ReGB Leaf-On dataset. Moreover, the ReGB Leaf-On dataset was the least sensitive to the addition of any feature on top of the spectral features.

In general, point cloud features had a larger influence under leaf-off conditions, helping in discriminating trees when leaves are not present. Adding features to the spectral information under leaf-on conditions did not decrease the total disagreement, but a decrease was nevertheless observed in the SemiSup approach.

The high total disagreement achieved by the ST approach was particularly obvious for the ReGB Snow dataset, where the addition of the texture had a strong effect. The total disagreement of the ReGB Snow dataset was lower for every approach, except for the recall using the SemiSup approach. Overall, the ReGB Snow dataset yielded a relatively high recall but also a high total disagreement. Such observations can arise in the case of a high number of commission errors for less represented classes.

The user accuracy of the woody debris land cover had a substantial negative

influence on the classification accuracy for every dataset due to a low user accuracy. The user accuracy of woody debris ranged from 0.15 to 0.83, with a median at 0.49. The lowest user accuracies for woody debris were found in the classification maps produced with the ReGB Snow dataset.

2.4.2 Quantification of the land cover dynamics

The ratio between raw and error-adjusted change estimates indicated an accurate area estimation for certain land cover changes (Table 2.3). The diagonal values indicated an overall agreement in the classification maps, since most of the area did not change. A value far from 1 did not necessarily indicate large errors in the raw observed changes (such as in the case of the vegetation to water changes) because very small changes of a given kind would still lead to a very high ratio. The off-diagonal values closer to 1 were found for gravel in the natural reach and, with a weaker intensity, in the hydropeaking and residual reaches.

Among the changes of gravel, the observations closest to 1 were related to the changes from/to water for the natural and hydropeaking reach and also from/to vegetation along the residual reach. An accuracy of change estimate between water and gravel of $\pm 10\%$ is achieved along the hydropeaking and natural reaches and $\pm 300\%$ along the residual reach. In general, the raw observed dynamics, that had a ratio larger than 2, were far from the raw error-adjusted estimates, apart from the transitions cited above, which were in agreement.

Figure 2.4 presents the error-adjusted dynamics among the three reaches with the respective uncertainties and completes Table 2.3 for the interpretation of the accuracy assessment of the dynamics. The observed changes of land cover were normalized by the area of the source land cover. As such, the total area of all the changes occurring within the same land cover in the source image was equal to 1. The uncertainty is presented by the italic number on the top of the bars, which shows the log of the coefficient of variation (CV) based on the standard error estimation by Olofsson [96]. Therefore, a low negative value indicates a better precision in the dynamics estimation. The uncertainty is high when numerous omission errors are found in relatively small classes. A large difference in the estimations (Table 2.3) but with low uncertainty (CV in Figure 2.4) is often observed when rare changes are mistakenly mapped. In such a case, the relative area mapped is far from reality, but the error-adjusted estimation captures the absence of this change from the ground truth and adjusts the estimate with high certainty.

Most of the observed land cover changes were linked to the gravel land cover. The CV values were small due to the high proportion of labeled areas for the error-adjusted estimates, comprising $> 50\%$ of area per class. The error-adjusted changes 'gravel to water' and 'water to gravel' presented the lowest CV along the natural reach and along the hydropeaking reach. The same changes also exhibited low CV along the residual reach. However, the lowest CV along the residual reach was

TABLE 2.3: The table shows the ratio of the raw classification change estimates by the error-adjusted change estimates. The rows are the initial land cover classes; the columns are the final land cover classes. A high off-diagonal value indicates an over-estimation of the change. The off-diagonal large values indicate commission error of changes, mainly due to classification errors. The off-diagonal values closer to 1 are represented darker for easier readability.

RESIDUAL	water	vegetation	gravel	woody debris
water	0.85	14.52	3.28	NaN
vegetation	43.11	0.97	2.95	44.54
gravel	2.72	2.32	0.58	NaN
woody debris	4.27	2.13	NaN	0.91

HYDROPEAKING	water	vegetation	gravel	woody debris
water	0.94	54.89	1.19	1.32
vegetation	10.04	0.97	8.21	2.75
gravel	1.04	3.24	0.74	NaN
woody debris	1.24	1.54	NaN	0.93

NATURAL	water	vegetation	gravel	woody debris
water	0.9	16.14	1.05	2.22
vegetation	1.47	0.96	3.37	7.96
gravel	1	4.64	0.92	8.96
woody debris	1.75	3.83	38.04	0.56

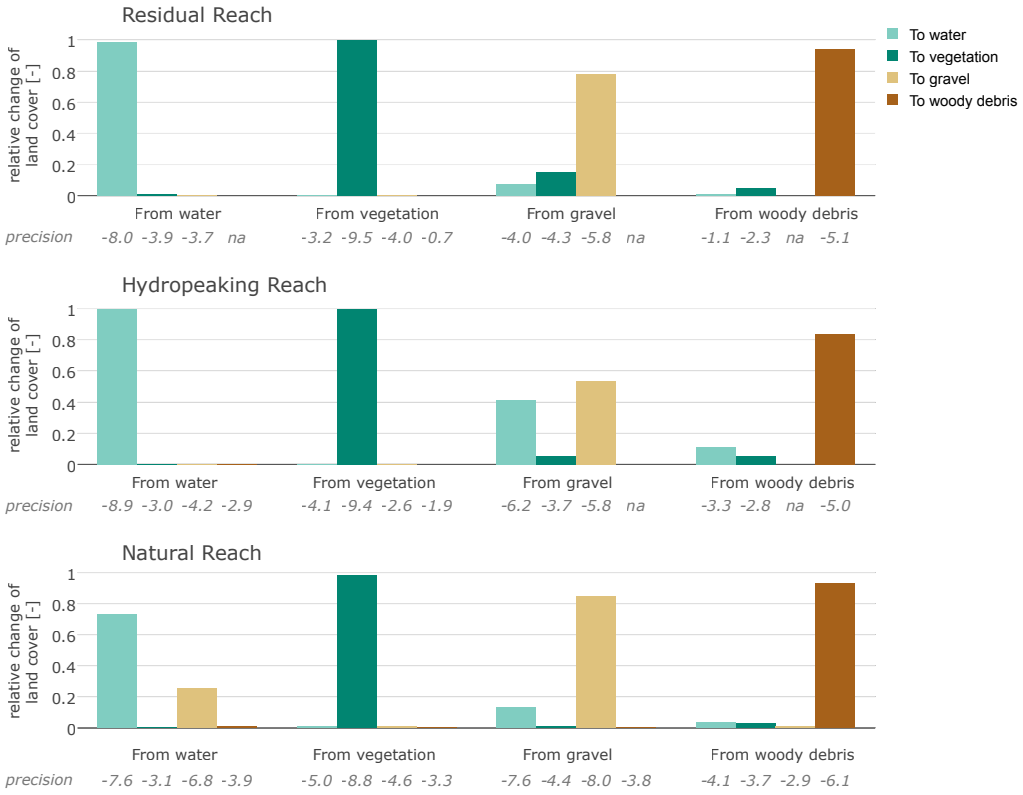

FIGURE 2.4: Error-adjusted change estimates expressing the land cover dynamics. The results are normalized with respect to the source of land cover change. The log of the coefficient of variation is displayed in italics under the bars. Land cover with large changes and smaller coefficients of variation are better candidates for dynamics estimation since related classification errors have less effect on the dynamics estimation. The changes between gravel and water exhibit the larger changes along with the smallest coefficients of variation.

found for the change 'gravel to vegetation'. In general, the CVs along the natural reach were higher than the CVs along the hydropeaking and residual reaches.

The raw observed dynamics contained substantial errors for rare dynamics changes, such as changes from vegetation to water (Table 2.3). The error-adjusted dynamics did not contain such errors, thus compensating for low change likelihood in the raw observations. The dynamics between gravel and water were already well captured in the raw observed dynamics, meaning that most of the observed changes were likely land cover changes.

2.4.3 Feature Importance

The feature importance was computed on each dataset independently (Figure 2.5). Excluding the ReGB Snow dataset, the patterns of feature importance varied more among different sensors rather than among seasons. The RGB datasets relied more on the texture and point cloud than other datasets. This was also visible by observing the increase in the recall when including these features.

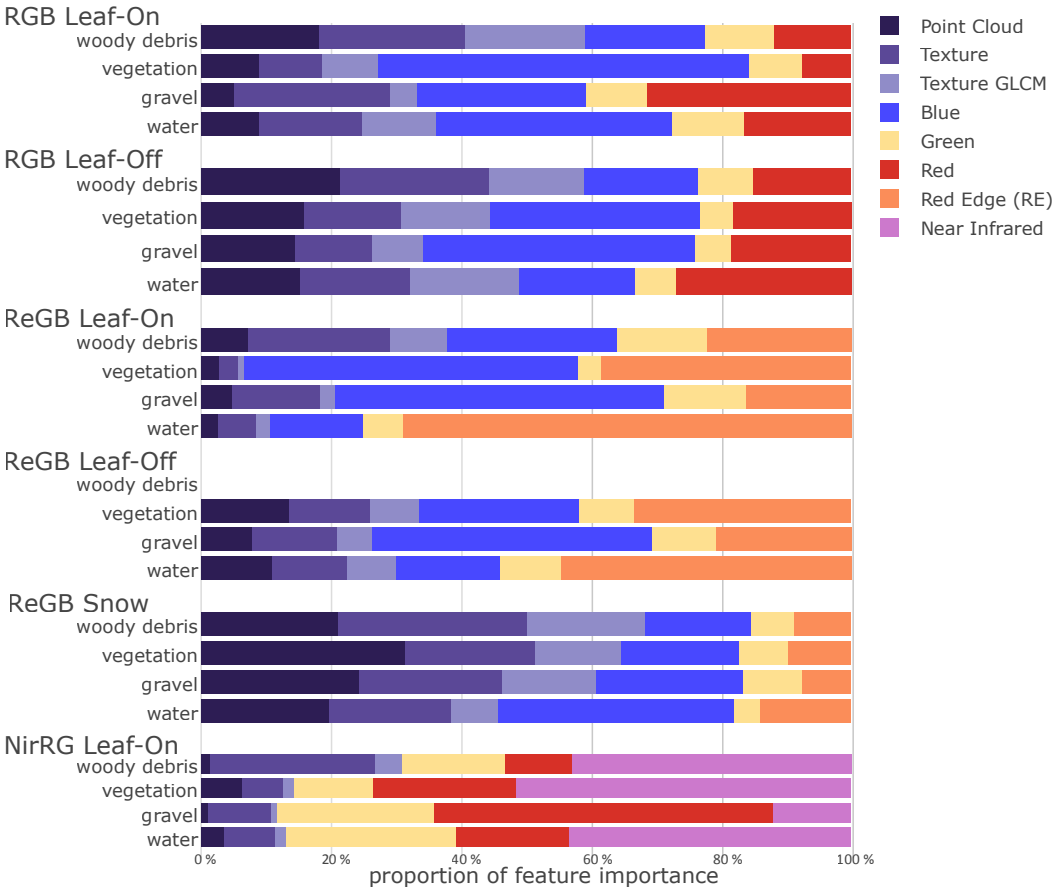

FIGURE 2.5: Feature importance for each dataset for all land cover classes. The calculation was based on the Gini importance of the random forest classifier.

Along with sensor differences, feature importance showed clear dependencies on the class to be modeled. Texture and point cloud descriptors were very important to discriminate woody debris in all the datasets. In the presence of snow, the point cloud and texture features were important for all classes, even for the water class, while classification based on spectral information yielded poor results (Table 2.2). These observations qualitatively validated the feature set we built, since the addition of a feature group increased the accuracy in parallel to a share of the feature importance between the groups.

As expected, the importance of spectral features varied substantially depending on the wavelength band. In general, infrared and blue bands were always useful apart from the above-mentioned ReGB Snow dataset. The green band was the least important, independently of the sensor or season, probably because of the high correlation to the blue channel and some class-specific redundancy with the near-infrared channel. In parallel, the green band gained importance in the NirRG dataset in which the blue band was not available.

The importance of texture and point cloud for the woody debris detection was shared by all datasets. Texture and point cloud were, in general, of equal importance, except in the case of the ReGB Leaf-On and NirRG Leaf-On datasets, in which the standard texture features were more important than the point cloud and GLCM features. In presence of snow, the point cloud and texture features were important for every class.

2.5 Discussion

2.5.1 Classification accuracy

The accuracy assessment allows us to analyze the effect of the different feature sets and the impact of semi-supervision on the classification accuracy. Furthermore, studying a global accuracy metric allows us to understand the effects of sensor and seasonal changes on the classification accuracy and on the change mapping quality.

Overall, the semi-supervised setting helps to overcome failures in the training set definition by active learning and by generalizing the training set. We argue that the better performance is due to better coverage of class-conditional variances, making the training set more representative of the modes of variation needed to discriminate classes. Since the increase is shared among all datasets covering different sensors, it suggests that a semi-supervised approach should be integrated as often as possible in land cover classification of a riverscape. The SemiSup approach could also be extended, for example, to include annotations of low confidence patches directly [100] instead of misclassified areas only.

Neither the type of sensor nor the season has a marked influence on the considered metrics unless the landscape of interest is covered by snow. However, the inclusion of the point cloud features has a strong influence on the leaf-off datasets,

which is linked to the loss of discriminating power by the spectral features. The importance of point cloud features for leaf-off datasets remains despite the reduced quality of the image matching and the point cloud generation carried out by the image processing software under leaf-off conditions. The season and the sensor type have a large effect on the woody debris mapping, related to i) the high reflectance of surrounding gravel with an RGB sensor, ii) the mix with young vegetation, and iii) the difficulties to segment woody debris patches (Figure 2.3). Observed changes among the classifications are both due to natural variation and to classification errors. With the proposed semi-supervised approach, our study outperforms results of previous works that aimed, among others, at woody debris classification, improving the producer accuracy of woody debris classification by [101] and [102] by 9% and 16%, respectively. These performances suggest that the point cloud information and texture features are key components for mapping woody debris. Other studies have also shown the importance of structure information for delineating riverscape land covers [81, 103] using Lidar data.

The textural features show different patterns and reveal their failure to improve the accuracy. The radical decrease in performance of the ST approach for the ReGB - Snow dataset shows that the texture features should be carefully used. In fact, parameterization of texture features has been highlighted in other studies [67]. In our case, we argue that texture provides conflicting information to the classifier, probably over- or under-representing statistics for some classes, in particular when used jointly with only spectral features. Furthermore, the results suggest that the importance of the textural features has to be related to the intrinsic properties of the acquired image, such as spatial resolution and image noise. The texture features were more relevant for the RGB camera, suggesting a loss in the image quality of the infrared camera due to a wider point spread function of the infrared cameras. The observed increase of total disagreement for the RGB Leaf-Off dataset (+0.008) using texture features is linked to the conditions of the acquisition in which large shadows were present due to the sun's position in autumn, generating many more commission errors of vegetation and woody debris classes on gravels land cover.

2.5.2 Accuracy of the observed land cover dynamics

The classification accuracy has a direct effect on the change mapping accuracy but does not determine it in total. Very high classification accuracy might not be enough to study the dynamics of a system, given the stability of the overall land cover in a post-classification framework [87, 104]. Note that error-adjusted dynamics allow estimations of overall changes but cannot correct the classification maps.

In general, the high ratios in Table 2.3 show that many commission errors are occurring homogeneously across classes. The large differences between the direct

estimation of changes and the error-adjusted estimates signal that the whole processing chain is inadequate for studying the dynamics of every land cover type assessed in this study. The larger uncertainties are associated with smaller classes, mostly due to the influence of registration errors and classification errors around class boundaries, where a small change has a great impact on the observed dynamics. Land cover classes with a small total extent and related lower classification accuracy (e.g., woody debris) can contribute largely to the observed dynamics of the post-classification change maps. Change mapping errors due to image acquisition and preprocessing are well known, and their mitigation is still an open problem [105, 106].

The 'gravel - water' changes are well captured and exhibit a high accuracy. First, the raw values of dynamics extracted from the consecutive classification map were close to the error-adjusted values, with a ratio close to 1. Hence, the interface between water and gravel is a candidate for a robust quantification of the dynamics using raw classification. Second, this change exhibits one of the lowest coefficients of variation according to the error-adjusted uncertainty analysis. The performance based on the observed 'gravel - water' changes can be explained by a better 3D reconstruction and co-registration given the objects' simple geometry found close to a planar surface. The detection of these land cover classes was also weakly influenced by seasonality. Therefore, a metric based on the changes from gravel to water and from water to gravel is a candidate for robustly quantifying the dynamics of riverine land cover by remote sensing. Moreover, changes between water and gravel land covers are linked to important hydromorphological processes in river systems and important processes maintaining floodplain biodiversity. As a consequence, the deployed UAS shows potential for an accurate estimation of land cover influenced by erosion and deposition processes inside a semi-automated framework. Furthermore, the relatively good estimation of 'water - wood debris' changes encourages further study of the spatial dynamics of such land cover using remote sensing.

2.5.3 Relevant features for post-classification change mapping

As a supplement to the accuracy analysis, feature importance is analyzed to understand what are the factors conditioning the accuracy of specific classes in a given dataset.

The texture features are important to classify woody debris for all datasets including the NirRG, shown as well by the increase in the recall for all datasets. However, the total disagreement does not decrease by adding texture features, which is sign of potential uselessness. As discussed above, the parameterization of texture features extraction is critical, particularly for land cover like woody debris, which exhibits very complex shapes. However, when employing diverse features, the importance the texture is evident for the woody debris class. In particular for the SemiSup approach, textural descriptors are often coupled to a decrease in total disagreement

showing the necessity of these features. When compared to the STP approach, the SemiSup approach shows improved performance from its ability to integrate relevant information from texture and point cloud features.

Since we rely on a statistical method to assign labels with an independent fit on each dataset, we did not consider atmospheric correction as would be required by physical modeling methods to retrieve reflectance values for direct image comparison. The high importance of the blue band in almost all datasets and for most of the land cover classes makes it the most relevant acquired data. Its importance has been observed in studies on other environments such as rangelands or urban areas [107, 108]. It has also been reported as the most important information for classification of similar land cover types as in our study [109], e.g. forest, meadow, water and rock. The higher degree of light diffusion of the blue wavelengths can have a positive impact in shadowed parts, which may explain the high importance. Relying on a statistical method, we cannot further determine the physical reason of the importance of the blue band in the end. On the contrary, the green band is never important for any dataset apart from the NirRG in which the blue band is absent. The lower importance of the green band has been raised in other studies as well [110], possibly due to the redundancy of information with the blue bands. In our study, it is clear that the green band is not useful when the blue band is available. However, the green band affects the texture and point cloud feature generation. For each dataset, the infrared bands are always important when available. It is well known that the infrared bands are useful in wet or waterlogged environments [111]. However, in the case of the ReGB Snow dataset, the importance of the infrared band is weak. In this case, the point cloud and texture are the most important features, since spectral information is not a discriminant when snow cover is present.

Finally, the ReGB and the NirRG grant high importance to the blue and infrared features for mapping gravel and water land cover, while the RGB dataset gives more importance to point cloud and texture features. Given this observation and following the high accuracy of change mapping for the 'gravel - water' changes, the features used by the classifier should be adapted to the sensor used to target the changes between gravel and water land cover.

2.6 Conclusion

This study demonstrates the suitability of high-resolution imagery from UAS for riverine land cover change mapping in a post-classification setting. In our study, we built a set of ground truths based on the changes observed across several image acquisitions in order to capture the errors introduced by the different image processing steps at different levels and not only in terms of image classification. Several processing steps have been implemented to optimize the land cover classification, taking into account the specificities of the targeted riverine environment. The registration

of high-resolution images from different sensors under different environmental conditions (shadows, vegetation seasonality, snow, etc.) is achieved by using algorithms relying on the optimization of mutual information metrics, overcoming differences in feature representation. Despite the successful inter-modal registration, local misregistrations were still present, leading to over-estimation of land cover dynamics. The semi-supervised approach, built upon a spatial mixing of segments, patches and pixel-based inference, is well suited to the temporal monitoring of dynamic and heterogeneous riverine landscapes. Results indicate that land cover dynamics are best observed by detecting changes at the interface between gravel and water only. The semi-supervised approach generated error of 10% of observed changes along highly dynamic reaches. Overall, the best UAS set up to observe the land cover dynamics is built on spectral information based on blue and infrared bands with the support of texture and point cloud metrics under leaf-off conditions.

Nevertheless, the use of post-classification change mapping generally has limited accuracy for short time scales when riverscape-changing events (such as floods or fire) do not occur between image acquisition, since the errors of the classification map have a greater impact on the accuracy when fewer land areas change. In such a case, an error-adjustment procedure based on a reference set can help to extract a precise estimation of the dynamics. Given this fact, a possible metric of riverine dynamics should focus on land cover changes between gravel and water covered area, since they can be detected robustly under many different seasonal conditions and sensor characteristics. Furthermore, these changes are important to quantify erosion and deposition processes, which are in turn pivotal for many ecosystem processes as they serve as pioneer habitats. Finally, the results support the extension of land cover dynamics quantification by UAS campaigns to the study of hydromorphological processes in a post-classification setting.

Overall, this study highlights how remotely sensed data can support ground observations made at a local level when focusing on river systems. Based on this study, new observations of riverine dynamics can be derived in order to optimize data acquisition, data processing chain, and accuracy evaluations of UAS campaigns.

2.7 Acknowledgments

This research project was part of the National Research Programme "Energy Turnaround" (NRP 70) of the Swiss National Science Foundation (SNSF). Further information on the National Research Programme can be found at www.nrp70.ch.

2.8 Appendix

2.8.1 Classification

Feature Sets

Spectral (S) The spectral group was composed of locally sorted pixel values for each color channel. Specifically, the pixels of the orthoimage were ordered from the darkest to the brightest for each band in non-overlapping windows of 5 pixels size, generating a common feature in many computer vision processing chains [112]. This step ensured invariance to rotation because sorted values are no longer dependent on their relative spatial location. In short, considering a window size of 5 pixels with three bands at a resolution of 8 cm creates a stack of 75 pixels (corresponding to the dimensionality of the feature) covering an area on the ground of 40×40 cm. Each feature block originating from the same color channel was considered as a sub-group for the feature importance analysis. Hence, the importance of spectral channels across images can be compared.

Textural (T) The texture group was composed of two sub-groups, namely standard texture features and gray-level co-occurrence matrix (GLCM) metrics and standard texture features [113] such as entropy, local gradients, mean, median, and the 0.1 and 0.9 quantiles. The 'salt-and-pepper noise' of the entropy and gradient features was removed by applying median filtering in their spatial representation. The entropy and gradient features were calculated on a circular window of 6 pixels in diameter, while the median smoothing was calculated on a disk of 48 pixels in diameter. Median and quantiles were calculated by considering circular windows with a diameter of 16 pixels. The disk sizes were selected in a way that the features showed a visually consistent representation of the objects. The second sub-group included features based on the GLCM metrics [114], namely dissimilarity, correlation, homogeneity, energy, contrast and second angular moment.

Point cloud (P) The point cloud features group was composed of features calculated on the point clouds generated by the photogrammetric process of dense image matching. Note that this set of features was less commonly employed to perform analyses, with standard processing schemes often relying on the more common spectral and textural features [115]. The point clouds of the individual UAS datasets were registered horizontally (on the image plane) and vertically (based on reference elevation). The horizontal corrections of co-registration were directly extracted from the image registration phase. The vertical registration is carried out in two steps. First, the vertical shift with respect to an external DEM is calculated using the flattest areas of the point cloud in terms of local standard deviation and gradient. In such areas, the ground was expected to be flat; therefore, the correspondences to the external DEM were robust and the vertical shift can be removed globally. In a

second step, the external DEM was subtracted from the point cloud, generating a normalized point cloud, which contained only the aboveground elevation of the objects. Finally, features based on the point cloud were computed at a resolution of 1m. These features were minimum, maximum, mean, standard deviation, density and the volume of the 3D convex hull defined by the points inside each cell.

Classification approaches

The three feature groups were combined to create five different approaches to classification. The S, ST, SP and STP approaches were based on variations in the feature sets described above. GEOBIA procedures are not considered in these approaches to extract a consistent link between the feature sets selected and the classification accuracies. The last approach (SemiSup) involved an additional classification step and was built based on concepts from recent studies including GEOBIA and active learning [116, 117, 118, 100, 119]. However, our approach was specifically tailored to take into account the specificities of the riverine environment rather than to produce general land cover mapping.

The SemiSup approach was developed to make use of the patchy structure of the riverscape without degrading the classification in highly heterogeneous areas (Figure 2.6). The first step corresponded to a Simple Linear Iterative Clustering segmentation (SLIC) of the orthoimages [120] through the implementation of the Scikit-learn library [121]. SLIC produced segments with the purpose of simplifying a feature-based classification. Segments are spatial clusters represented by homogeneous properties defined by color or texture statistics. The orthoimages were resampled by a factor of 5 prior to segmentation to keep a reasonable computational load, but not lose important image details. SLIC depends on three hyperparameters, i.e., the number of segments, the compactness and a smoothing parameter sigma. The first parameter was set in a way that each segment consisted of a size of approximately 100m^2, that corresponded to segments of around 625 pixels, corresponding to the typical area of homogeneous land cover expected in the considered riverscape. The compactness and sigma parameters were empirically set to 10 and 1, respectively. Following the segmentation, we extracted non-overlapping patches, which are squared areas fully included within segment boundaries. Four different grids were used to extract patches. Each grid cell completely encapsulated within a segment defined a new patch. The grids were defined by a shift of half a grid cell in the X or Y direction with respect to the previous one, with the first grid set at an arbitrary origin. A set of rules was applied such that every new patch intersects neither a segment boundary nor a patch from a previous grid.

At this stage, an expert-labeling procedure is carried out to build the training set based on the patches. We employed a random forest classifier [98] due to its property

to ingest heterogeneous features without constraints. Other advantages of a random forest classifier include 1) the straightforward and interpretable parametrization which can effectively avoid an overfit if necessary (limitation of depth, non pure leaves, limitation of impurity to split, etc.), 2) the computational complexity, which is rather low compared to other classifiers, and 3) the ease to extract variable importance from the trees and its interpretability. In our python implementation, we used the scikit-learn package, offering different classifiers. Random forests are among the best performing classifiers in this setting. The number of trees was set to 100. On each tree, a leaf was defined as soon as it was pure. After the first classification, the expert performed several iterations to improve the classification, specifically by looking at misclassified areas (arrow loop in Figure 2.2). The classification training was consistently applied across the five tested approaches to provide baselines that are directly comparable (arrow C1 in Figure 2.6).

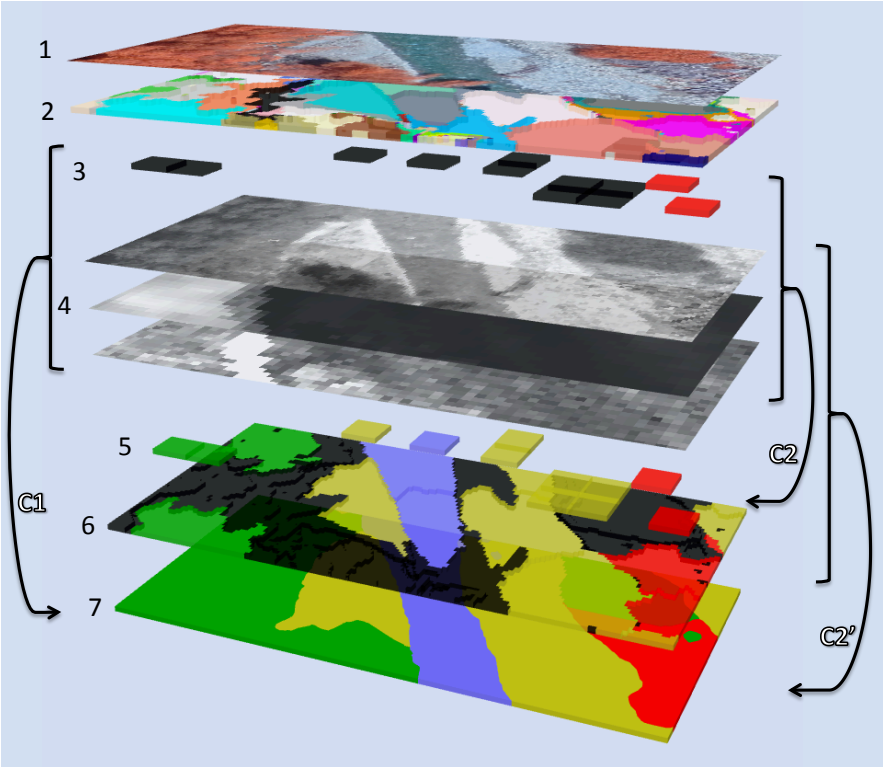

FIGURE 2.6: Stacked layers used in the processing chain. 1) orthoimage, 2) segmentation, 3) patches with an example of two labeled patch for training, 4) three examples of feature, 5) classified patches, 6) classified segments by overlapping patches, 7) final land cover map. The C1 arrow represents the S, ST, SP and STP approaches based on a direct-supervised classification. The C2 and C2' arrows represent the first and second classifier of the SemiSup approach. Some of the processing steps and intermediate products such as probabilistic classification and smoothing operations are not visible here.

The SemiSup approach implemented a transductive approach to increase the size of the training set. The classifier predicted the labels of the patches not annotated by the expert (arrow C2 in Figure 2.6). Then, patches classified with high confidence

were retained. We modeled such confidence as being the difference between the first and second most probable classes. A threshold value of 0.3 was set as a confidence measure. All the patches showing equal or higher confidence values were retained. As such, the layer of classified patches contained only patches in homogeneous areas classified with high confidence. The classified patches of high confidence were subsequently used in two ways. First, the classification probability and the corresponding label of the patch were propagated to the segment in which it was contained. Through this operation, the segments were classified without taking into account the information present close to the edges of the segment (the edge of the patch was in general not close to the edge of the segment), being often misleading due to extreme values and object border effects. Second, an additional classifier was trained on the pixels found inside the high confidence patches to classify remaining areas at the pixel level (arrow C2' in Figure 2.6). For this step, we again employed a random forest classifier with the same parameter settings as in the previous classification. Since the probabilities of the patches were transferred to the corresponding segments, only remaining segments needed to be classified (black patches in layer 6 in Figure 2.6). These segments were expected to be highly heterogeneous since they were either too small to contain a patch or their confidence value was too low in the first classification. The second classifier was based on the same sets of features, however, excluding the edge-dependent features (i.e., entropy and gradient for texture; standard deviation, the volume of convex hull and point density for point clouds), which exhibited extremely high or low values along the edges of objects. The second classifier implicitly includes a multi-scale component of GEOBIA by considering an extreme pixel-based scale.

Finally, the pixel-based and segment-based class probabilities were merged. In order to enforce spatial smoothness in the output domain, we applied a two-step filtering on the classification map. This filtering step was applied to all the tested approaches. Both steps were based on a circular window with a diameter of 6 pixels. Both filters contained weights sampled from a bivariate Gaussian distribution with 1-pixel standard deviation. For each class, the filter returned a posterior probability map based on a weighted sum. Hence, the probability of a given pixel belonging to a given class depended on its neighbor's classification output values as well After filtering, we performed maximum *a posteriori* inference by assigning the most probable class to the pixel. The second filter implemented a weighted max-voter filter on the labels to remove remaining salt-and-pepper noise. The classification maps were eventually vectorized and generalized with the Chaiken algorithm [122] using the implementation of the GRASS software [123].

2.8.2 Accuracies

TABLE B.1: Mean and median errors of misregistration on six pairs of images. The values are calculated using ten ground control points on every image spread over the entire image. The highest values are observed for the residual reach, where the terrain is the most variable.

Reach	Dataset 1	Dataset 2	Average [m]	Median [m]
Natural	RGB Leaf-On	NirRG Leaf-On	0.43	0.39
Natural	ReGB Snow	ReGB Leaf-On	1.03	1.04
Hydropeaking	RGB Leaf-Off	ReGB Leaf-Off	0.38	0.36
Hydropeaking	NirRG Leaf-On	RGB Leaf-Off	0.70	0.60
Residual	RGB Leaf-On	NirRG Leaf-On	2.42	2.65
Residual	ReGB Leaf-Off	ReGB Leaf-On	0.81	1.09

TABLE B.2: Total area for the reference dataset manually delineated for each class for each dataset. The ReGB Leaf-Off dataset contains a smaller area of woody debris, since it was acquired on the Sarine only. The ReGB Snow dataset contains a larger area of gravel (proportion: 0.31), since it was acquired on the Sense only. The total of each row corresponds to the Reference area entry in Table 2.1.

[square meters]	water	vegetation	gravel	woody debris	total
RGB Leaf-On	107'733	475'064	119'823	8'643	711'264
RGB Leaf-Off	164'116	778'268	171'632	10'824	1'124'840
ReGB Leaf-On	173'364	739'996	71'418	9'420	994'197
ReGB Leaf-Off	49'671	228'858	5'287	48	283'864
ReGB Snow	8'062	102'063	48'736	3'346	162'206
NirRG Leaf-On	164'116	689'852	107'717	10'631	972'316
total	667'063	3'014'100	524'612	42'912	
[proportion]					
RGB Leaf-On	0.15	0.67	0.17	0.01	
RGB Leaf-Off	0.15	0.69	0.15	0.01	
ReGB Leaf-On	0.17	0.74	0.07	0.01	
ReGB Leaf-Off	0.17	0.81	0.02	0.00	
ReGB Snow	0.05	0.64	0.31	0.02	
NirRG Leaf-On	0.17	0.71	0.11	0.01	
overall proportion	0.16	0.71	0.12	0.01	

TABLE B.3: Producer Accuracy

Dataset	Approach	Water	Vegetation	Gravel	Woody Debris
RGB Leaf-On	S	0.795	0.982	0.951	0.672
RGB Leaf-On	ST	0.816	0.975	0.946	0.798
RGB Leaf-On	SP	0.828	0.972	0.933	0.768
RGB Leaf-On	STP	0.834	0.974	0.951	0.807
RGB Leaf-On	SemiSup	0.881	0.984	0.956	0.754
RGB Leaf-Off	S	0.799	0.968	0.924	0.536
RGB Leaf-Off	ST	0.800	0.962	0.889	0.803
RGB Leaf-Off	SP	0.861	0.980	0.934	0.672
RGB Leaf-Off	STP	0.863	0.976	0.907	0.817
RGB Leaf-Off	SemiSup	0.897	0.974	0.934	0.823
ReGB Leaf-On	S	0.863	0.971	0.901	0.675
ReGB Leaf-On	ST	0.864	0.970	0.886	0.739
ReGB Leaf-On	SP	0.862	0.971	0.895	0.704
ReGB Leaf-On	STP	0.864	0.970	0.888	0.756
ReGB Leaf-On	SemiSup	0.864	0.971	0.909	0.781
ReGB Leaf-Off	S	0.944	0.950	0.878	
ReGB Leaf-Off	ST	0.942	0.950	0.887	
ReGB Leaf-Off	SP	0.949	0.961	0.893	
ReGB Leaf-Off	STP	0.951	0.968	0.899	
ReGB Leaf-Off	SemiSup	0.976	0.971	0.885	
ReGB Snow	S	0.827	0.987	0.831	0.512
ReGB Snow	ST	0.781	0.940	0.804	0.718
ReGB Snow	SP	0.782	0.981	0.820	0.774
ReGB Snow	STP	0.801	0.970	0.835	0.799
ReGB Snow	SemiSup	0.861	0.968	0.881	0.830
NirRG Leaf-On	S	0.827	0.980	0.899	0.824
NirRG Leaf-On	ST	0.836	0.981	0.903	0.838
NirRG Leaf-On	SP	0.848	0.986	0.904	0.815
NirRG Leaf-On	STP	0.858	0.986	0.906	0.852
NirRG Leaf-On	SemiSup	0.887	0.988	0.930	0.885

TABLE B.4: User Accuracy

Dataset	Approach	Water	Vegetation	Gravel	Woody Debris
RGB Leaf-On	S	0.889	0.961	0.938	0.609
RGB Leaf-On	ST	0.891	0.969	0.930	0.483
RGB Leaf-On	SP	0.866	0.970	0.924	0.568
RGB Leaf-On	STP	0.893	0.972	0.923	0.559
RGB Leaf-On	SemiSup	0.895	0.978	0.959	0.828
RGB Leaf-Off	S	0.908	0.962	0.919	0.242
RGB Leaf-Off	ST	0.880	0.963	0.926	0.255
RGB Leaf-Off	SP	0.917	0.973	0.938	0.470
RGB Leaf-Off	STP	0.903	0.974	0.939	0.396
RGB Leaf-Off	SemiSup	0.892	0.981	0.945	0.486
ReGB Leaf-On	S	0.877	0.969	0.903	0.578
ReGB Leaf-On	ST	0.873	0.970	0.913	0.509
ReGB Leaf-On	SP	0.880	0.969	0.905	0.533
ReGB Leaf-On	STP	0.877	0.970	0.913	0.512
ReGB Leaf-On	SemiSup	0.879	0.970	0.946	0.506
ReGB Leaf-Off	S	0.843	0.988	0.558	
ReGB Leaf-Off	ST	0.848	0.989	0.533	
ReGB Leaf-Off	SP	0.882	0.988	0.616	
ReGB Leaf-Off	STP	0.912	0.990	0.576	
ReGB Leaf-Off	SemiSup	0.919	0.993	0.656	
ReGB Snow	S	0.839	0.978	0.966	0.146
ReGB Snow	ST	0.567	0.973	0.968	0.156
ReGB Snow	SP	0.901	0.964	0.963	0.211
ReGB Snow	STP	0.799	0.979	0.965	0.201
ReGB Snow	SemiSup	0.812	0.988	0.970	0.246
NirRG Leaf-On	S	0.891	0.968	0.956	0.473
NirRG Leaf-On	ST	0.900	0.970	0.961	0.461
NirRG Leaf-On	SP	0.913	0.972	0.955	0.519
NirRG Leaf-On	STP	0.924	0.974	0.961	0.486
NirRG Leaf-On	SemiSup	0.945	0.979	0.966	0.553

Chapter 3

Remotely Sensing Variation in Ecological Strategies and Plant Traits of Willows in Perialpine Floodplains

Milani, G., Kneubühler, M., Tonolla, D., Doering, M.,
Wiesenberg, G. L. B., & Schaepman, M. E.

This chapter is based on the peer-reviewed article:
Journal of geophysical research: biogeosciences, 2019, 124(7), 2090-2106
DOI: doi.org/10.1029/2018JG004969
and has been modified to list all cited references in the Bibliography Chapter.
The layout has been adapted to uniform the current thesis.

G. Milani, M. Kneubühler and M. E. Schaepman conceptualized the study. G. Milani, M. Kneubühler, D. Tonolla, M. Doering and G. L. B. Wiesenberg elaborated the methodology. G. Milani, M. Kneubühler, D. Tonolla, M. Doering and G. L. B. Wiesenberg performed the investigation. G. Milani, M. Kneubühler, D. Tonolla, M. Doering, M. E. Schaepman performed the formal analysis. G. Milani wrote the first draft of the manuscript. G. Milani, M. Kneubühler, D. Tonolla, M. Doering and M. E. Schaepman participated in the writing and editing of the final manuscript.

3.1 Abstract

Natural floodplains are characterized by a complex habitat mosaic. However, damming, water storage and hydropower production affect many floodplains by altering their natural habitat diversity. Field sampling data and imaging spectroscopy are used in combination with statistical models to assess resource allocation strategies of willow stands in perialpine floodplains. Three contrasting floodplain reaches located along two rivers in Switzerland serve as testbeds: the Sarine River is partitioned into an upstream and downstream segment under the influence of a dam and a hydropower plant, while the Sense River represents an undisturbed, natural floodplain. Airborne imaging spectrometer data allows mapping of spatially distributed Competitor / Stress tolerator / Ruderal (CSR) strategies using a partial least square modelling approach. Using cross-validation, we demonstrate that a statistical modelling approach can reveal variations in CSR scores based on the StrateFy model. Such intra-specific variation of CSR scores cannot be captured by a strategy categorization based solely on the species. Results reveal that willows shifted towards more competition and less stress-tolerance along hydrologically altered reaches compared to the willows' strategy along the natural control. Moreover, the overall distribution of strategies indicates that stress factors (i.e., limiting growth factors), rather than disturbance (i.e., events leading to partial or total destruction), shape the plant traits of alluvial willow trees. Detailed assessments of resource allocation strategies contribute to a more complete understanding of the continuous and reciprocal shaping between flow regimes, landforms and alluvial vegetation.

3.2 Introduction

Natural floodplains comprise diverse, dynamic and complex ecological habitats found in the transition zones between aquatic and terrestrial realms. The habitat mosaic is shaped by the flow regime, and its variations impact the alluvial zones through direct impacts such as flood events, seed dispersal, water table variations or sediment accretion. The interactions between flow regime and vegetation also have an important influence on the river system [124, 125] and can be conceptually described using the concept of plant traits [126, 125]. In general, the concept of plant traits enables the description of complex physiological patterns using simple observables [34, 127]. More specifically, plant traits have been considered in the context of floodplain as descriptors of response to disturbance [128, 129].

Classifications of plant variables have been developed to capture sensible phenotypes that often occur jointly. Models of plants' main resource allocation strategies, or economic strategies, simplify the description of plant interactions with the energy and matter cycles [130, 131]. In other words, the economic strategies of plants can provide comprehensive groups of plant trait expressions summarizing the interactions with their environments. Although the understanding of plant resource

allocation strategies is not complete, today it is accepted that grouping plant trait expressions into strategies is sensible and supports a comprehensive understanding of environmental processes [132, 133].

3.2.1 CSR Strategies

A scheme of plant strategies allows the description of multiple differences between plants using few variables. Such a scheme, the CSR theory [134], expresses the positioning of an individual among three constrained axes: competitor (C), stress tolerator (S) and ruderal (R). More recent developments of the CSR theory have introduced the twin filter model in concordance to the original model [135]. Initially developed in a theoretical frame and applied to grasslands [136], the CSR theory has recently been generalized to a universal description of resource allocation strategy for vascular plants [137]. Most recent developments by Pierce et al. (2017) [35] include the quantification of strategies based on leaf traits only. This model allows deriving the CSR scores for every individual independently. It is therefore possible to quantify an alteration of the strategy among similar individuals that would present morphological differences due to environmental variations. Moreover, a model based on leaf traits allows the strategy to be estimated at the individual level and can be upscaled to the floodplain level.

3.2.2 Remote sensing of ecological strategies

To date, few attempts have been mad e to derive CSR strategies from remotely sensed data. Radiative transfer models have been used to retrieve CSR strategies by inverse modeling [138]. Statistical models, such as the partial least square regression, have been used to link plant strategies with measured spectra from airborne imagers [139, 140]. However, all reviewed methods used a description of CSR strategies based on a weighted average of species scores depending on the relative abundance of each species inside the plots. By allocating a single CSR score to every species, these methods cannot reveal morphological adaptation among similar individuals exposed to different environmental conditions. In other words, a CSR score based solely on the species cannot reveal any plasticity of traits. By using leaf traits to derive CSR scores, we are able to observe shifts triggered by environmental stress or disturbance at a local scale. In brief, mapping of CSR scores sensible to plasticity of traits enables the observation of spatial patterns.

3.2.3 Application to alluvial vegetation

Variations of plant strategies among similar communities can be linked to variations in environmental conditions. Plant strategy, or more generally plant physiomorphology, can be altered by changes in the flow regime of a river [12, 141, 142]. For example, a change of flooding characteristics can be responsible for variability in

litter production and can modify the accessibility of nutrients to plants [143]. In general, the main interactions between alluvial vegetation and river morphodynamics have been described and modeled [144, 145]. Recent studies have given prominence to the concept of economic strategies for describing these interactions [146, 147, 148]. In this context, a spatial observation of CSR scores can be used to complement the description of the river system's dynamic response.

The aim of the current study was to characterize the impacts of hydrological control on alluvial willow trees and to observe relative patterns in their spatial distribution by retrieving an indicator of resource allocation strategies of plants based on airborne imaging spectroscopy. We used the recent model of CSR scores based solely on leaf traits [35] to derive a statistical model from spectroscopy data. This new approach allowed us to observe variations of strategies among willow stands located in the floodplains. The observation of CSR scores was completed by an analysis of pigment ratios to gain insight into the fluvial processes altering the plants, particularly related to drought events. Differences in CSR scores patterns could ultimately inform about interactions between vegetation and flow regime. We note that the impact of flow-regime changes on vegetation can be indirectly caused by unmonitored processes of the aboveground or underground ecosystems. Therefore, we do not intend here to prove causality links between the complex processes of the river system. Rather, we provide a new methodology of observation and try to interpret the possible shaping of vegetation states within the limited knowledge gathered on the considered complex floodplains.

3.3 Material and Methods

3.3.1 Study site

The study area consists of three hydrologically different floodplain-reaches of two perialpine rivers located in Switzerland: two reaches are located along the Sarine (46°45'N 7°7'W) and one along the Sense (46°44'N 7°18'W) (Figure 3.1 and SI Figure S2). Both rivers are located in the region of Fribourg, in western Switzerland, and share similar climatic conditions: a warm temperate climate prevails in the region, with regular rainfall throughout the year. The weather stations of Fribourg and Plaffeien, respectively, are located next to the Sarine and the Sense reaches at an elevation of 646m and 1042m. They recorded annual averages of temperature of 8.7°C and 6.9°C, precipitations of 1075mm and 1253mm, and water vapor pressure of 9.5hPa and 8.2hPa during the years 1981-2010 according to MeteoSwiss [149]. For this study, we assume that the willow stands found along the various reaches would exhibit similar plant parameters if no water flow alteration would be in place.

All leaf sampling sites located along the three reaches can be found within a 10km radius (SI Figure S1). Hydropower installations have a significant impact on the Sarine flow regime. The Sense River near Plaffeien, however, is one of the last

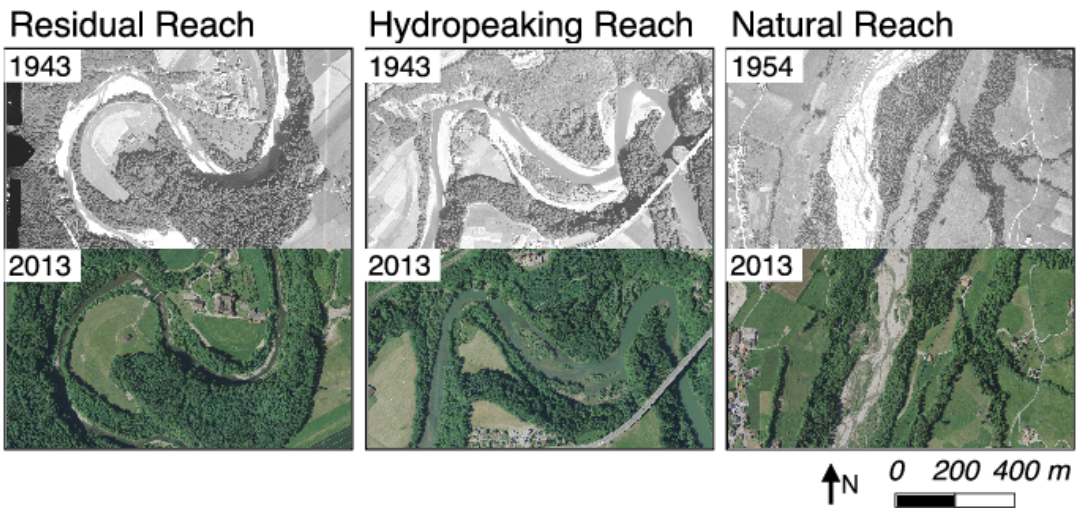

FIGURE 3.1: Aerial images recorded before and after the construction of the hydroelectric complex formed by the Rossens Dam and the Hauterive hydroelectric plant in 1945. The image excerpts are located, from left to right, close to the Hauterive Abbey (residual), the Pérroles bridge (hydropeaking) and the village of Plaffeien (natural). A large riparian zone subsists only to a broad extent along the natural reach. Almost all bars along the residual and the hydropeaking reach are covered by mature vegetation, mainly hardwood vegetation. Image Source : Swissimage Geodata © swisstopo.

rivers in Switzerland to have a near natural flow regime. The selected reaches represent three different flow dynamics, namely, i) a residual reach (constant low flow), and ii) a hydropeaking reach (unnatural, hourly and daily flow changes) along the Sarine, as well as iii) a natural reach along the Sense (irregular natural flow changes). The regular and frequent changes observed in the hydropeaking reach are due to the operation of a hydropower plant upstream of the reach.

The natural reach exhibits a considerable portion of transitional ecosystems between aquatic and terrestrial environments, such as low stands of willow bushes or pioneer vegetation on gravel bars, which is not the case along the altered reaches (unvegetated gravel bars and islands in Figure 3.1). The stabilization of the riverbanks along the altered reaches followed the construction of the dam in 1945. Willow trees were selected for this study, found in large patches of bushy wood along the three reaches. *Salicaceae*, composed of willows and poplars, form the most represented family in the active floodplains of the northern temperate zone [150]. In addition, a strong dependence between the characteristics of alluvial willows and the environmental gradient from the aquatic to the terrestrial ecosystem has been observed [151, 152]. The willow stands form homogeneous areas along each reach, allowing the remote sensing system to capture spectrally pure data by reducing disturbances due to adjacency effects [153, 154]. Compared to sparsely vegetated gravel bar, willow stands have a canopy with a relatively high fractional cover, even if variations exist between and within stands. We also restricted the considered willow trees to those detected inside the floodplain areas.

3.3.2 Airborne remote sensing data

Imaging spectroscopy data were acquired by the APEX imaging spectrometer [155] during four campaigns in 2015 and 2016 for all three reaches. APEX has been operating since 2011 and produces datasets composed of 316 spectral bands ranging from 380-2500nm. The data were acquired on June 24th and August 21th, 2015 and on July 7th and September 7th, 2016 at a ground resolution of 2m.

The spectra-radiometric calibration of the APEX instrument was carried out using the APEX Calibration Information System [156]), within which radiometric gains and offsets are recalculated for every spatio-spectral pixel. The acquired APEX data were processed to radiances and calibrated in the APEX Processing and Archiving Facility [157]. The ATCOR software was used to convert radiance data to reflectance factor [158]. The geo-referencing of reflectance data (L2 products) was based on the PARGE software [159]) and utilizes the swisstopo swissALTI3D digital elevation model. The signal-to-noise ratio of the radiance measurements is on average higher than 625 [155]. Similar datasets acquired by the APEX instrument have been used to study various aspects of the vegetation [160, 161, 162].

Three datasets were acquired to cover the reaches of interest (SI Figure S1). A first flight line covered the upper part of the residual reach. A second flight line covered the hydropeaking reach and the lower part of the residual reach. The considered portion of the residual and the hydropeaking reaches were, respectively, 10km and 5km in length. A third flight line covered the natural reach, representing 5km of river length. The three flight lines were acquired on each of the four acquisition dates. Only the two acquisitions from 2016 were used to map plant parameters, while all four acquisitions were used together to detect willow trees. In summary, six groups of parameter maps were produced: residual, hydropeaking and natural reaches in July 2016 and residual, hydropeaking and natural reaches in September 2016.

3.3.3 Laboratory data

Simultaneously to the two image acquisition campaigns of 2016, we sampled five willow individuals at ten different sites along each of the two rivers, resulting in a sample set of 100 individuals (SI Table S1). Each individual was subject to repeated measurements (four in the case of leaf area, leaf dry and fresh matter measurements, and two in the case of pigments). We sampled fully expanded leaves exposed to direct sunlight from the top of the canopy whenever possible. When the tree was too high along the Sarine, we sampled the highest possible leaves found under direct sunlight for most of the day. The samples mainly comprise the species *Salix elaeagnos*, *S. viminalis* and *S. alba* in varying proportions among the sites. For each individual, we sampled leaves and leaf rings according to recommendations by Cornelissen et al. (2003) [163], with adaptations due to the limited equipment available on-site, since the topography made it too difficult to transport heavy equipment over

the floodplains. Consequently, the leaves were directly frozen in dry ice at the collection site due to the unavailability of a fridge. The applied nomenclature used to group the plant parameters is given in Figure 3.2. The sampled individuals were geolocated using hand-held GPS devices and high-resolution imagery acquired by drone to manually set the exact locations. Since the accuracy of the hand-held GPS was not sufficient to fit the apex data (error of $\pm$ 10 m), we took at least four pictures of every sampled individual. To geolocate the individuals sampled, we used as support ortho-images at a 4cm resolution acquired using a Ebee drone from Sensefly equipped with an infrared-modified camera Canon IXUS 125HS [90] and notes taken on-site. More information on similar drone data and there use on the considered floodplains can be found in Milani et al. (2018) [36].

A leaf rehydration procedure preceded the weighing and measurement of the leaf surface. From the three initial leaf traits, namely, leaf area, leaf dry weight and leaf hydrated weight, we calculated the CSR scores based on the tool StrateFy [35]. The StrateFy model allows a calculation of the continuous values for the CSR scores. Since this model approximates CSR strategies such as defined by Grime (1974) [134], but might possibly differ in some aspects, we refer to them as "CSR scores" instead of using the term "CSR strategies". The CSR scores mapped in this study are therefore explicitly considered as strategy values provided by the StrateFy model, rather than representing the categorical strategies defined by the model of Grime (1974) [134]. In the StrateFy model, the specific leaf area (SLA) and the leaf dry matter content (LDMC) are derived from the base leaf traits. The CSR-score calculation is then based on a calibrated regression of the three traits: SLA, LDMC and leaf area itself (Figure 3.2). SLA and LDMC were stored and further used in our subsequent analysis, along with the base leaf traits, since they support the interpretation of the link between leaf traits and CSR score. All leaf traits measurements were based on four leaves per individual and averaged to produce one sample (per quantity) per individual.

Pigments were extracted from frozen leaf discs using a high-performance liquid chromatography (HPLC) system. A sequence of pigment extraction was carried out using the following solvents: Acetone, Acetone:Deionized Water, and Isopropanol:Hexane solutions. We then concentrated them using a centrifugal vacuum concentrator after freezing the solution in liquid nitrogen. A reference standard was measured before every batch of measurements with the HPLC to check the stability of the measures. The following pigments were investigated: chlorophyll A, chlorophyll B, xanthophylls and carotenes. We performed a qualitative analysis based on pigment ratios by normalizing the detected peak areas with respect to chlorophyll A value directly without conversion to content or concentration.

We worked with pigment ratios rather than pigment content or concentration due to limited resources available for extracting calibrated concentration or content measurements. The main motivation of considering ratios instead of an absolute quantity is therefore purely logistic. Also, the use of ratios suppresses some error

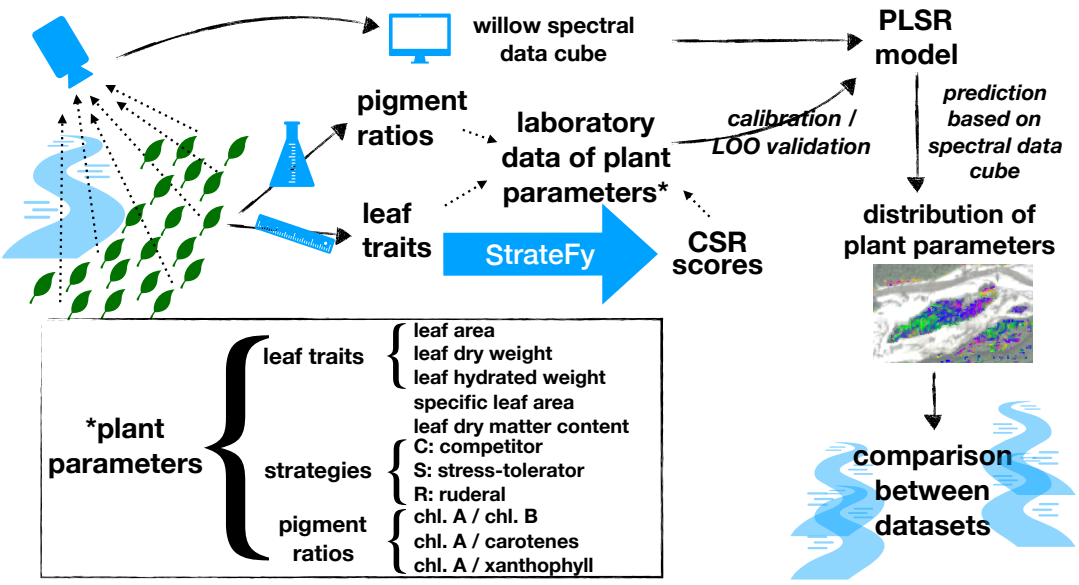

FIGURE 3.2: Data processing scheme from the leaf sampling and image acquisition to the production of plant parameter maps. The laboratory data are used to fit the PLS regression and to assess the prediction accuracy. The plant parameter maps support the statistical analysis of the differences between reaches. PLSR: Partial least square regression, LOO: leave-one-out validation.

sources such as variation in leaf discs or a possible degradation of pigments as long as it stays constant among the samples. Information regarding environmental stress is extractable from pigment ratios [164]. We refer here specifically to water stress, since variation in water availability stands as one of the major processes influencing floodplain vegetation [144, 165]. Water stress leads to water deficit in the photosynthetic process, which triggers changes in the cell physiology to handle light excess. Increase of chlorophyll A - chlorophyll B ratio has been observed under water stress [166, 167]. Decrease of chlorophyll - carotenoids ratio has been observed under water stress [168, 169], also specifically for the chlorophyll - xanthophylls ratio [164]. Recent studies in remote sensing have made use of pigment ratios [170, 171]. However, remotely sensing pigment information from imaging spectroscopy data is still challenging [172].

We replicated each pigment extraction using other leaf discs of the same individual. We averaged the pigment ratios of both extractions for further analysis. The accuracy of the replicated pigment extraction indicated that inter-sample variability was often close to the overall variation in the retrieved pigment ratio. Observations based on pigment ratios have to be read by keeping in mind the possible inaccuracy of the measurement (SI Figure S7). While the replicability of pigment ratios measurements failed in some cases, consistent patterns can be observed among the sampling sites (SI Figure S8). The pigment ratios were further used to gain more information on the comparison of CSR score between the reaches. In particular, we underline that pigment ratios are not used to predict CSR scores.

3.3.4 Regression of laboratory data on airborne imagery

In general, CSR scores can be retrieved by remote sensing if the physiological properties influence the light propagation strongly enough to be captured by the imaging system. However, a statistical model directly includes the influences of external variables, unlike a physical model [173, 174]. For example, a positioning of a plant individual towards a high S-score can be linked to soil properties such as low organic carbon content. The low-organic carbon soil would strongly influence the reflection of light in the case of a low-density canopy and could then allow an indirect estimation of the high S-score. By the definition of strategies, the measured traits are representative of a whole set of plant traits and linked to environmental properties. Therefore, it is reasonable to expect a statistical relationship between imaging spectroscopy data and CSR scores. Based on the assumption of such a statistical relationship, we built a statistical model to predict CSR scores and plant traits from imaging spectroscopy data.

We used a partial least square (PLS) regression to link imaging spectroscopy information to laboratory data (Figure 3.2) on a single pixel basis. Two independent PLS regressions were realized using the respective samples and imagery acquired in July and in September, leading to a 'July distribution' and a 'September distribution' of plant parameters. PLS regression is widely used in the field of imaging spectroscopy data analysis [175, 176, 177], notably because of its capability to deal with high-dimensionality input data. Prior to the regression analysis, the imaging spectroscopy data were transformed using the continuum removal method [178]. The continuum removal method is a standard method used in spectroscopy to emphasize absorption features and reduce potential data biases for example due to change in scene illumination. The laboratory data were normalized using a cox-box transformation and subsequently scaled to the interval [-1, 1] based on the minimum and maximum values prior to the regression analysis. Spectroscopic measurements were regressed on eleven plant parameters: the three CSR scores, the three leaf traits (leaf area, leaf dry weight, leaf hydrated weight), SLA, LDMC, and the three pigment ratios. We used the PLS regression implementation of the python library scikit-learn [179]. The number of latent components to retain in the PLS regression was set to 9, following an optimization based on the coefficient of determination of the fitted data (SI Figure S4), specifically called R^2_{cv}, Q^2 or Q^2_{cv}. To test the goodness of fit and the robustness of our algorithm, we followed a leave-one-out procedure for each sample. As a result, the final coefficient of determination of the PLS regression was based solely on models that exclude validation samples.

The regression analysis allowed us to predict the plant parameters of willow trees based on imaging spectroscopy data. The detection of willow trees followed a semi-automatized procedure based on a random forest classifier from the scikit-learn library [179] using the four available image acquisitions in a multi-temporal setting. To form the training set, we selected areas in which the presence of willows

was known based on a field investigation and on the basis of high-resolution images acquired with the drone. Pictures taken from the field were analysis to check the presence or absence of willow stands. We selected 318 points flagged as non-willow and 149 points flagged as willow to form the training set. We divided the training set into two subsets (75% training, 25% validation) to calculate the classification accuracy. In addition, a further validation area along the second flight line was used to check the consistency of the willow detection based on visual interpretation (SI Figure S1). Finally, the plant parameters were predicted based on imaging spectroscopy over each pixel detected as willow in the alluvial areas. The acquired drone ortho-images, the 3D model reconstructed during the processing of drone-acquired images to ortho-images, and the ground pictures taken during the field sampling helped to interpret the resulting maps.

3.3.5 Statistical comparison of means

T-tests were applied to assess inter-reach differences between the distributions of each of the eleven plant parameters. We also assess in a same manner the inter-date differences between in July and September 2016. The null hypothesis states here that the average of each plant parameter is similar between the reaches or between the season. Since geographic data, and more specifically remotely sensed data, contain a high degree of spatial autocorrelation, we corrected the statistical test based on the effective sample size calculated using a semi-variogram method [180]. The use of a semi-variogram model for estimating the effective sample size [180] prevents the application of complex methods to account for autocorrelation [181]. The degree of freedom dropped by a factor ranging from 12 to 60 depending on the parameter and the site considered. The main consequence was a reduced probability of type I error.

3.4 Results

3.4.1 Statistical modeling based on imaging spectroscopy

We found a moderate prediction power of the PLS regression based on imaging spectroscopy data to predict ten of the eleven considered parameters, as shown by the R^2 coefficient of determination based on the leave-one-out validation (Figure 3.3). A weak prediction power ($R^2 = 0.082$) was found for the chlorophyll A — chlorophyll B ratio. Overall, the predicted values are centered at the average of the sampled values and less dispersed than the sampled values. This is an indication of robustness against over-fitting for the PLS regression (Figure 3.3). The CSR scores were overall predicted with a higher R^2 than the leaf traits and LDMC, but with a lower R^2 than SLA. The C-score had an R^2 close to the one of leaf area, with which it is strongly correlated in the StrateFy model. The pigment ratios generally exhibited lower R^2 values.

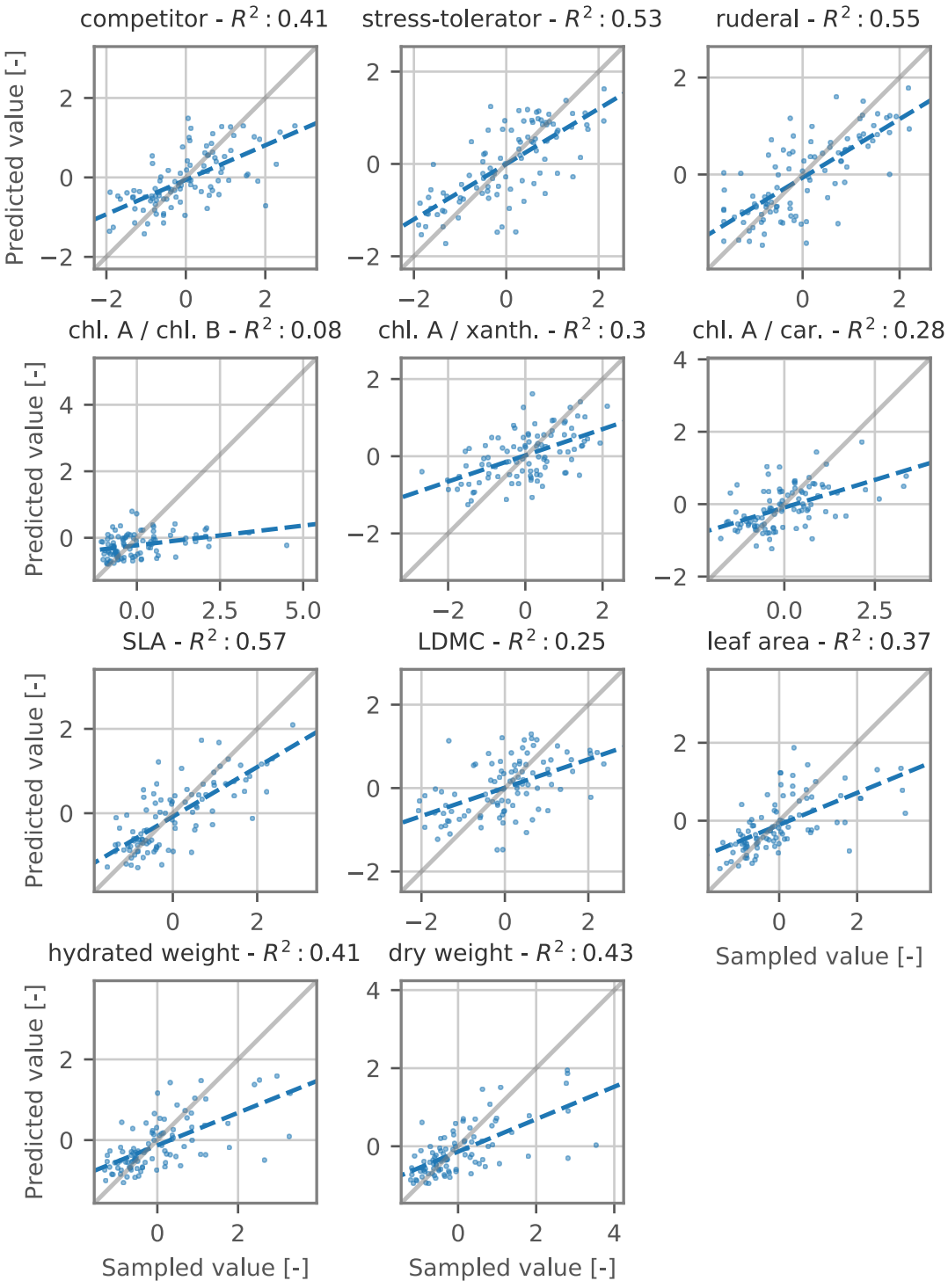

FIGURE 3.3: Scatter plot of sampled values versus predicted values from the leave-one-out validation of the PLS regression. The sampled and predicted values are here normalized based on the mean and variance of the sample set for better visualization. The coefficient of determination (R^2) is based on the PLS regression. The statistics of the regression line can be found in SI Table S2.

3.4.2 Prediction of plant parameters by imaging spectroscopy

The willow detection reached an overall accuracy of 95%. Within the additional validation area, the willow detection presented a consistent pattern corresponding to the field investigation. We considered the accuracy level of the willow mask good enough to be used for further analysis without modification. The prediction of CSR scores of the detected willows presents certain patterns at local scale (Figure 3.4). Coupled with the field observations, the patterns observed in our maps reveal some similarities among the sites. In general, tall willows at the front of islands tended towards a high C-score (yellow and red patches in excerpts d, e, h & g) while smaller trees, sometimes with lower fractional cover as observed on the field, tended to have a higher S-score (light green patches in excerpts b, d, f, g & h). Along the altered reaches, more individuals with high S-score were found on islands and sediment banks not regularly flooded (b, c & f). Specifically along the hydropeaking reach, taller individuals found on islands tended towards higher C- and R-score (d & e). Along the natural reach, more heterogeneous patterns were present on islands and in the alluvial forest (g, h & i). Individuals with a high C-score were found on islandheads and on first terraces, while more individuals with high S-score were found in the center of islands where the soil is less developed and the bushes are sparse.

The predicted plant parameters were aggregated for each reach and season to get the empirical density function (SI Figure S6). For each distribution, we calculated the mean and the variance to statistically analyze the differences between reaches and between seasons. For each difference, we extracted the direction of the change (i.e., which reach or which season had a higher value) and the statistical significance of the change (Table B.1). The plant parameters based on imaging spectroscopy data showed, as expected, a higher number of significant differences than the differences based on laboratory data only (Lab vs Im).

All the significant differences of functional parameters averages observed using imagery were in agreement with differences observed using laboratory data only, i.e., significant differences observed by imagery corresponded in direction to (weakly) significant differences observed in laboratory data. For example, the average C-score was higher along the residual and hydropeaking than along the natural reach, as shown by a weak difference using laboratory data for the residual reach — natural reach comparison and for the hydropeaking reach — natural reach comparison. The same findings were confirmed by the significant differences in the averages of plant parameters retrieved from imaging spectroscopy data. Moreover, the laboratory data distribution corresponded to the range of values spanned by the predicted distribution (SI Figure S6). As such, laboratory data suggested a reliable prediction of the considered plant parameters by imaging spectroscopy. A deviation from the predicted distribution could be observed in some cases, for example in the prediction of chlA — chlB for the natural reach in September.

The predictive power of the statistical model was weak for pigment ratios, and

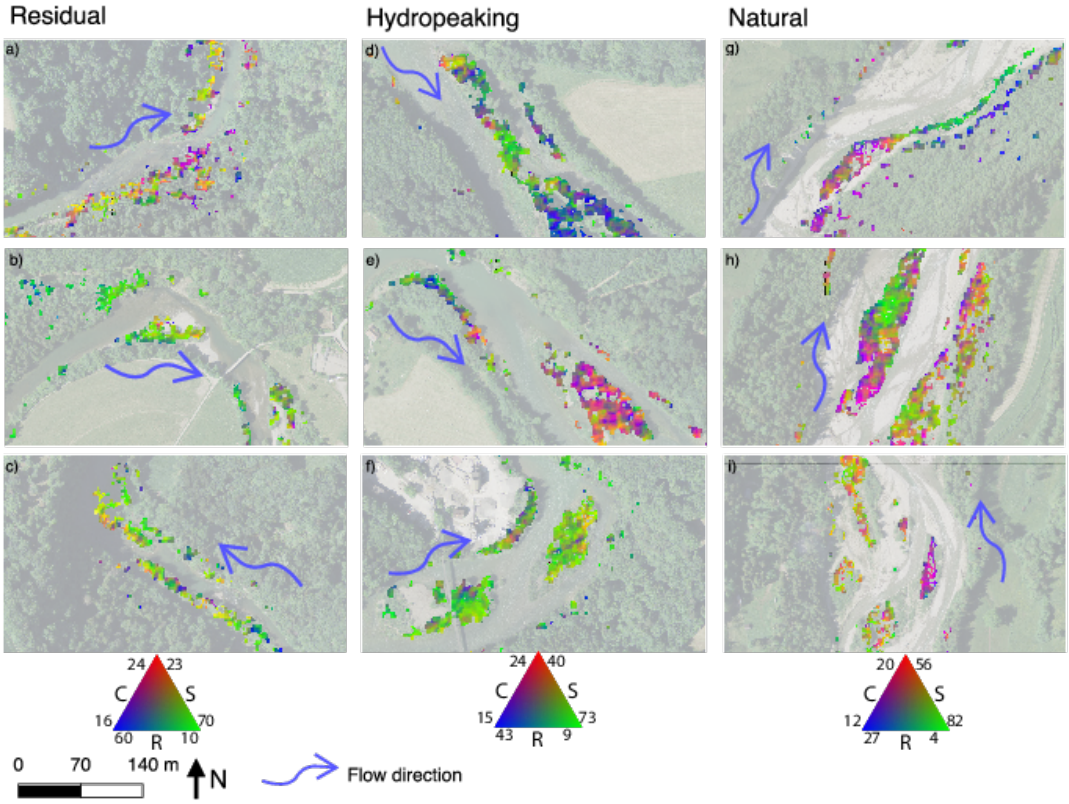

FIGURE 3.4: Excerpts of maps displaying CSR scores along the three reaches. The red, green and blue channels are respectively allocated to the C, S and R-score. The color rendering is stretched independently for each reach depending on the range spanned by the respective distributions. The CSR scores are mapped only for pixels included in the willow mask based on the multi-temporal willow classification.

the laboratory measurements showed high variability. However, the differences obtained from imaging spectroscopy data were consistent with each other: the same trends were observed along the season for the three reaches. Further, the differences between the natural and the residual reach were similar to those between the natural and the hydropeaking reach. In any case, the low R^2 obtained over the pigment ratios does not allow a deep interpretation of the patterns observed.

3.4.3 Differences between reaches

The significant differences between plant parameter distributions showed a dependency on the reach, displayed mainly by the differences between the natural and the two others reaches (Table B.1, left part). Indeed, significant differences were found for the CSR scores, leaf traits and pigment ratios. Willows along the natural reach had a higher S-score compared to willows along the altered reaches, which had higher C- and R-scores. Between the hydropeaking and residual reach, the differences in leaf traits were significant, but no differences in SLA or LDMC could be observed. A significant difference in C-score is also observed, notably linked to its

TABLE B.1: Difference of averages for all plant parameters between reaches and between dates. The differences were based on the laboratory data (Lab) and on the imagery predictions (Im). On the left side, the letter (R/H/N) refers to the respective reach indicated in the header having the highest average (R: residual reach, H: hydropeaking reach, N: natural reach). On the right side, the sign (+/-) refers to the increase or decrease of the parameter along the season. Significance indication : * := no significance (p>0.01), +*/-*/R*/H*/N* := weak significance (0.01 >p>0.0001), +/-/H/R/N := strong significance (p<0.0001)

Plant parameter	Difference between reaches						Shift along the season					
	R & N		H & N		H & R		N		R		H	
	Lab	Im	Lab	Im	Lab	Im	Lab	Im	Lab	Im	Lab	Im
Competitor	R*	R	H*	H	*	R	*	-	*	*	*	+
Stress tolerator	*	N	N	N	R*	*	*	+	*	+	*	+
Ruderal	*	R	H*	H	H*	*	*	-	*	-	*	-
chlA / chlB	*	N	*	N	*	H	+*	+	*	+*	*	+
chlA / xanthophylls	*	R	*	H	*	H	*	-*	*	-	-*	-
chlA / carotenes	R*	R	H*	H	*	H	*	-	*	-	*	*
SLA	*	R	H*	H	*	*	*	-	*	-	*	-
LDMC	*	N	N*	N	*	*	*	-*	*	*	*	-*
Leaf Area	R*	R	H*	H	*	R	*	-	*	*	*	*
Leaf hydrated weight	*	R	*	H	*	R	*	-	*	*	*	+
Leaf dry weight	*	R	*	H	*	R	*	-	*	+*	*	+

distribution in July. Ratios of chlA — xanthophyll and chlA — carotenes were lower along the natural reach compared to the altered reaches, while the chlA — chlB ratio was higher. The differences of pigment ratios all showed a higher relative content of chlA along the residual reach with respect to the hydropeaking reach. In addition to the difference of averages, the shapes of plant parameter distributions varied according to the reach (SI Figure S6). residual and hydropeaking reaches generally showed overlapping distributions. The distributions were in general more diversified for the altered reaches, which exhibited broader ranges. The distributions in July exhibited a singular pattern, where the leaf hydrated and dry weight distributions of the residual reach were close to the distributions of the natural reach. Simultaneously, the CSR score distributions were distinctly different between the natural and the altered reaches.

3.4.4 Shifts along the season

A shift of plant parameters from July to September was observed for all three reaches. We observed opposite shifts of leaf traits between the natural reach and the altered reaches, while the shift of pigment ratios and the shift of CSR scores were similar. The CSR scores showed a homogeneous pattern of development, with an average increase in S-score along the three reaches. Along the natural reach, smaller, lighter

and drier leaves were observed, occurring with a shift towards a higher S-score. Along the altered reaches, larger, heavier and wetter leaves were observed, accompanied by a shift towards more stress toleration and more competition. We observed similar shifts of pigment ratios among the three reaches: the chlA — xanthophyll and chlA — carotenes ratios decreased, while the chlA — chlB ratios increased.

3.4.5 Ternary representation of CSR scores

The ternary representation of strategies discriminates the reaches based on the strategy values present along each reach and their respective spreads (Figure 3.5). The distribution of CSR scores spanned along the stress tolerator axis but had a smaller range along the competitor direction. The CSR scores showed a wide range of distribution along the ruderal axis. While the competitor direction is strongly correlated to the leaf area, the stress tolerator axis is more correlated to the SLA and LDMC trait. Our results reveal a large intra-reach variance of CSR scores, particularly along the S-axis, corresponding to variation in SLA, and LDMC to a lesser extent. The extent of the score distribution covered a substantial portion of the ternary triangle parameterized in the StrateFy model [35]. The dispersion of laboratory data (Figure 3.5, upper graphs) in a ternary graph revealed the discrimination among the reaches, while no pattern could be observed along the season. A few cells of the ternary graph, away from the center of the CSR score distribution and at the edge of the triangle, were considered as outliers. Outlying cells, defined as a cell containing a single pixel, were therefore masked out. The presence of outliers could be due to imprecision in the willow detection or in the PLS prediction.

3.5 Discussion

3.5.1 Statistical model based on imaging spectroscopy data

The selection of specific willow stands and the use of simple but efficient statistical tools allow relevant statistics to be extracted from remotely sensed data. The large areal extent of the willow stands is ideal for capturing remotely sensed measurements by offering a stable spectral response over multiple pixels. The remotely sensed plant parameters are not spatially independent, hindering the direct use of t-tests. The correction of the degree of freedom of the t-tests helps to reduce the number of type I errors where the null hypothesis is rejected, which in our case impacts several t-tests that we carried out. The correction of effective sample size appears to be crucial here, since multiple t-tests do not reject the null hypothesis after the decrease in degree of freedom.

In our study, the benefit of imaging spectroscopy is two-fold: it increases the information available for the statistical analysis between reaches (regional scale), and it reveals the pattern of CSR score distribution on islands and over alluvial forest. The spatial range of variability in plant parameters, visible in figure 3.4, is too small

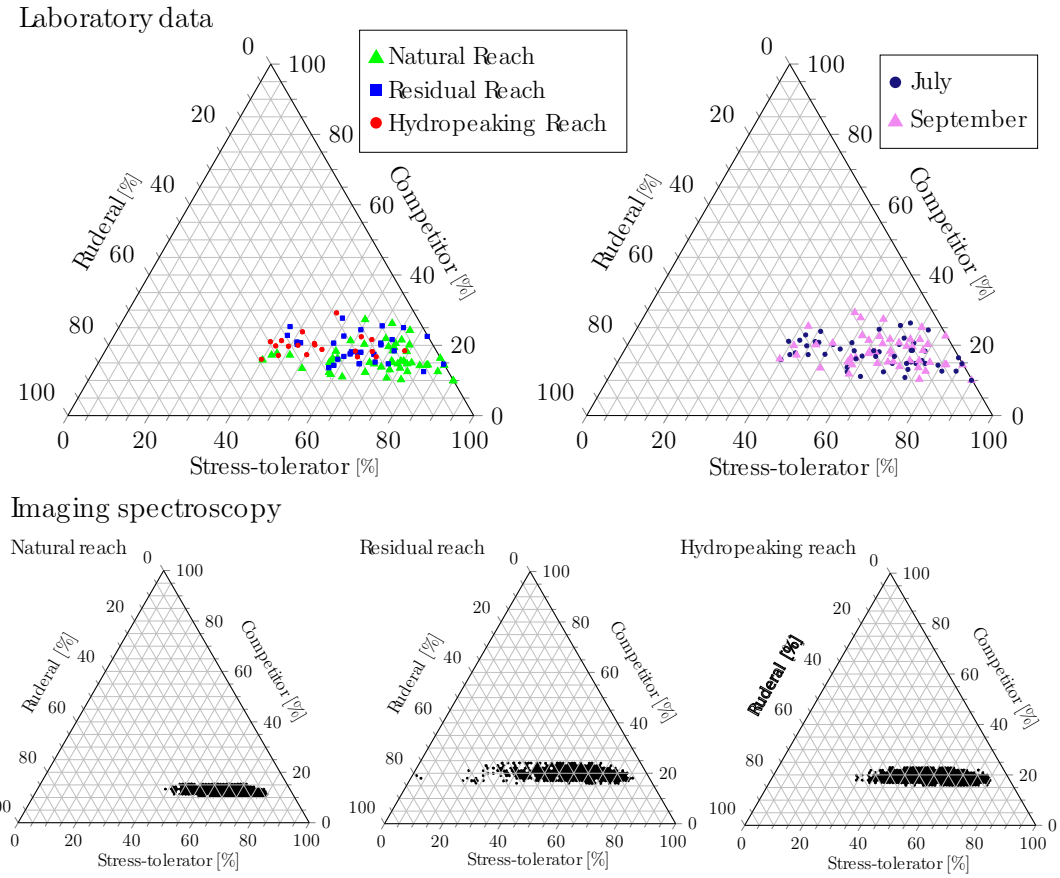

FIGURE 3.5: Ternary plot of distributions of laboratory data (upper graphs) and remotely sensed CSR scores (lower graphs). Upper left: laboratory data colored by reach. Upper right: laboratory data colored by season. Bottom: distribution detected by remote sensing along the three reaches for July. Colored cells represent the presence of pixels with corresponding CSR scores along the reach. Cells with single pixels, considered as outliers, were removed.

to be depicted by ground sampling. An exhaustive ground sampling targeting all individuals would be inappropriate for the sites along the rivers, sometimes particularly hard to reach.

The statistical model is able to predict the CSR score from imaging spectroscopy data with a relatively high R^2. PLS regression models from other studies [182, 183, 175] were able to predict plant traits with a comparable or higher prediction power. However, the compared models focused on communities formed by heterogeneous vegetation, while here the considered willow stands form a particularly homogeneous set of targets, thus creating a setting in which the parameters to retrieve are subtle changes of each individual. On the contrary, a set of heterogeneous individuals offers a larger spread in variation to be detected, and is therefore less affected by measurement noise. In brief, the leaf area, SLA, and LDMC are better retrieved than the pigment information, which is in line with other PLS regression models predicting plant traits [182, 183, 175, 184]. Moreover, the CSR-score group shows the highest prediction power among all the plant parameters predicted.

The ternary representation of predicted values along each reach allows us to compare the range of CSR scores spanned and to assess their link to other parameters (Figure 3.5 and SI Figure S5). The large variations in CSR score between individual willow trees suggest that a description of strategies based on a purely species-based approach does not take into account a substantial plasticity of the parameter. A certain range of possible strategy values for a single species or family has already been identified in the StrateFy model [137, 35]. The observed overall wide spread of plant parameters can be linked to the known polymorphism and adaptive capabilities of willows [150]. It is, in any case, unexpected to observe such a large spread in CSR scores for a single type of vegetation. Such variation could be a possible sign that the number of samples per individual was too small and that the overall spread represents an intra-individual variability. However, the sampled alluvial willows growth in a specific environment where few tree species are found. The large spread of CSR scores can therefore be linked to the environmental changes occurring in the alluvial environment due to flood, drought and changes in morphology in particular. On the considered sites, stands of willow trees can also be found on a nutrient-rich soil on which the growth of forest trees is only a question of time. Therefore, it is here not clear if the large spread in CSR scores is actually due to the particular conditions of the floodplain or if it is an artifact of sampling. However, in the case of an actual variations among willow stands, our observations show that a species-based quantification of CSR scores does not capture a possibly large range of strategy. Instead, a quantification based on physio-morphological features such as the StrateFy model is able to reveal possible intra-species variations.

3.5.2 Processes influencing plant parameter retrieval

The higher prediction power of CSR scores compared to leaf traits can be explained by two factors. First, the difference in prediction power can be due to a non-linear relationship between the parameters and the spectra [185]. Second, and more likely, the higher prediction power compared to the leaf traits is probably linked to external variables of the StrateFy model, such as fractional cover or soil properties, including any other plant traits. Thus, it can be expected that plant strategies are more likely to be retrieved than single plant traits.

The PLS regression based on imaging spectroscopy data is affected by any environmental variable that can influence the reflection of light from the canopy or from the ground. Subsequently, an influence of environmental changes (such as ground surface composed of understory vegetation, gravel and litter) can also explain the patterns observed in the plant parameter distributions for July between the natural and the residual reach [186]. Changes in canopy reflectance would therefore be a plausible cause of the difference in leaf trait distributions between the seasons, while the CSR-score prediction, possibly relying on environmental variables, does not change as much.

According to the field investigations, the fractional cover was often lower for the willow patches along the natural reach. Patches presenting low fractional cover showed particularly high S-scores. This observation can be explained by the thin layer of soil present in locations particularly exposed to flood events. Similar observations have linked sparse vegetation to a high S-score [187, 188]. Additionally, the determination of a PFT based on spectral response can be linked to canopy structure, as it has been demonstrated using simulated spectra [184]. These arguments support the need for a direct statistical estimation of CSR scores based on remotely sensed imagery without intermediate calculation. Finally, since we expect the method to possibly rely on environmental variables without proof of evidence, the statistical model used to predict CSR scores based on remotely sensed data might not be generalizable to any environment.

The low R^2 obtained for pigment ratio possibly relates to the measurement accuracy of the laboratory data. It has been observed that separating plant functional groups via reflectance does not strongly profit from pigment content variation [184]. This observation indicates that the failure of linking pigment information with the retrieved reflectance does not prevent us from retrieving CSR scores with a higher accuracy.

3.5.3 Shaping of of plant parameters related to alterations of the flow regime

It is well known that alterations of the natural flow regime (sensu [189]) downstream of reservoirs have large impacts on flood events and erosion, transport and deposition of sediments [190, 83, 191, 192] with variable responses of riparian vegetation properties [141]. Along the hydromorphologically altered reaches of our study we observed a trend to more homogenized and denser vegetation pattern [193, 15], a change of vegetation communities [194, 195] and a decrease in pioneer species recruitment [196, 197] leading to an increase of the overall vegetation biomass and a stabilization of the river system ultimately leading to channel narrowing [144, 145]. This stabilization may decrease environmental stress (e.g., accumulation of nutrients or stabilization of water table), leading ultimately to a shift in plant strategies, e.g. in composition or by plastic adaptation.

Our results showed a shift of plant parameters towards values associated with a competition strategy for willows located along the altered reaches. This strategy shift towards higher C-scores is in line with known vegetation responses, for example after a flow regime altered by damming, which results in a rapid stabilization of riverbanks through the extension of vegetation roots [6]. This vegetation response can in turn amplify the initial stabilization triggered by the flow regime alteration, or in other words, create a positive feedback loop. In brief, while our results are in line with previous observations linked to the development of vegetation along altered reaches [12], the perspective of plant resource allocation strategy summarizes here

the various observations in a conceptual framework. In any case, our results cannot explain any causality in the interaction processes between the flow regime and the change in plant parameters.

While the prediction of plant parameters based on imaging spectroscopy is primarily used to extract their distributions, the observed spatial patterns of CSR scores can be linked to various processes of the alluvial ecosystem. In general, the distribution of alluvial vegetation is closely related to fluvial landforms and fluvial processes [198]. Moreover, environmental factors (e.g., substrate characteristics, areal extend, or light availability) exhibiting large variations in floodplains are known to have an impact on plant communities [199]. Further, hydromorphological alterations can lead to various changes in the substrate characteristics [141], ultimately affecting plant strategies.

The spatial distribution of the CSR scores observed reveals patches particularly present along the hydropeaking and the natural reaches. This high spatial autocorrelation might indicate a shaping of the CSR scores by long-term processes, such as those cited above, as opposed to short-term processes. While a high spatial autocorrelation is present at the decameter-scale, we do not observe a gradient of CSR scores along the channel or away from the channel. The absence of a lateral gradient can be explained by the relatively small width of the willow stands found along the reaches. The absence of a longitudinal gradient observed in plant parameters might be related to the relatively small-scale length of river considered, since the flow conditions stay almost stable along the reaches considered.

3.5.4 Strategies, stress and disturbance

It is commonly accepted that species composition of floodplains is primarily shaped by floods that partially or completely destroy the vegetation and the substrate, leading to a cycle of recolonization of the freed spaces [200, 145]. Though the species composition is mainly driven by disturbance, our observations indicate that the shaping of plant traits is also driven by stress factors, as discussed in the following paragraph. To begin with, the common shift of plant parameters along the season reveals that environmental factors influence the alluvial vegetation at the regional level. A dry period preceded the second data acquisition campaign, explaining the shift of plant parameters observed from July to September 2016 (SI Figure S3). The observations on possible water stress (see next section) also indicate a substantial impact of stress on plant traits. While the spread of predicted values is quite large along the ruderal axis, we were unable to find any clear link with other observations or components of the floodplain. In particular, the distribution of higher R-scores for the altered reaches was not expected, since the altered reaches are less affected by floods than the natural reach. The spread along the ruderal axis, already found data to a lesser extent in the laboratory, might be linked to the underlying SLA. It has been observed that seed dispersal of some *Salicaceae* species follows complex spatial

and temporal patterns [201]. Then the observed variation in R-score can be linked to the restrictive conditions under which *Salix* trees release seeds.

Next, while it might not be expected that willow trees are found in the S/SR region of the CSR triangle, it not a surprising result. Willow trees, though having a relatively tall canopy and long life cycle in the overall vegetation kingdom, have much shorter and in general smaller canopies than most trees found in forested environments. The generally shorter canopy of alluvial willows can be explained by the influence of disturbance (floods, asphyxia of roots, destruction of the substrates through erosion, etc.) and the influence of stress (summer droughts, lack of nutrients on gravel bars, temporal saturated conditions of the soil, etc.). Therefore, the CSR scoring of the observed alluvial willow as S/SR is not in contradiction with the original assumptions of Grime (1974) [134] Other studies have revealed a classification of willows towards S or R strategies: some willow species considered in our study are found as S/CS [35] and *Salix Alba* has even been reported as R [202]. The colonization capabilities of alluvial willows have been described as belonging to species following an R strategy [203]. Also, Grime (2006) [204] described the *Salix* genus as being close to certain herbaceous species in their regenerative strategies involving numerous wind-dispersed seeds.

Furthermore, the broad range of plant parameters along the altered reaches can be a sign of differentiation caused by stress removal [205, 206]. Disturbances generally increase trait differentiation among communities [204], clear ecological niches and physical space, thus increasing the biodiversity [207, 208]. On the contrary, trait convergence is observed among communities influenced by various stress factors [209, 210, 211, 212]. In our case, the system where disturbances occur, i.e., the natural reach, shows a smaller range in plant parameters than the altered (stabilized) floodplain reaches. Since the larger spread of plant parameters along the altered reaches is certainly not due to an increase in disturbance, their divergence can be here a sign of stress removal. Given all these observations, it is possible that the plant traits of willows are mainly shaped by stress rather than disturbances.

3.5.5 Support from leaf traits and pigments

The observations of pigment ratios and leaf traits support the observed changes in CSR score. While it is difficult to link the leaf traits and pigment ratios to an increase of the C-score, it is likely that these plant traits are connected to a decrease of S-score compared to the natural reach. The deviation of the predicted distribution of pigment ratios is in line with the low R^2 achieved by the PLS regression, possibly linked to the accuracy of pigment measurements in the laboratory. Observed changes in pigment ratios could correspond to water stress. Such water stress could also be a possible cause for the difference observed between the natural and the altered reaches, though we do not have evidence for these causality links. The distribution of pigment ratios along the natural reach compared to the altered reaches

exhibit a higher proportion of photo-protective pigments, both at the beginning and at the end of summer (SI Figure S6). Water stress has been described as an important component of natural alluvial ecosystems [213, 214, 215]. A water stress along the natural reach would also be supported by the shift in CSR scores. A plausible water stress along the natural reach might be linked to the soil characteristics of the floodplain, which is more gravelly along the natural reach, while a thicker soil has developed along the altered reaches. Decreased water stress along the altered reaches can be a result of an increase of water availability indirectly caused by alteration of the hydromorphological processes. An increase of water availability can be linked, for example, to soil formation, to the height of the impermeable bedrock, or to the location of alluvial vegetation at the time of low water. All these environmental variables are linked to the hydromorphological processes of a river [216], and are therefore prone to be modified under an alteration of the flow regime. However, it is also possible that the various observation on the CSR score, LDMC and pigments ratios are due to one or multiple causes unrelated to water stress. We would like to underline that the mentioned links between water stress and our observations are plausible interpretations not relying on evidences. Also, the observed differences in plant parameters could be due to variations assumed to be negligible in this study due to the sites setting, such as variations in geology or land use of surrounding areas.

3.6 Conclusion

The willow stands along the investigated reaches offer an appropriate subject of study to predict CSR scores from imaging spectroscopy. The convenience of the willow stands was found to be both ecological, due to their importance in floodplains and their adaptive capabilities, and methodological, since they form relative homogeneous and dense vegetation stands compared to other kinds of vegetation found in floodplains. The PLS regression model achieved a prediction of CSR score among willow stands with an R^2 of 0.4 to 0.55 over alluvial vegetation using airborne imaging spectroscopy. The correction of the effective sample size in the statistical test was successfully set up to analyze the river systems based on dense spatial data. In brief, the mapping of strategies based on leaf traits revealed spatial patterns as well as a large variation among individuals, supporting the quantification of resource allocation strategies based on individual traits.

Our main observations relate the shaping of the willow resource allocation strategies to an alteration of the flow regime. The natural reach exhibited a CSR-score distribution shifted towards higher S-scores compared to the altered reaches. Both altered reaches under the influence of residual flow or hydropeaking flow exhibited a displacement of strategies with respect to the natural reference. All the leaf traits and pigment observations indicate a possible presence of water stress affecting the willow trees located along the natural reach. We note that changes in vegetation

properties can be indirectly caused by alteration of the flow and sediment regime through various mechanisms such as soil formation, bank stabilization or properties of the soil parent material. Finally, our observations indicated that among the willow stands of the floodplains considered in this study, stress, rather than disturbance, drives the shaping of plant traits. These observations add a new component to assess the adaptive capabilities of alluvial willows.

The dynamics of biophysical processes of interaction between the vegetation and the flow regime still need to be further detailed. While environmental water protection policies try to warrant the re-activation of the flow regime variations (environmental flow, functional flow), further research is needed to fully understand the continuous and reciprocal shaping of the flow regime, landforms and alluvial vegetation. Towards this goal, the framework of resource allocation strategies offers new insights into these interactions and has proven to be a promising descriptive model. The use of imaging spectroscopy data complements the traditional view of plant communities by bringing new and explicit information on spatial distribution. Nonetheless, the transferability of the approach chosen in our study to different ecological environments remains to be assessed.

3.7 Acknowledgments

This research project was part of the National Research Programme "Energy Turnaround" (NRP 70) of the Swiss National Science Foundation (SNSF). Further information on the National Research Programme can be found at www.nrp70.ch.

Data are and code are available at https://doi.org/10.5281/zenodo.2585396

3.8 Appendix

Introduction This supporting information provides figures and a table with detailed information on the study sites. It provides as well figures and tables on the distributions of predicted plant parameters and validation of the PLS regression. It also provides a text and figures on pigment ratios and their use in the article.

Text S1.

The main processes affecting established alluvial vegetation on a seasonal scale are erosion of vegetation (through substrate erosion or direct uprooting) by floods and variation in the water table [144, 165]. The use of pigment ratios in this study is therefore closely linked to changes in water availability given the typical setting of alluvial vegetation. An increase of chlorophyll A / B ratio, which has been observed under water stress [166, 167], can be theoretically explained by impacts on cell physiology [217]. The proteins associated with the reaction centers of light-harvesting complexes (i.e., core antennas) contain only chlorophyll A, while the outer binding proteins, the light-harvesting complexes II, (LHCII) contain chlorophyll A and B

[218]. It has been observed that short-term drought stress, understood equally as excess light, caused a rapid disassembly of the LHCII [219]. Also, higher light intensities can lead to a reduction of LHCII [220] or their downsizing [221]. A proportional reduction of the outer complexes with respect to the central antennas would lead to an increase in chlorophyll A / chlorophyll B ratio. A decrease of chlorophyll / carotenoids ratio, which has been observed under water stress [168, 169], and specifically of chlorophyll / xanthophyll ratio [164], can be explained by the functions and variations of pigments expected under such events. Carotenoids, apart from participating in light harvesting, are also involved in photoprotection [164]. Photoprotective pigments can experience increasing levels under excess of light [222, 223], following preceding water stress. A replenished pool of carotenoids, along with a decreased level of chlorophyll pigments [224, 225] can explain decreasing chlorophyll A / xanthophyll and chlorophyll A / carotenes ratios during water stress.

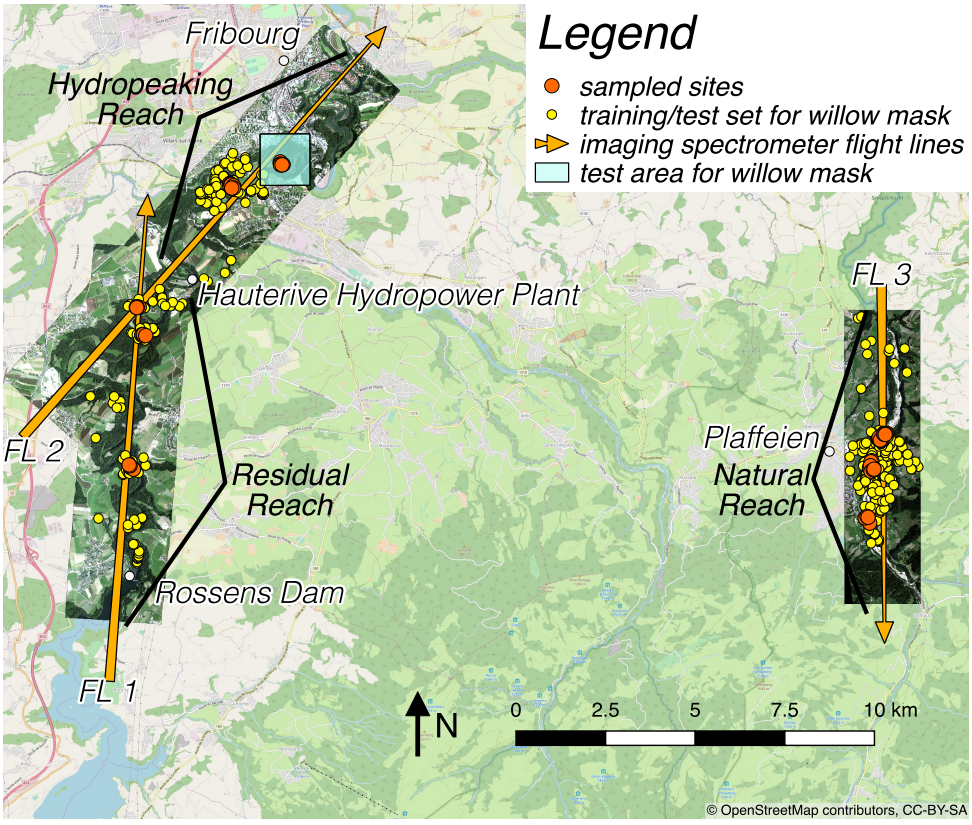

FIGURE 3.6: Imaging spectrometer flight lines (FL) and distribution of sites for laboratory data sampling. The arrow directions depict the direction of the plane. All three flight lines were acquired on each of the four acquisition dates.

FIGURE 3.7: Location of the study sites in Switzerland. The main rivers and lakes in Switzerland are represented in blue color.

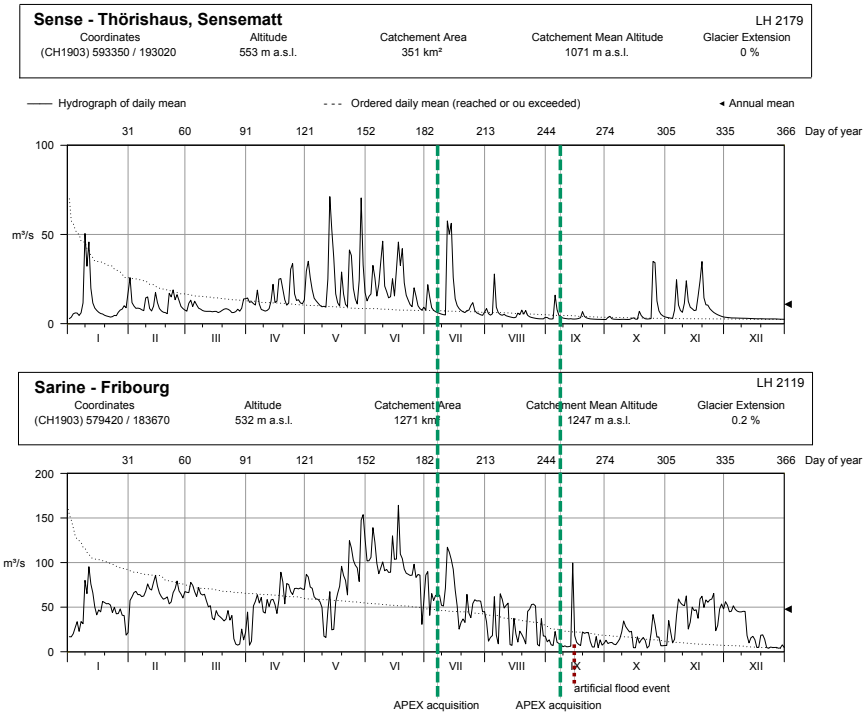

FIGURE 3.8: Reports provided by the Federal Office for the Environment FOEN, division Hydrological data and forecasts. The discharge data are obtained from gauging stations located a few kilometers downstream of the reaches of interest along both the Sense and the Sarine river, therefore not showing an exact discharge measurement of the study sites. The months of July and August exhibit a low discharge, particularly along the Sense river.

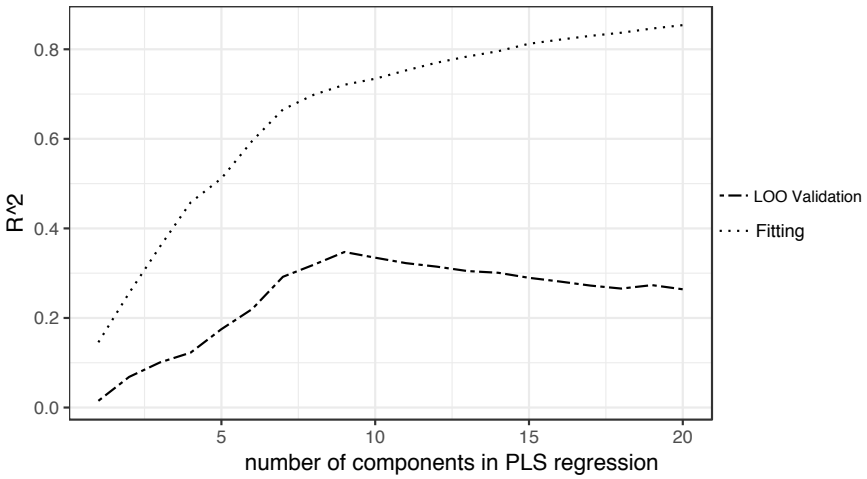

FIGURE 3.9: Coefficient of determination for the PLS regression with respect to the number of latent components. The fitting score and the validation score are based on the mean achieved by every leave-one-out validation step. The maximum achieved by the validation score indicates an optimal number of latent components of 9. The coefficient of determination is the mean of all coefficients calculated on each variable. LOO validation: leave-one-out validation.

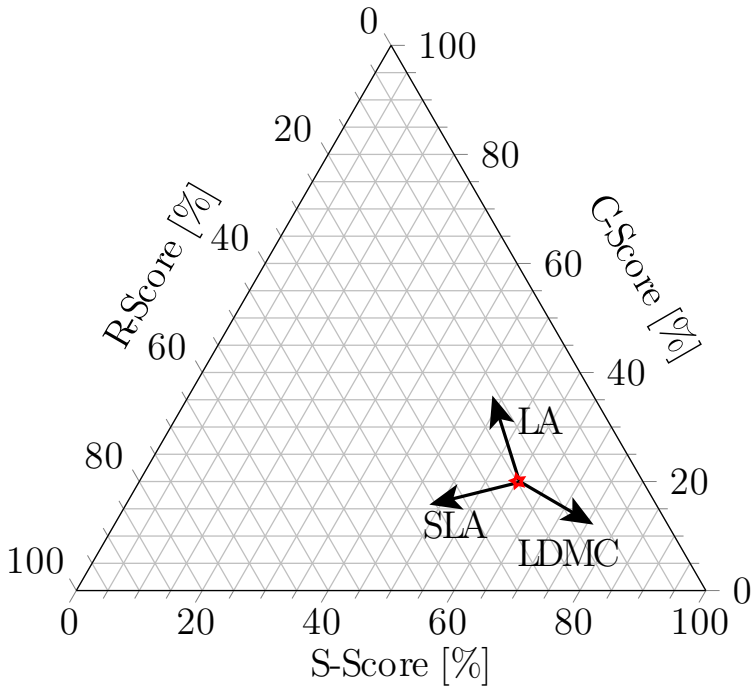

FIGURE 3.10: Directions of changes of strategies depending on the changes in leaf area (LA), specific leaf area (SLA) and leaf dry matter content (LDMC) independently. Here, the origin point of the arrows has been selected in the range of the observed data. The length of the arrows is arbitrary.

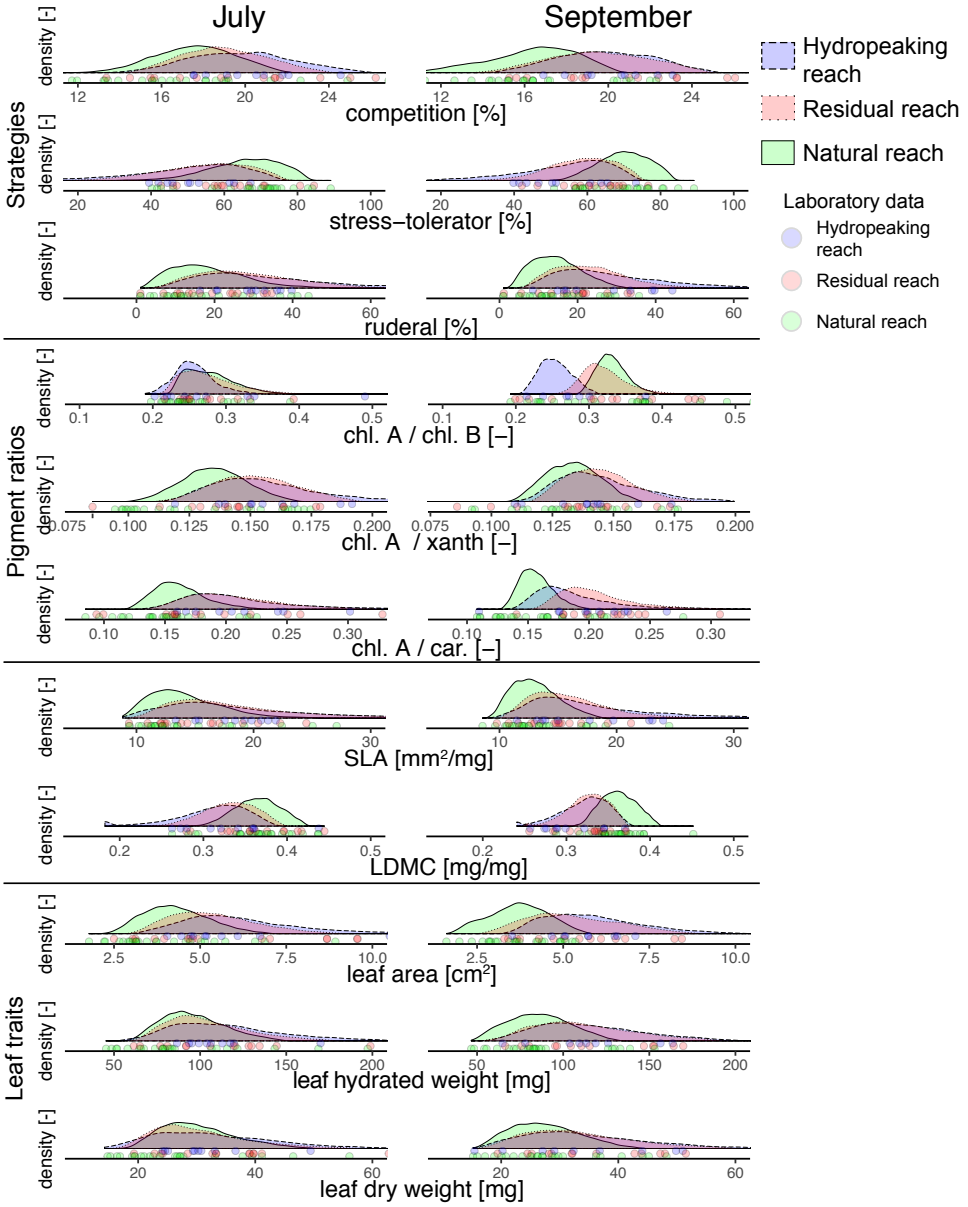

FIGURE 3.11: Histograms of plant trait distributions predicted by imaging spectroscopy. Distributions are represented as density normalized over the total number of observations along each reach. The scale of the x-axis is adapted for each plant trait to cover the full range of the distributions and laboratory data. The scale of the y-axis is similar for the dataset of July and September for each plant trait. The points below the histograms represent the laboratory data in respective colors. The three leaf traits (leaf area, leaf hydrated weight and leaf dry weight) represent the average of the respective trait per leaf (e.g., leaf dry weight is the mean dry weight per leaf found at a location).

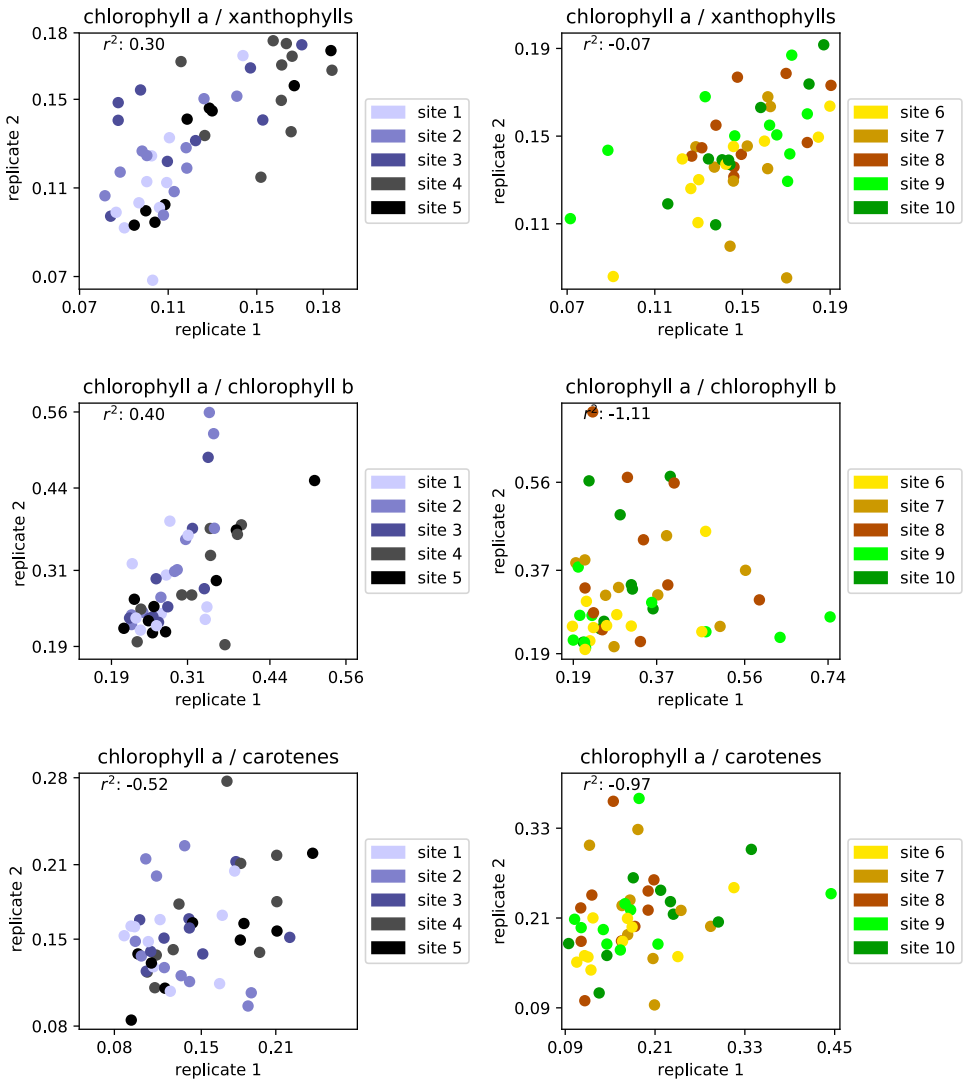

FIGURE 3.12: Scatter plots of replicates for the three pigment ratios. The sites 1 to 5 (in blue) are found along the natural reach; the sites 6 to 8 (in yellow-red) are found along the residual reach; the sites 9 and 10 (in green) are found along the hydropeaking reach.

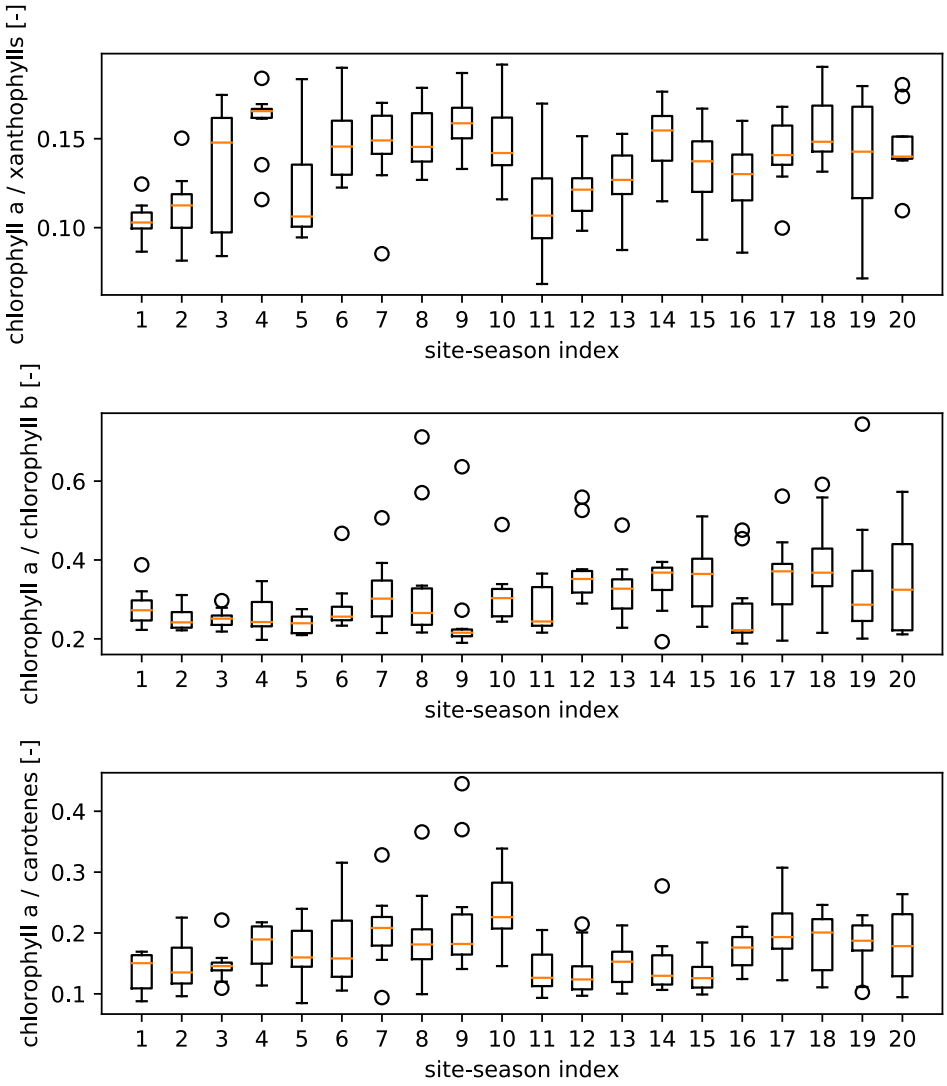

FIGURE 3.13: Boxplots of pigment ratios of laboratory data with respect to an ordered index. The index is built following the site order from 1 to 10, including a shift of 10 for the season of September. The indices from 1 to 10 refer therefore to July and 11 to 20 refer to September. The box extends from the 25 percentile to the 75 percentile in the data. The middle line is located at the median. The whiskers extend from the box to the last data closer to 1.5 times the interquantile range. Points are outliers out of the whiskers. Although large variations exist in the replicates of laboratory data, the differences between reaches and seasons can be visually retrieved here, corresponding to Table 1 in the article.

TABLE B.2: Summary of the number of sampled individuals per reach. Five individuals were sampled on every site at a distance of roughly 5 to 10 m from each other.

	July			September		
	Natural	Residual	Hydropeaking	Natural	Residual	Hydropeaking
number of sites	5	3	2	5	3	2
total number of samples	25	15	10	24	15	10

TABLE B.3: Statistics of the linear regression between sampled and predicted values (Figure 3). The coefficient of correlation should not be mixed with the coefficient of determination R^2_{cv}. While the first one describes the linearity between the sampled and predicted value, the second one describes the accuracy of data retrieval. For example, perfectly aligned predictions in Figure 3 with a slope different from 1 would have here an R^2 of 1, but an R^2_{cv} smaller than 1.

	R^2	p-value
competitor	0.63	<0.01
stress-tolerator	0.72	<0.01
ruderal	0.74	<0.01
chl. A / chl. B	0.33	<0.01
chl. A / xanth.	0.54	<0.01
chl. A / car.	0.52	<0.01
SLA	0.75	<0.01
LDMC	0.50	<0.01
leaf area	0.61	<0.01
hydrated weight	0.64	<0.01
dry weight	0.66	<0.01

Chapter 4

Characterizing Flood Impact on Swiss Floodplains using Inter-Annual Time Series of Satellite Imagery

Milani, G., Kneubühler, M., Tonolla, D., Doering, M., & Schaepman, M. E.

This chapter is based on an article submitted to the peer-reviewed IEEE Journal of Selected Topics in Applied Earth Observations and Remote Sensing in 2019. The article was submitted under the title « Impacts of flow alteration on Swiss floodplains observed by remote sensing », which will be amended according to the above title in the following steps of the publication procedure.

G. Milani, M. Kneubühler and M. E. Schaepman conceptualized the study. G. Milani, M. Kneubühler, D. Tonolla and M. Doering elaborated the methodology. G. Milani, M. Kneubühler, D. Tonolla and M. Doering performed the investigation. G. Milani, M. Kneubühler, D. Tonolla, M. Doering performed the formal analysis. G. Milani wrote the first draft of the manuscript. G. Milani, M. Kneubühler, D. Tonolla, M. Doering and M. E. Schaepman participated in the writing and editing of the final manuscript.

4.1 Abstract

Pressure on the biodiversity of ecosystems along many rivers is growing continuously due to the increasing number of hydropower facilities regulating downstream flow and sediment regimes. Despite a thorough understanding of the short-term processes and interactions at this hydro-biosphere interface, long-term analyses of the impacts on floodplain dynamics are lacking. We used inter-annual Landsat 4, 5, 7 and 8 time series to analyze the effects of hydrological events on floodplain vegetation in four mountainous floodplains in the Swiss Alps. Using a spectral mixture analysis approach, we demonstrate that the floodplain vegetation dynamics of mountainous rivers can be recovered at a spatial resolution of 30 meters. Our results suggest that interactions between floods and floodplain vegetation are complex and not exclusively related to flood magnitude. Of the four reaches analyzed, only data gathered along the sub-mountainous reach with a quasi-natural flow regime show a clear link between remotely sensed vegetation indices and floods. In addition, our 29-year time series shows a continuous upward trend in vegetation indices along the floodplains, strongest in the reaches affected by hydropower facilities. The approach presented in this study can be easily replicated in other mountain ranges by providing available flow data to verify the impact of hydropower on floodplain vegetation dynamics.

4.2 Introduction

Rivers and their floodplain provide essential ecosystem services worldwide while under pressure from hydropower production, agricultural expansion and climate change [4, 226, 227]. The changes imposed on the flow regime largely impact the floodplain vegetation through the modification of natural hydrogeomorphic processes [228], since the forms of floodplain vegetation are largely related to flood characteristics [229, 230]. Although alterations of the flow regime usually result in changes in the floodplain ecosystem, such as vegetation encroachment or increase in non-woody vegetative cover, prediction of changes based on planned alterations are challenging [192, 15]. The flow regime also shapes vegetation distribution through flow-related processes, such as sediment transport and deposition processes [231], which are also globally triggered by anthropogenic alteration of the hydrographic network [232, 233]. Observation and monitoring of floodplain vegetation development and recovery are necessary to assess flow regime management needs and the achievements of restoration projects along river systems [16].

4.2.1 Remote Sensing of Floodplains

A range of remote sensing technologies have been developed to observe numerous aspects of floodplains. For example, aerial and unmanned aerial systems (UAS)

have been deploy to classify river land cover [234, 36]. Moreover, lidar technology has been used in combination with aerial images to study long-term changes in vegetation [235]. Further, floodplain tree species have been classified by using high-resolution imaging spectroscopy data [236, 37]. Satellite remote sensing provides near-continuous coverage of data in space at a high temporal frequency of acquisition. Its important advantages are currently unmatched by airborne remote sensing platforms. For floodplain applications, satellite remote sensing characteristics are attractive because rivers are generally widely distributed and often difficult to access due to obstacles such as valleys, cliffs and dense forests.

Despite decades of research on the use of satellite remote sensing for floodplain vegetation [237], its actual use for floodplain studies is still very rare. In the past, previous studies have shown that decameter-scale satellite imagery can be used for studying floodplains in a multi-temporal setting [238, 239, 240]. However, the use of satellite remote sensing in floodplains has been mainly limited to two main objectives: the delineation of geomorphological units and the monitoring of water quality parameters [241, 242]. High or medium-resolution satellite images were used to delimit geomorphological units, flood extent and land use, for example by using the ASTER sensor [47] or the QuickBird Satellite sensor [243]. High-resolution satellite imagery has also been used to map bar crest movement over a relatively short time scale [244]. On the other side, the spectral resolution of available satellite imagery allows monitoring of water quality parameters, such as the concentration of suspended sediments, for example by using the ETM+ sensor [245] or the MODIS sensor [246]. However, these studies were mainly limited to large rivers such as the Danube or the Amazon. Landsat Tasseled Cap inter-annual products have been used to classify the land cover of large floodplains and inter-annual changes [247, 248]. The average annual values of the normalized difference vegetation index (NDVI) on riparian forests were also extracted from time series based on Landsat satellites [29]. Finally, satellite imagery has been used very rarely over mountainous floodplains due to the relatively narrow width of the object of interest. In brief, available time series of satellite imagery with high temporal resolution have not been widely considered for studying vegetation dynamics of complex river floodplains.

4.2.2 Floodplain Vegetation Dynamics

While processes linking vegetation to the flow regime have already been the subject of several studies [144, 145, 141], temporal series of remotely sensed data can potentially reveal influences of flood events characteristics on vegetation. The frequency and timing of floods, in addition to the magnitude of single flood events, determine the impact of the flow regime on floodplain vegetation [249, 250]. Although changes in floodplain characteristics have been linked to major flooding, vegetation development appears to have a more complex relationship with the flow regime [251]. For example, the development of vegetation is influenced by groundwater [165] and

variations in groundwater depth [252]. The dynamics of vegetation recovery after flooding has also been documented in the past [253, 47], including the consideration of recovery after extreme events [254, 255]. However, it appears that there is a lack of studies on vegetation recovery dynamics with inter-annual data spanning several decades.

Satellite imagery allows to study vegetation recovery after major flood events using data covering several years before and after the event. Bertoldi (2011) [47] demonstrated the usefulness of medium-resolution satellite imagery over the Tagliamento River in Italy, where changes in riparian vegetation caused by changes in flow conditions were successfully observed. However, the use of satellite imagery in this case was limited to the delineation of vegetation areas classified as sparsely or densely vegetated.

In our study, we contribute to the discussion on riparian vegetation changes led by modification of water flow by adapting the idea of Bertoldi (2011) [47] to consider mountainous and sub-mountainous rivers. We apply this approach to time series of images geo-located over four Swiss Alpine river floodplains. While previous studies have used satellite imagery to delineate plots and vegetation classes, the analysis of satellite imagery in our study furthermore provides information on the state of riparian vegetation, such as the rate of vegetation growth or the detection of dry periods. Compared to natural floodplains showing a correlation between flood events and vegetation dynamics, we expect a decoupling of such mutual effects along floodplains with altered hydrological and sediment regimes. This hypothesis is motivated by the loss in habitat dynamics expected along reaches with an altered flow regime. We assume that observed changes in vegetation conditions are mainly triggered by flood events affecting the floodplains.

4.3 Material and Methods

4.3.1 Study Sites

The four Swiss Alpine study sites were selected on reaches of the Sense, Allenbach, Maggia and Brenno river floodplains where unvegetated gravel bars are large enough to be detected by the remote sensing data considered (Figure 4.1). The width of the floodplains considered is therefore linked to the theoretical minimum width required for a continuous detection of the surface, which encompasses two pixels. This minimum width is here 60m on the ground, given that the imagery used has a 30m spatial resolution. The study area was delineated by the extent of the Swiss federal inventory of floodplains of national importance. The last inventory was carried out from 2012 to 2017. The selected reaches each have a gauging station few kilometers upstream or downstream of the reaches of interest. A summary of some of the characteristics of each reach is presented in Table B.1.

TABLE B.1: Characterization of the study reaches in their actual state. The natural flow regime was extracted from data made available by the Swiss Federal Office for the Environment (FOEN). The substrata classification is based on the map GK500 of the Swiss Geotechnical Commission (SGTK). The width refers to the mean of the detected floodplain area based on the satellite imagery.
Abbreviations: GS: gauging station, HP: hydropower plant, C: crystalline, U: unconsolidated, S: sedimentary.

	Maggia	Brenno	Sense	Allenbach
Strahler number	7	6	6	4
Lengh [km]	8	4	4	2.2
Mean floodplain width[m]	304	104	163	128
Area [ha]	243	42	65	28
Mean Elevation [m asl]	365	447	820	1'470
Natural Hydrological Regime	meridional nivo-pluvial	meridional nivo-pluvial	transition nival	meridional nivo-pluvial
Distance to GS [km]	3.5, upstream	1, downstream	15, downstream	0, downstream
Distance to upstream HP [km]	5.3	8	-	-
Substrata	C (hills) / U (valley)	C and S (hills) / U (valley)	U	U / S

The first reach is located along the Sense River next to the village of Plaffeien, an investigation site of previous studies about its hydromorphology [256], floodplain habitats [257] and the use of aerial imagery [258, 36, 37]. The Sense River is one of the last rivers in Switzerland to have a near natural flow and sediment regime.

The second reach is located along the Allenbach, a mountainous stream located next to the village of Adelboden. The Allenbach is prone to flood events triggered by short storm events due to the low storage capacity of the watershed [259]. Supplementary information on the Allenbach watershed can be found in Collins (2006) [260].

The third reach is located along the Maggia River, between the villages of Boschetto and Lodano. A large hydropower system, Officine Idroelettriche della Maggia SA, impacts the floodplain ecosystem due to flow regulation since ca. 1995, resulting in a residual flow regime [261]. The flow regulation has led to a 75 percent decrease in the average annual discharge, while the annual peak discharge was not decreased [261]. Supplementary information on the flow and sediment dynamics can be found in Perona (2009) [253] and, along with landscape composition information, in Rohde (2004) [257].

The fourth reach is located along the Brenno River. The reach considered along the Brenno spans a total length of circa 4km, which we divided into three sections. Such division was necessary to eliminate river sections along which agriculture and roads were close to the channel and thus would influence the retrieval of the vegetation indices. The first section is located next to the village of Loderio, the second is located upstream of the village of Motto Blenio, and the third section is located next to the village of Prugiasco. This reach has also been affected by hydropower facilities since circa 1960, leading to a 73 percent decrease of annual discharge and a substantial decrease in small and medium-sized floods, while the number of flood events does not show any change [262].

4.3.2 Satellite Imagery

Our methodology was developed to reflect changes in vegetation indices in medium-resolution satellite imagery (ground resolution $\sim$30m), with the aim of using time series covering three decades along mountainous and sub-mountainous rivers. Here, the size of the objects under study was considered to be small for a remote sensing application since the extent of the minimum size under consideration (i.e. the minimal width of the floodplains) is of the same magnitude as the size of the ground sampling distance of the imagery.

Since vegetation indices tend to accurately capture differences in vegetation cover at low fractional cover [263], we make use of the large variation in fractional cover typically found in mountainous floodplains for a robust retrieval of vegetation properties by remote sensing. The central idea is therefore to focus on the sparse vegetation areas of the floodplain in order to extract reliable information on changes in

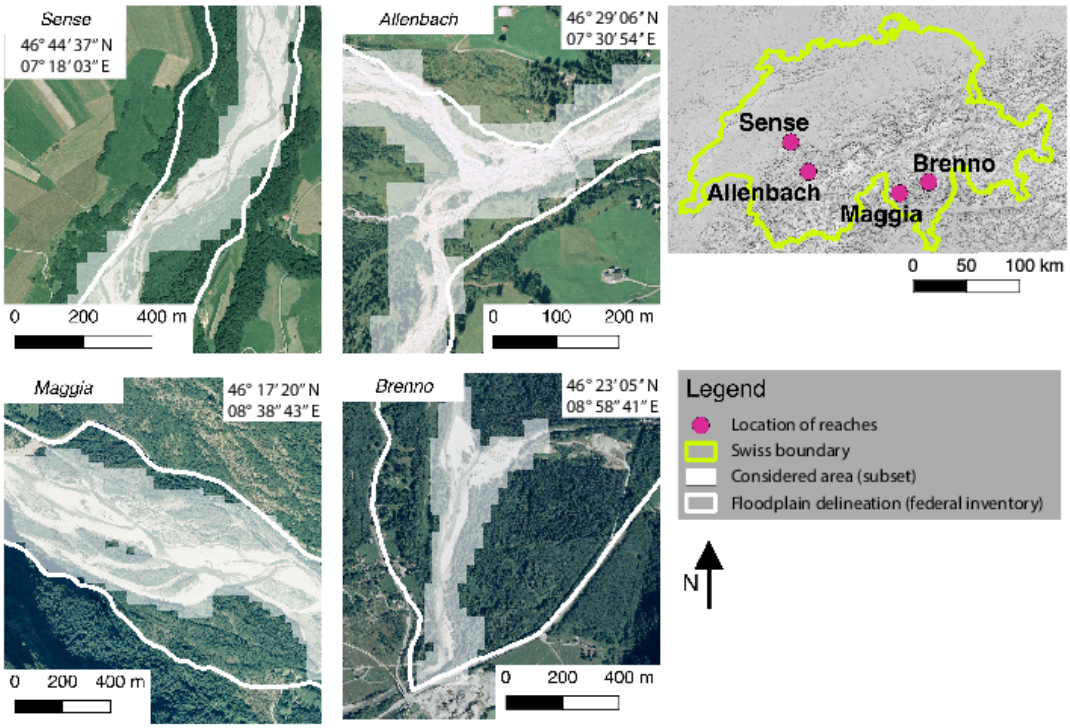

FIGURE 4.1: Subsets of the considered reaches exhibiting the delineation of the floodplains (white line) and the total considered area in the study (white pixels). The floodplain delineations are extracted from the Swiss federal inventory of floodplains of national importance. The total considered area (in white) represents all locations that were included in the mask for the normalized difference vegetation index (NDVI) and the vegetation fraction (VF) calculation for at least one acquisition in the time series. The coordinates refer to the image center. Background Image Source: orthophotos of the years 2004 and 2005 (Swissimage Geodata © Swisstopo).

vegetation conditions.

We used remotely sensed images acquired by Landsat missions 4, 5, 7 and 8 to construct inter-annual time series of vegetation indices [264]. Independent time series were built for each reach. A list of all selected images can be found in the additional material (SI Section 1). The calibrated top-of-atmosphere reflectance [265] at a resolution of 30 m was used. For each reach, only one image was selected per year from 1988 to 2016. This period was chosen as a compromise between data availability, the size of the data set and the occurrence of large-scale flood events in the sectors of interest. The best image was selected based on minimum cloud coverage over the target area and an acquisition date as close as possible to July 31 to represent the vegetation period. The images used were all from the Landsat series, including the operational land imager (OLI) on Landsat 8, the enhanced thematic mapping system Plus (ETM+) on Landsat 7 and the thematic mapping instrument on Landsat 5 (TM05) and Landsat 4 (TM04). Limiting our analysis to the Landsat image collection allowed a consistent comparison of the information remotely acquired over the period. Where possible, we tended to include data from a single sensor in order to

further minimize the biases that could occur due to small but existing differences in sensor characteristics [266]. Therefore, when available, Landsat 7 was chosen instead of Landsat 5, and Landsat 5 images instead of Landsat 4 images. If no suitable images were found in July or August, the images acquired in June were considered as potential candidates. The images from ETM+ were chosen to minimize the Scan Line Corrector (SLC) problem [267]. If the SLC issue affected a large part of the area of interest, images of OLI and TM05 were considered instead.

Although we did not apply atmospheric correction ourselves, we provide some details on these corrections here since the results of this study depend on these processing steps. We used already atmospherically corrected images, as provided by the USGS via the Google Earth Engine platform. The image acquisitions by TM04, TM05 and ETM+ have been corrected using the LEDAPS algorithm (Landsat Ecosystem Disturbance Adaptive Processing System) [268]. Average residues of $\sim$0.004 to 0.010 have been reported for the accurate recovery of the surface reflectance of ETM+ [269]. Image acquisitions by OLI were corrected using the Landsat Surface Reflectance Code (LaSRC). While LEDAPS uses meteorological services to evaluate the parameters of atmospheric correction, LaSRC uses parameters estimated from the MODIS satellite constellation. The surface reflectance is considered to be captured more accurately by OLI than by previous sensors [270, 271, 272]. We selected only images without clouds or shadows on or close to the reaches. On each image, the cloud and shadow areas were masked according to the internal flags available in the product quality assessment (QA) layer.

4.3.3 Image Post-Processing and Vegetation Indices

The normalized difference vegetation index (NDVI) [273] was used in our study. NDVI varies according to the Leaf Area Index (LAI) and vegetation health among other sources of variation [274, 275, 276]. NDVI has been widely used in a broad range of applications such as estimation of productivity, response to environmental changes or trophic interactions [277]. However, NDVI has shown some inconsistencies in a few cases when comparing the state of vegetation at a given location over time [278, 279]. To complement the use of NDVI, we also extracted the vegetation fraction (VF) for each pixel, derived from Spectral Mixture Analysis (SMA) [280]. SMA, or unmixing, aims at retrieving the abundances of a number of selected spectra from a single pixel. The sparse vegetation and small patches of vegetation found on floodplains underpin the need for SMA (Figure 4.1). The SMA uses a restricted selection of spectra to estimate the contribution of pre-defined materials to the measured reflectance. A spectral library can be formed from the selected spectra, called spectral endmembers. The algorithm assumes that each pixel is a linear combination of the library's endmembers. We used a fully constrained linear spectral unmixing algorithm provided by the Google Earth Engine platform. While it has been shown that nonlinearity is important to retrieve accurate subpixel fractions [281, 282, 283],

we are here interested in relative changes, making the retrieval of absolute values not a necessity. For this reason, we consider the VF as an index in our study.

NDVI and VF are complementary rather than completely independent. By using them concurrently, potential issues in the data can be detected, such as hazy conditions or large variation in the water cover. The SMA allowed us to estimate the VF present in each pixel. We used a selection of 19 spectra from the ASTER spectral library as spectral endmembers [284]. Among the 19 spectra, three were vegetation spectra. To complement the selected 19 spectra, we included three additional vegetation spectra and two rock material spectra extracted specifically from the selected images, leading to a total of 24 spectra. The image post-processing includes three main components, i.e., (i) the delineation of a floodplain mask, (ii) the extraction of the NDVI distribution and (iii) the extraction of the VF distribution. The mask was created from the same center line for each year. First, we digitized a line in the center of the unvegetated area. The line was then rasterized, defining an initial mask at a resolution of 30m. Then, two steps were repeated iteratively. First, the initial mask was extended by one pixel in all directions. Then, pixels that contain a VF larger than or equal to 50 percent were removed from the mask. Repeating these steps several times results in a mask that covers all pixels in the section that have a VF smaller than 50 percent. Six repetitions extend the mask to a maximum width of 360m. The last step in the construction of the mask consisted of a final expansion of one pixel in all directions. This last step creates a mask robust to one-pixel variations of co-registration. The distributions of the NDVI and VF values were finally extracted for each year within the limits defined by the mask.

The theoretical range of NDVI is from -1 to 1. Negative values can be found over water bodies. The low positive values observed here generally correspond to bare soils, areas of unvegetated gravel, or a mixture of gravel and water. In general, the NDVI increases with vegetation cover and vegetation health. The possible values of VF range from 0 to 1. A VF value of 0 indicates a total absence of vegetation within a pixel, while a VF value of 1 indicates that the entire pixel is covered with vegetation. An intermediate value indicates that parts of the pixel are covered with vegetation. An intermediate value can be observed over different configurations, for example, if vegetation is sparse or because there is a clear boundary between land cover types. Also, intermediate values of NDVI and VF may indicate the presence of large woody debris in the pixel. It is indeed almost impossible to differentiate between very sparse vegetation and the presence of woody debris in a pixel because of the similar spectral signature of the two types of land cover.

4.3.4 Flow Variables

The discharge data were made available by the Swiss Hydrology Division of the Federal Office for the Environment (FOEN).

We chose gauging stations as close as possible to the study reaches (Figure B.1): Maggia - Bignasco, Ponte Nuovo 2475, Brenno - Loderio 2086, Allenbach - Adelboden 2232, and Sense - Thörishaus, Sensematt 2179.

Eight variables, which are expected to be related to floodplain vegetation dynamics, were calculated from maximum daily flow data of the selected hydrological stations for each period between satellite images (SI Table B.7). Only flow data until the exact image acquisition date were considered as part of the period. For example, if a satellite image was acquired over the Sense on July 17, 2014, the flood occurring on August 11, 2014, was then considered in the subsequent period (image 2015). The eight flow variables used in the analysis were:

- *Q2*, *Q10* and *Q30*: number of floods with return periods of n=2, 10 and 30 years. Commonly used to describe recurrence of floods with a certain magnitude [285]. *Qn* were extracted from the FOEN report for each gauging station, without catchment correction. For example, a *Q2* event is defined here as a day presenting a peak discharge equal or higher than the *Q2* discharge. A flood can be considered in multiple groups (i.e. if one *Q10* occurred, it was also considered as *Q2*, since it raises above both thresholds).
- *Qmax*: yearly maximum discharge [286, 287]
- *NM7Q2*: number of days with a daily average discharge lower than the lowest average discharge observed over seven consecutive days with a return period of two years (extracted from the FOEN reports). Commonly used to describe the effect of droughts periods [288, 289].
- *Q2 spring*, *Qmax spring*, *NM7Q2 spring*: *Q2*, *Qmax* and *NM7Q2* for the same growing season as the image acquisition, defined as starting from the first of April and lasting until the date of the image acquisition.

We then calculated the Spearman's rank correlation between the eight flow variables and the changes in NDVI median and VF median. A threshold of significance was set at an alpha value of 0.05 for the correlation. We did not apply a correction of type-I errors due to the limited sample size. The number of type-I errors is here inflated due to the number of tests carried out.

4.4 Results

4.4.1 Spearman's Rank Correlation

The *Q2*, *Q10* and *Qmax* and *Qmax spring* variables were negatively correlated at a significance level of 0.05 with changes in NDVI and VF along the Sense (Table B.2). Correlation coefficients were slightly higher for VF changes than for NDVI. Variables limited to the spring period showed similar statistical trends as the full-year variables, although they have lower correlation coefficients. Along the Maggia, the variables *NM7Q2* and *NM7Q2 spring* showed a statistically significant relationship

TABLE B.2: Coefficient of Spearman's rank correlation for the mask size (MS), NDVI and VF changes against the flow variables for the four reaches. Only the correlation coefficients statistically significant at an alpha value of 0.05 are shown.

	Sense			Allenbach			Maggia			Brenno		
	MS	NDVI	VF	MS	NDVI	VF	MS	NDVI	VF	MS	NDVI	VF
Q2	-	-0.52	-0.65	-	-	-	-	-	-	-	-	-
Q10	-	-0.5	-0.64	-	-	-	-	-	-	-	-	-
Q30	-	-	-	-	-	-	-	-	-	-	-	-
Qmax	-	-0.55	-0.65	-	-	-	-	-	-	-	-	-
NM7Q2	-	-	-	-	-	-	0.54	-	-	-	-	-
Q2 spring	-	-	-0.52	-	-	-	-	-	-	-	-	-
Qmax spring	-	-0.4	-0.53	-	-	-	-	-	-	-	-	-
NM7Q2 spring	-	-	-	-	-	-	0.43	-	-	-	-	-

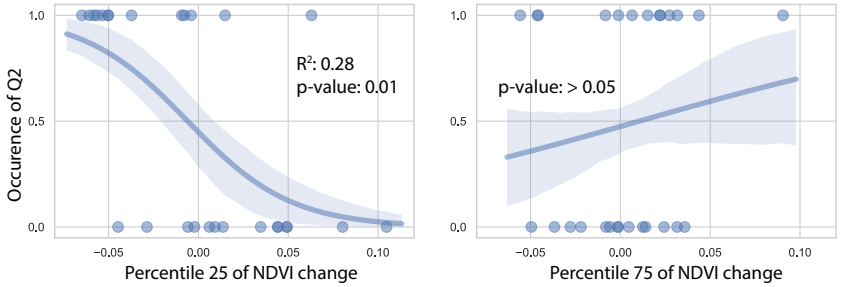

FIGURE 4.2: Logistic regression between the normalized difference vegetation index (NDVI) and the occurrence of preceding *Q2* events. For each image acquisition, absence of preceding events leads to a value of 0 and presence of at least one preceding *Q2* event leads to a value of 1.

with the change in mask size. No significant relationship was found between flow variables and variation of indices along the Allenbach and Brenno rivers.

Along the Sense, the regression between the occurrence of *Q2* events and the change in NDVI was examined more closely (Figure 4.2). The more detailed logistic model was restricted to the Sense, since the other reaches did not show statistical relations between the median of the indices and the flow variables. In particular, along the Sense, about half of the years in which at least one *Q2* event was present showed a negative change in the indices larger than the most extreme change observed without preceding *Q2* events. A logistic model was therefore tested between the occurrence of *Q2* events and percentiles of NDVI distribution. On the one hand, the 25th percentile of the NDVI distribution was correlated at a significance level of 0.05 with the occurrence of at least one *Q2* event. However, the 75th percentile of the NDVI distribution was not significantly correlated with the occurrence of *Q2* events. A very similar result was obtained from the VF distributions (SI Figures 4.7).

4.4.2 Indices Dynamics

Besides statistical analysis, a qualitative analysis between individual events and changes in indices was carried out (Figure 4.3).

In general, along the Sense, the Maggia and the Brenno rivers, presence of *Q10* or *Q30* events coincides with a decrease in indices. Periods with few flood events exhibit an increase in indices, such as from 1990 to 2005 along the Sense, from 2002 to 2007 along the Maggia (particularly on the NDVI), and from 1994 to 1999 and 2009 to 2015 along the Brenno. Along the Sense, the large flood event of 1990 ($489 m^3 s^{-1}$, return period: >150 years) coincided with an observed decrease in NDVI and VF, although the magnitude of the decrease is not as unique in the time series as the peak discharge.

Along the Allenbach, no pattern is qualitatively visible in the dynamics of the indices. The low VF values found in 2014 and 2015 coincided with relatively dry periods preceding the image acquisitions. Also along the Allenbach, the second part of the time series, from 2003 to 2016, showed some positive statistical relation between changes in indices and the occurrence of large floods, although this was not significant (SI Figures 4.5 and 4.6).

Overall, the NDVI values showed less variability than the VF values, both for mean values and for complete distributions (violin charts, SI Section 4). The presence of a statistical mode in the upper half of the NDVI and VF distributions, around 0.7 and 0.9 respectively, represents pixels that are found on entirely vegetated areas. Another mode in the lower half of the NDVI and VF distributions, around 0.3 and 0.1 respectively, typically represents pixels that are completely free of vegetation.

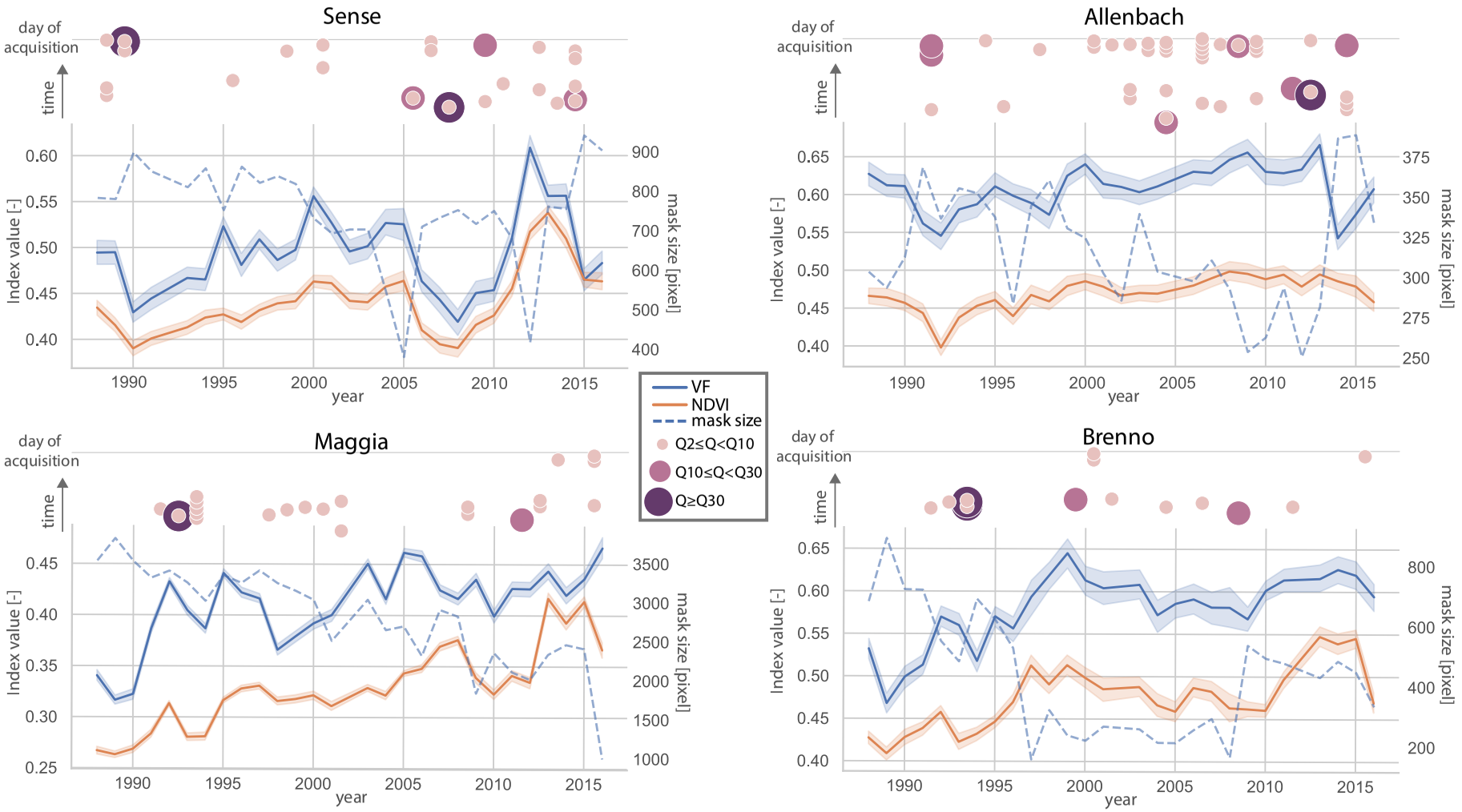

FIGURE 4.3: Mean values of the normalized difference vegetation index (NVDI) and Vegetation Fraction (VF) from 1988 to 2016 along the four investigated reaches (scale on the left axis) and mask size over which the indices were extracted for each year (right axis). The bands along the curves indicate a 68 percent ($\pm 1\sigma$) confidence interval. The x-axis depicts the year of image acquisition. The flood events happening between two acquisitions are centered between the image acquisitions along the x-axis. The flood event discs are vertically distributed (close - far) according to the time length preceding the next image acquisition.

4.4.3 Trend in the Time Series

The trends of the indices over the years were analyzed. Overall, the NDVI and VF distributions increased over the years (Figure 4.4). The median of the NDVI showed a significant increase over the years for all four reaches. The median of the VF only increased significantly over the years along the Maggia and Brenno reaches. The coefficient of determination (R^2) of the linear regression on the NDVI along the Maggia River was particularly high at 0.75.

An analysis of the auto-correlation function of the detrended time series did not reveal a significant level of auto-correlation beyond a one-year lag along the Sense, Allenbach and Brenno rivers. A significant level of autocorrelation was detected with a three-year delay for NDVI along the Maggia River. A significant level of autocorrelation with a one-year lag for all reaches has a small but existing impact on the significance of statistical tests performed on linear trends, which increases the rate of Type I error.

4.5 Discussion

4.5.1 Sensibility of Remotely Sensed Indices

The VF distribution is known to be sensitive to variations in the spectral characteristics of the land cover [290]. Therefore, changes in the spectral properties of a pixel can lead to variations in the estimated fraction of vegetation. The sensitivity of the VF is visible in the dynamics of the indices: some periods show variations in the VF, while the NDVI remains relatively stable between consecutive years. However, the changes described by spectral mixture analysis (SMA) may be more accurate than the changes described by NDVI [291], although NDVI and results from SMA are known for providing consistent information over a variety of environments [292, 293].

The violin charts (SI Section 4) revealed that flooding affects the shape of the NDVI and VF distributions by inflating the lower mode. An overall decrease in the two distributions indicates that individual flood events erode parts of the floodplain vegetation. In the representation of the complete distribution (SI Section 4), large variations in VF cannot be entirely attributed to shifts in the presence of vegetation, due to the high temporal resolution of image acquisition relative to the vegetation growth rate at high VF values. Although some pioneer species can develop rapidly on unvegetated gravel bars, some changes in VF associated with high VF values are typical of forest cover. It is therefore more likely that the variations observed in the higher mode of VF distribution are related to the reflective properties of the forests and grasslands surrounding the floodplain.

The variability in mask size has an influence on the change of indices. The mask size is expected to be inversely proportional to the average of the indices, since a greening of the floodplain should result in a smaller number of pixels with an FV

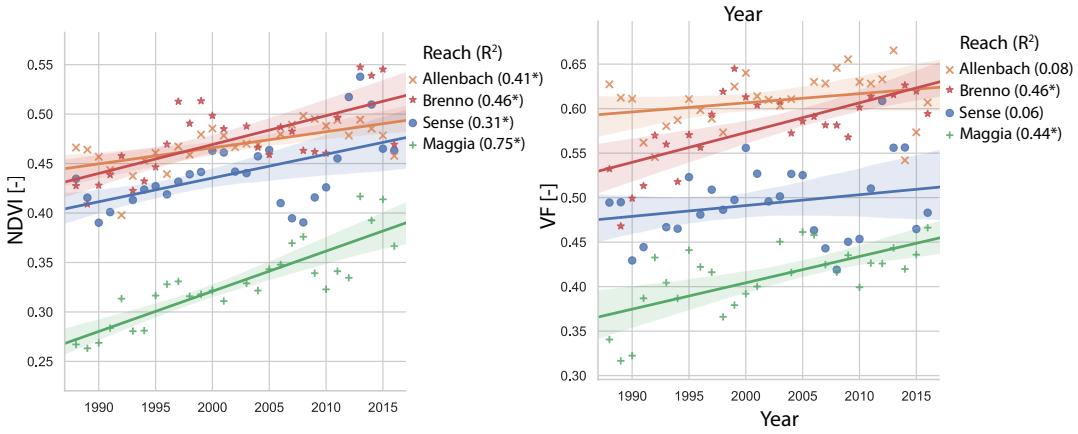

FIGURE 4.4: Linear regression between the year of image acquisition and median of NDVI and VF. The colored areas represent a confidence interval of 68% for the regression line. An asterisk (*) indicates a p-value smaller than 0.05.

below the 50 percent threshold. As a consequence, the NDVI and VF distributions can raise over the years either due to an overall greening or due to a thinning of the floodplain width.

4.5.2 Relation between Flow Variables and Remote Sensing Indices

Sense Reach Along the Sense River, periods with flood events generally coincide with decreases in NDVI and VF values, while no linear relationships are observed along the other three reaches. The magnitude of the flood events (represented by *Qmax*) and the number of flood events with a return period of 2 and 10 years (*Q2* and *Q10*) are statistically related to changes in the extracted indices. These observations are in line with the general principle that floods are one of the main drivers of habitat dynamics in floodplains [294, 295].

The impact of the major flood of 1990 on the indices ($489 m^3 s^{-1}$) is of the same magnitude as for the 2005 and 2014 floods ($246 m^3 s^{-1}$ and $299 m^3 s^{-1}$). The 2007 flood had less impact on the indices, probably due to erosion caused by the 2005 flood two years earlier. A remarkable difference between these events can, however, be found in the average daily flow. The average daily flow during the 1990 floods was $34.6 m^3 s$ and $32.9 m^3 s^{-1}$ on July 29 and 30, while the average daily flow was $147 m^3 s^{-1}$ on July 22, 2005 and $130 m^3 s$ on August 9, 2007. The very short duration of the flood event of 1990 can therefore be part of the explanation of a relatively weak change of indices despite the exceptional character of the flood event. This observation supports the fact that not only the flood peak is important, but also other characteristics such as the duration or the total energy of the flood event [296].

Another fact that can explain the relatively low impact of the flood of 1990 on the indices is that the retrieved indices do not necessarily reflect all the impacts of a flood on the floodplain land cover. Although large floods (*Q50*) have been observed to have significant effects on channel morphology [235], the impacts on floodplain

morphology may not be proportionally reflected by the impacts on the riparian vegetation [297]. In addition, the effects of flow regulation on vegetation structure may still be incomplete after several decades [298]. These elements can therefore explain the lack of change in vegetation indices after a single flood event with a very large peak discharge.

Instead, some studies have found a clearer statistical relationship between the frequency of moderate flooding (*Q1* to *Q10*) and changes in vegetation [299, 238, 251]. Furthermore, influences of major flooding (*Q100*) on specific vegetation characteristics, such as poplar recruitment on high terraces, have also been observed [238]. Nevertheless, the effect of floods on vegetation is still challenging to predict nowadays [300]. Given the complex processes linking flood events to the riparian vegetation structure, it is not surprising that the large flood of 1990 does not impact the indices in a prominent way.

Maggia and Brenno Reaches Along the two hydropower affected reaches of the Maggia and Brenno, although we observed a decrease in indices for most major floods, the absence of correlation can be explained by the presence of changes in the indices over years without flood events. The dynamics of the indices along these reaches are presumably related to the alteration of water flow by upstream hydropower facilities, in addition to other factors such as land use change or weather variation. The modification of the natural flow regime by dams or hydropower plants has a strong impact on erosion, transport and sediment deposition [191, 83] along with a variable response of floodplain vegetation [141]. Another study on the Maggia reach indicated that flow changes resulted in a loss of natural vegetation dynamics and a decrease in non-vegetated gravel bars [261]. Since the frequency of large flood events has not decreased [261], the absence of a statistical link between floods and the indices can suggest that the alteration of the sediment regime has a large influence on the development of the vegetation in the floodplains [233].

The co-occurrence of dry periods with an increase in mask size observed along the Maggia is probably related to the canopy leaf angle distribution, which changes the retrieved vegetation-free fraction per pixel in the spectral mixture analysis [301]. Consequently, it is expected that dry periods lead to a higher estimation of the vegetation-free fraction.

Along the Brenno, some years without *Q2* events show a decrease in the indices, leading to an absence of a statistical relationship. The observed decrease in the indices may result, in this case, from a limitation of the chosen approach: the construction of the floodplain mask for each single year may independently mask the areas of the floodplain in which strong plant growth occurs, resulting in a shrinking of the area under consideration and thus an "artificial" decrease in the indices. It is not possible to disentangle the effect of the mask size change from other changes without external data. Changes of the mask size are smaller along the other reaches, although present as well.

Allenbach Reach Along the Allenbach, no statistical relation was found between flow variables and indices. In contrast to the Sense, Brenno and Maggia reaches, the Allenbach floodplain is subject to fast variation in water flow and recurrent flood events due to storms [302]. Given the smaller size of the watershed, the Allenbach is subject to reduced variations in the intensity of flood events compared to the other reaches. This results in a floodplain with almost no presence of pioneer species and a well defined floodplain boundary. The delimitation between the surrounding vegetation areas and the vegetated zones of the floodplains is clearly defined. Such a floodplain structure is in line with an absence of statistical link between flow variables and NDVI and VF, therefore supporting the method developed in this study, since, as it would be expected along this reach, the flood events have a limited direct impact on the floodplain vegetation.

Periods with Few Disturbances Flood-free years generally coincide with an increase in NDVI and VF (Figure 4.3), although these links are not statistically significant. Vegetation growth in size and space has been observed during periods without flooding [251]. Also, some dynamics in NDVI and VF can be linked to previous floods, most likely representing recovery after a disturbance. Vegetation recovery after a major flood can occur in the short term [303, 304]. However, the vegetation can still be altered for decades [305, 298]. Periods of increased vegetation productivity following flooding have been observed using coarse resolution imagery in semi-arid environments [306]. Although floods are the main source of erosion of floodplain vegetation, they also create conditions favorable to the establishment of seedlings through the deposition of sediment and nutrients [307, 308]. The increase of NDVI and VF distributions after major floods may also be influenced by the deposition of woody debris on sediment bars, islands and terraces, as it occurs in the Sense River [36], introducing bursts of nutrients to these areas [309, 310, 311]. Finally, the floodplains of alpine rivers have been described as being very resistant and having a high recolonization capacity [312]. The dynamics observed over flood-free years show the importance of disturbance to support floodplain ecosystems by enabling habitat turn-over [238] and thus supporting establishment of unvegetated gravel bars, as well as pioneer vegetation.

4.5.3 Trends in Time Series

The indices retrieved along the Maggia and Brenno reaches and, to a lesser extent, along the Sense and Allenbach reaches, show an increase in the averages of the indices over the period considered. Such an increase in vegetation is in line with observations made in other studies along the Maggia [261] and Brenno [262]. The observed trends in vegetation dynamics may also be related to longer-term climate-related processes [3]. In general, river systems have been described as very sensitive to climate variation [313, 314].

An overall increase in vegetation cover leading to a shrinking of riparian areas is consistent with the expected response to climate change [315, 316, 317]. Changes in the flow regime of the Allenbach and the Sense River can potentially be triggered by climatic variations, since, to our knowledge, no large changes in the land cover have occurred in the watershed for the considered period. For example, from 1950 to 2016, three of the five largest peak discharges recorded by the Sense - Thörishaus station occurred in 2011, 2012 and 2015. A stable increase of the magnitude of *Qmax* is also visible in the flood statistics of the Allenbach - Adelboden station from 2011. Given all these elements, it would not be surprising that the observed changes in the indices retrieved over the floodplain vegetation are effects of climate variations in the Alps, although they could also be triggered by different causes such as land use changes or a combination of both.

The detected trends in the NDVI values may be partially affected by artifacts present in the satellite imagery. It is also possible, however unlikely given the rigorous calibration of the Landsat time series [267], that a shift in sensor performance affects the NDVI. It has previously been reported that the combination of LC07 acquisitions with TM acquisitions can lead to an artificial underlying trend in NDVI [318]. In addition, some differences were reported regarding the data acquisition by OLI and previous satellites sensors [319]. More specifically, lower values in the visible range were consistently observed for OLI, corresponding to a slight increase in the NDVI. However, the variations of the on-orbit gains (in the order of 0.5%) are lower than our observed dynamics [320]. It is also likely that the VF is less affected by a possible shift in the Landsat series surface reflectance data. In brief, while the NDVI shows a trend along all reaches, suggesting a climate-induced change, the VF index shows a trend only along the Brenno and Maggia rivers, suggesting a change induced by hydropower. In conclusion, while the trends may be affected by sensor performance, they are most likely caused by land use or climatic variations or a combination of them.

4.5.4 Limitations of Satellite Imagery

The satellite imagery used in our study captures multiple types of land cover changes that occur in a floodplain. However, it is not always possible to clearly separate the various types of change. For example, floods impact vegetation due to erosion from water or floating debris, or by prolonging the saturation of the root zone [11]. Substrate erosion is another cause of vegetation loss that can lead to changes in the indices, however on a longer time-scale. The erosion and deposition of substrate influence vegetation growth on the floodplains [321]. Change in resources availability can also lead to changes in the floodplain vegetation. Droughts, for example, have an important influence on floodplain vegetation [322]. Variations in water availability or in nitrogen availability are, however, not easily detectable using satellite imagery. Although water is frequently available for floodplain vegetation, the lack of soil or

the relatively coarse size of soil gravel do not store large amounts of water, making floodplain vegetation subject to significant and rapid changes in water availability [323, 324]. Also, the response of riparian vegetation to variation in groundwater can vary [323, 325].

In our observations, the periods of low water discharge are not well retrieved by the remotely sensed indices, although drought events have been observed by remote sensing through the NDVI statistics [326, 327]. The lack of sensitivity can be explained by the fact that the NDVI and VF values recovered in the poorly vegetated areas are mainly related to the proportion of vegetation, rather than the vegetation state. Since a stressful event, such as a drought, primarily affects vegetation health, it is expected that remotely sensed indices will not change substantially, as the relative proportion of vegetation is expected to remain stable. In other words, the variation in NDVI and FV over the floodplains is mainly driven by the vegetation fraction.

Another limitation of satellite imagery in our study relates to the description of changes in the sediment dynamics. Since such changes typically involves variation in the floodplain topography, generally without a large impact on the reflectance of the involved land cover, their observations from medium-resolution imagery are very challenging.

4.6 Conclusion

In conclusion, our observations confirm that satellite time series can support the study of floodplain ecosystems in mountainous and sub-mountainous river floodplains under the influence of flood events. The results suggest that it is important to take into account the sequence of flood events and their magnitude to contextualize the impact of a single flood on floodplain vegetation. To observe vegetation dynamics along rivers, we assessed the state of vegetation using NDVI and VF distributions of remotely sensed vegetation. Using NDVI in combination with a fraction of the vegetation estimated from a spectral mixture analysis has proven to be a robust approach to cloud disturbance and local reflectance variation. Therefore, time series of index distributions can be extracted in a robust way and thus be used to study inter-annual dynamics of vegetation conditions.

Overall, flood impacts were visible in the time series of indices averages and in the graphical representation of full indices distributions. We found a statistically significant relationship between changes in NDVI and VF distributions and flooding only along the sub-mountainous reach with a near-natural flow regime. A weak or non-existent statistical link was found along the altered reaches, as the flow alterations due to hydropower facilities modify or even completely disrupt floodplain dynamics. In addition, long-term trends in floodplain vegetation development were clearly depicted by the remotely sensed indices. However, it remains unclear whether the observed trends are caused by changes in the flow and sediment regime

due to hydropower production, watershed land use, climate variations, partly by sensor performance, or a combination of them.

We believe that the remote sensing approach used in this study can be transferred to other regions of the Earth, as it is not based on prior information. Satellite imagery can support river management at the catchment level [328], although the application of this approach appears to be limited to a large extent by the availability of accurate discharge data. Finally, we claim that satellite imagery has great potential, currently untapped, to better understand floodplain dynamics and anthropogenic impact to support the protection of floodplains worldwide.

4.7 Appendix

4.7.1 Satellite images

TABLE B.3: Information on satellite tiles used for the time series Sense 2003-2010. The *Discharge* column refers to the average daily discharge at the reference station of Sense - Thörishaus, Sensematt 2179. Blank years are due to the absence of appropriate images caused by cloudy conditions. OLI: Landsat 8 Operational Land Imager, ETM+: Landsat 7 Enhanced Thematic Mapper Plus, TM05: Landsat 5 Thematic Mapper, TM04: Landsat 4 Thematic Mapper

Year	Sensor	Tile	Date	Discharge
2016	OLI	196027	8.7.2016	6.17
2015	OLI	196027	7.4.2015	2.73
2014	OLI	196027	7.17.2014	6.60
2013	OLI	196027	7.14.2013	2.34
2012	ETM+	195927	8.29.2012	2.13
2011	ETM+	195028	8.11.2011	3.37
2010	ETM+	195027	7.7.2010	3.96
2009	ETM+	195028	7.20.2009	8.30
2008	ETM+	195027	8.18.2008	5.78
2007	ETM+	195027	7.15.2007	6.57
2006	ETM+	195027	7.12.2006	4.03
2005	ETM+	196027	8.17.2005	4.37
2004	ETM+	195027	7.22.2004	4.12
2003	TM05	196027	8.4.2003	1.54
2002	ETM+	195028	8.18.2002	5.50
2001	ETM+	195028	8.15.2001	3.19
2000	TM05	195028	8.20.2000	2.85
1999	TM05	195028	7.17.1999	6.80
1998	TM05	196027	8.6.1998	2.34
1997	TM05	196027	8.19.1997	3.26
1996	TM05	195027	8.9.1996	6.18
1995	TM05	195027	7.22.1995	4.13
1994	TM05	195027	8.4.1994	3.23
1993	TM05	196027	7.7.1993	10.55
1992				
1991	TM05	195028	7.11.1991	3.77
1990	TM05	195027	8.9.1990	3.10
1989	TM05	195027	7.5.1989	6.12
1988	TM04	195028	8.27.1988	4.73

TABLE B.4: Information on satellite tiles used for the Maggia reach. Please refer to caption of Table B.3. The reference station is Maggia - Bignasco, Ponte nuovo 2475.

Year	Sensor	Tile	Date	Discharge
2016	ETM+	195028	7.7.2016	1.83
2015	OLI	194028	8.7.2015	1.80
2014	OLI	194028	7.3.2014	1.87
2013	OLI	195028	7.23.2013	1.82
2012	ETM+	194028	7.21.2012	1.85
2011	ETM+	194028	7.3.2011	1.83
2010	ETM+	194028	8.1.2010	1.84
2009	ETM+	194028	8.14.2009	2.00
2008	TM05	195028	7.25.2008	1.84
2007	TM05	194028	7.16.2007	1.89
2006	ETM+	194028	7.21.2006	1.94
2005	TM05	194028	6.24.2005	1.90
2004	ETM+	194028	6.29.2004	1.93
2003	TM05	195028	8.13.2003	1.88
2002				
2001	ETM+	195028	7.30.2001	2.40
2000	TM05	195028	7.19.2000	1.96
1999	TM05	194028	7.26.1999	1.84
1998	TM05	194028	8.8.1998	1.91
1997	TM05	195028	8.12.1997	1.95
1996	TM05	194028	8.2.1996	1.88
1995	TM05	194028	6.29.1995	2.58
1994	TM05	195028	8.4.1994	1.92
1993	TM05	195028	8.17.1993	1.77
1992	TM05	194028	8.7.1992	1.82
1991	TM05	194028	8.5.1991	1.84
1990	TM05	194028	8.18.1990	1.75
1989	TM05	194028	8.31.1989	1.75
1988	TM05	195028	7.18.1988	1.76

TABLE B.5: Information on satellite tiles used for the Allenbach reach. Please refer to caption of Table B.3. The reference station is Allenbach - Adelboden 2232.

Year	Sensor	Tile	Date	Discharge
2016	ETM+	195028	8.8.2016	1.10
2015	OLI	195028	8.30.2015	0.65
2014	OLI	195028	6.8.2014	1.42
2013	ETM+	195028	7.31.2013	1.30
2012	ETM+	195028	7.12.2012	0.70
2011	ETM+	195028	8.11.2011	1.10
2010	ETM+	195028	7.7.2010	1.38
2009	ETM+	195028	7.20.2009	1.45
2008	ETM+	195028	8.18.2008	1.29
2007	ETM+	195028	7.15.2007	2.33
2006	TM05	195028	7.20.2006	1.21
2005				
2004	TM05	195028	7.14.2004	0.78
2003	ETM+	195028	8.5.2003	0.47
2002	ETM+	195028	8.18.2002	0.92
2001	TM05	195028	7.22.2001	2.39
2000	ETM+	195028	8.12.2000	0.91
1999	ETM+	195028	7.25.1999	0.98
1998	TM05	195028	8.31.1998	0.39
1997	TM05	195028	7.27.1997	2.07
1996	TM05	195028	8.9.1996	0.84
1995	TM05	195028	7.22.1995	1.21
1994	TM05	195028	8.4.1994	0.65
1993	TM05	195028	7.16.1993	1.19
1992	TM05	195028	8.30.1992	0.59
1991	TM05	195028	6.25.1991	3.45
1990	TM05	195028	8.9.1990	0.44
1989	TM05	195028	7.21.1989	0.78
1988	TM05	195028	8.19.1988	0.42

TABLE B.6: Information on satellite tiles used for the Brenno reach. Please refer to caption of Table B.3. The reference station is Brenno - Loderio 2086.

Year	Sensor	Tile	Date	Discharge
2016	ETM+	194028	7.16.2016	3.71
2015	OLI	194028	8.7.2015	1.86
2014	OLI	194028	8.4.2014	5.43
2013	OLI	194028	8.1.2013	2.37
2012				
2011	ETM+	194028	7.3.2011	2.12
2010	ETM+	194028	7.16.2010	3.05
2009	ETM+	194028	8.14.2009	3.97
2008	ETM+	194028	8.27.2008	2.38
2007	TM05	194028	7.16.2007	3.58
2006	TM05	194028	7.13.2006	1.43
2005	TM05	194028	6.24.2005	2.04
2004	ETM+	194028	6.29.2004	2.46
2003	TM05	194028	8.6.2003	1.41
2002				
2001	ETM+	194028	7.23.2001	7.22
2000	ETM+	194028	6.18.2000	3.24
1999	TM05	194028	7.26.1999	3.18
1998	TM05	194028	8.8.1998	2.81
1997	TM05	194028	8.21.1997	2.91
1996	TM05	194028	8.18.1996	2.57
1995	TM05	194028	6.29.1995	3.30
1994	TM05	194028	7.28.1994	2.77
1993	TM05	194028	6.7.1993	4.18
1992	TM05	194028	8.7.1992	2.42
1991	TM05	194028	8.5.1991	1.72
1990	TM04	194028	7.9.1990	3.91
1989	TM05	194028	8.31.1989	2.12
1988	TM05	194028	7.11.1988	7.76

4.7.2 Complementary Information on the Flow Variables

TABLE B.7: Extended definition of the flow variables. The thresholds defined for the flow variables (Q2, Q10, Q30 and NM7Q) were extracted from reports made available by the Hydrology Division of the Federal Office for the Environment (FOEN).

Q2	Number of days since the last image acquisition with a peak discharge equaling or exceeding the Q2 threshold, being the discharge with a return period of 2 years
Q10	Number of days since the last image acquisition with a peak discharge equaling or exceeding the Q10 threshold, being the discharge with a return period of 10 years
Q30	Number of days since the last image acquisition with a peak discharge equaling or exceeding the Q30 threshold, being the discharge with a return period of 30 years
Qmax	Maximum peak discharge observed since the last image acquisition
NM7Q2	Number of days since the last image acquisition with a peak discharge equaling or below a threshold defined as being the NM7Q with a return period of 2 years (The NM7Q extracted from FOEN report (see manuscript), is defined as "The annual minimum discharge levels recorded during 7 consecutive days").
Q2 spring	Similar to Q2, with flow data restricted from April 1st to the date of image acquisition
Qmax spring	Similar to Qmax with flow data restricted from April 1st to the date of image acquisition
NM7Q2 spring	Similar to NM7Q2 with flow data restricted from April 1st to the date of image acquisition

4.7.3 Complementary figures on links between flood events and indices

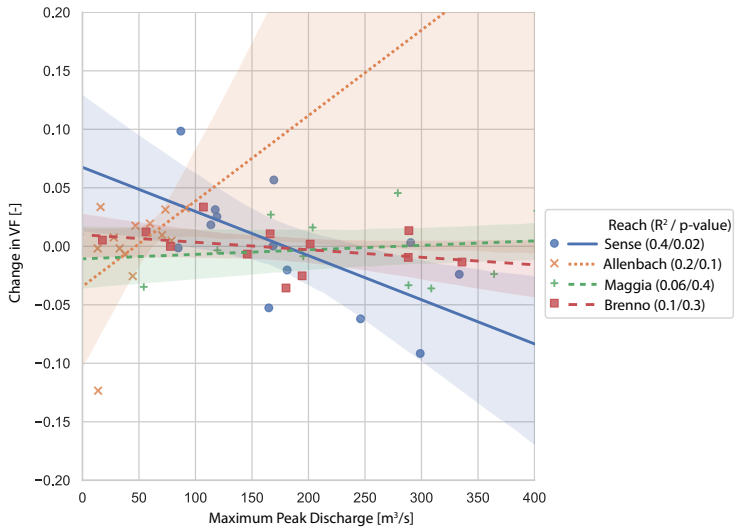

FIGURE 4.5: Linear regression between the maximum peak discharge and the change in the vegetation fraction (VF) along the four reaches for the years 2003 to 2016. A p-value under 0.05 is found for the slope coefficient along the Sense reach.

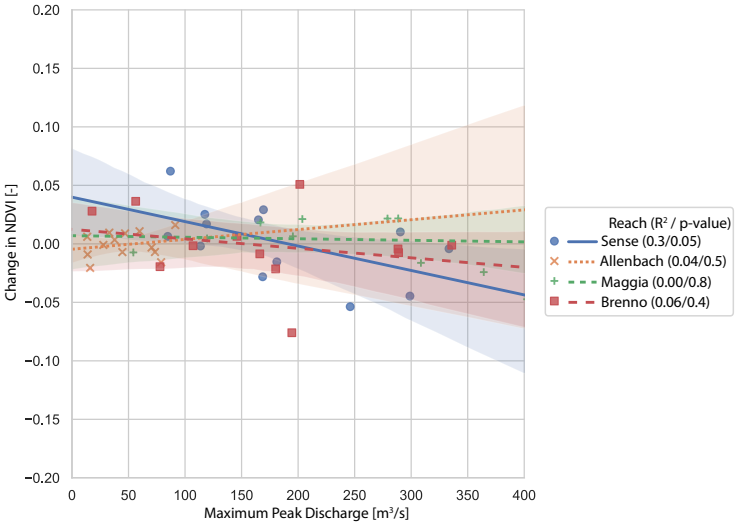

FIGURE 4.6: Linear regression between the maximum peak discharge and the change in the normalized difference vegetation index (NDVI) along the four reaches for the years 2003 to 2016. A p-value if 0.05 is found for the slope coefficient along the Sense reach.

4.7.4 Complementary figures of time series

For each time series, we present the distribution of NDVI and VF by violin graphs [329]. The violin graph displays a smoothed kernel density estimation of the underlying histogram. Violin graph ease the comparison of multiple distributions next to each other by smoothing extreme peaks and reducing the data noise.

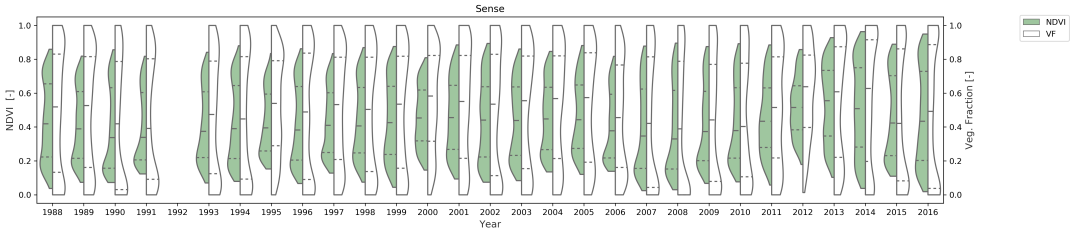

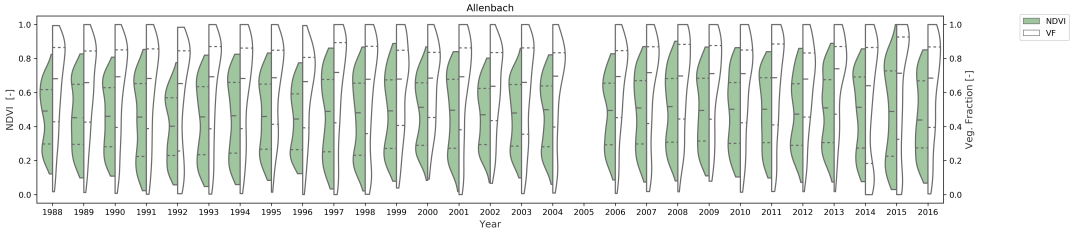

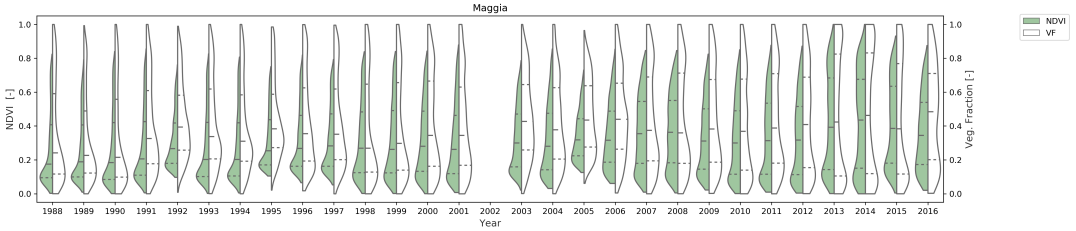

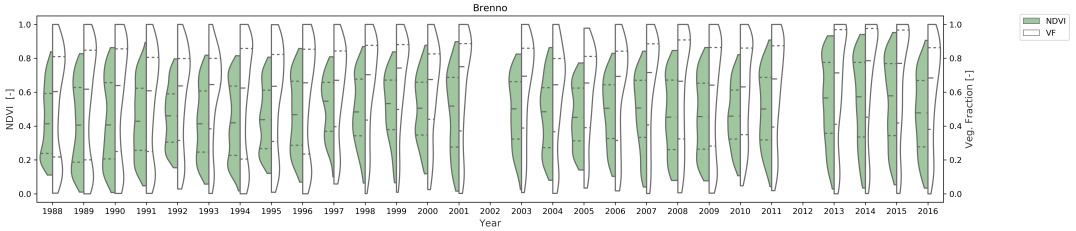

4.7.5 Complementary information on the link between VF and occurrence of $Q2$ events

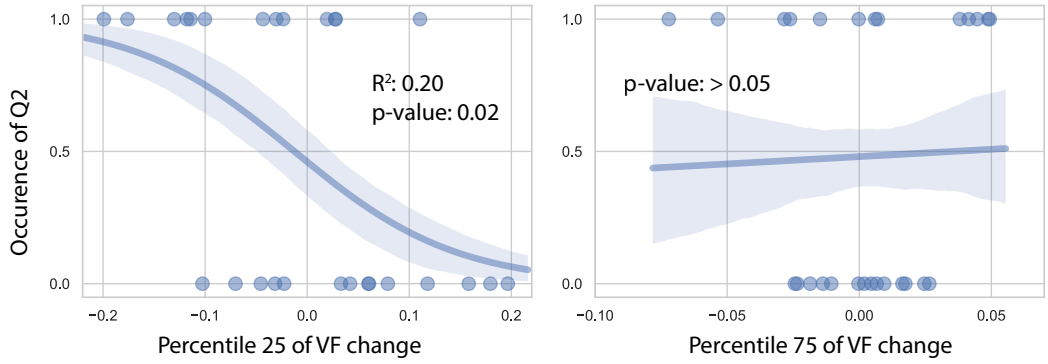

FIGURE 4.7: Logistic regression between the vegetation fraction (VF) and the occurrence of preceding $Q2$ events. Absence of preceding events leads to a value of 0 and presence of at least one $Q2$ event leads to a value of 1 for the samples.

Chapter 5

Synopsis

5.1 Summary

First, the main conclusions of each chapter are summarised through the answers to the questions asked in the Section 1.5. Then, the main questions of the thesis, as well as the implications of the results, will be examined and discussed in details.

5.1.1 Quantification of riverine habitat dynamics

Which habitats of the riverine landscape exhibit the largest changes between seasons? The interface between the water channel and gravel areas shows the most significant change. This interface has a particularly high dynamic range along the natural reach. Along the hydropeaking reach, a strong dynamics at this interface is also observed. However, this result is not valid along the remaining stretch, but this is not surprising given the very small size of the gravel areas found there.

Which components of the riverine landscape represents at best the riverine habitats dynamics? The interface between the water channel and gravel areas is also the best candidate to represent river habitat dynamics. The fact that this interface also presents important changes contributes to the good representation of the dynamics for this type of change, since the errors entered by the post-classification change detection framework are minimised by the strong signal of this interface. The high accuracy of change mapping on this interface is not obvious, as the boundary between gravel and water is not always clear.

Which characteristics of high-resolution imagery are the most important to map riverine habitats? The information on point clouds from the photogrammetric process improves the accuracy of the classification. In all cases considered, the use of a complex approach based on a spatially heterogeneous pixel-based / object-based classification gave the best results. Spectral data (as opposed to 3D information and texture) are the most important characteristics for mapping water and gravel areas using infrared cameras. The delineation between gravel and water can be expected to be well depicted using an infrared bands.

In short, some recommendations for quantifying river habitat dynamics by high-resolution imagery can be given. First of all, it is necessary to focus mainly on the interface between gravel and water to estimate the overall dynamics of the system.

This is more easily implemented with an infrared camera, regardless of the season. For best results, complex classification schemes involving the use of segmentation, texture and 3D information should not be feared. I believe that these results can help to monitor the state of rivers in Switzerland and other parts of the world and contribute directly to the objective of NRP70.

5.1.2 Impact of water flow alteration on plant traits

Can we map resource allocation strategies at the individual level using imaging spectroscopy? Partial least squares regression (PLSR) was used to predict CSR scores by imaging spectroscopy. A coefficient of determination (R^2_{cv}) from $\sim$0.41 to $\sim$0.55 was obtained for all three strategic directions. The CSR scores used to calibrate the PLSR were calculated with the StrateFy model [35]. The results are therefore only valid if the StrateFy model correctly captures changes in CSR scores at the intra-species level, which still needs to be proven.

Is there a difference between the resource allocation strategies found along the different reaches considered? A significant difference in the average CSR-scores among the different reaches. More specifically, the natural reach hosts individuals with a higher S-score while the altered reach hosts individuals with higher C and R-scores. A change is also observed in strategies towards a higher S score during the summer. This observation can be related to the dry month of August 2016, preceding the second data collection.

What are the processes shaping the plant traits of floodplain vegetation following a flow alteration? Although the study focuses more on describing levels than on processes, some hypotheses can be made about the formation of plant traits, but without providing solid evidence. According to Grime's theory, the difference in CSR scores between reaches is due to different levels of disturbance or stress. Here, the advantage of considering CSR scores is the grouping of a multitude of plant characters into a simple classification system. Based on observations, differences between the reaches may be due to higher stress levels along the natural reach and/or higher levels of disturbance along the modified reaches. However, it is unlikely that the level of disturbance will be higher along the altered reaches, as most of the dynamics observed in the floodplain have been reduced, such as flooding, sediment or the transport of woody debris. The difference between the reaches must therefore be controlled by a different level of stress. The differences observed in the CSR scores presented in the previous question are therefore in line with expectations: individuals along the natural reach generally grow on gravel banks with a thin layer of soil, making riparian vegetation subject to variations in water and nutrient availability.

5.1.3 Inter-annual dynamics of vegetation status

How can we extract information from medium-resolution satellite data archives on relatively small rivers ? In Chapter 4, I developed a method to use medium-resolution imagery

to obtain information on inter-annual changes in vegetation condition. The main idea was to focus on river reaches with open gravel and sparse vegetation to use areas with low fractional vegetation cover. This approach allows vegetation indices to be used in a more robust way than in fully vegetated areas, since most of them saturate at high fractional coverage. The areas of sparsely vegetated areas helped also to detect the increase or decrease in vegetation along the reach. Although this approach has produced consistent results in the floodplains examined in this chapter, it is not transferable to any form of river that does not have large enough gravel bars.

Which characteristics of the flood events sequence impact the vegetation status retrieved by remote sensing ? The results of chapter 4 show that only the Sense reach shows a significant correlation between flood occurrence and vegetation index dynamics. For the Allenbach reach, which is at a relatively high elevation and has a fairly clear boundary between the channel and shoreline vegetation and is subject to frequent storm-induced floods, it is not surprising to have an independence between floods and plant dynamics. However, the situation is more complex along the Brenno and Maggia rivers. hydropower production has an impact on the water flow of these sections, mainly by reducing the total annual flow. However, floods of the same magnitude as those that existed before the modification are still present. Large floods are key determinants of river geomorphology and shape the relief of floodplains, which in turn supports riparian vegetation. The lack of correlation between vegetation dynamics and flooding along the Maggia and Brenno rivers suggests that the formation of riparian vegetation is due to more complex characteristics of the flood sequence than large floods alone. These results, although not clearly established, may be of crucial importance for floodplain management in Switzerland in the coming decades.

Does the vegetation of Swiss alpine sub-mountainous braided rivers exhibit a trend over recent decades, and what are the most likely drivers of the trend? Along the Maggia and the Brenno rivers, since the implementation of the hydropower facilities in the middle of the 20th century, there has been an increase in riparian vegetation and a narrowing of the channel. This narrowing is also visible in the dynamics of vegetation indices extracted from satellite imagery. Along the Sense and Allenbach rivers, there is also an increase in the NDVI index throughout the year, but not on the fractional coverage extracted by mixing spectral analysis. It is not clear whether the observed trend is due to natural variations, bias introduced by changes in sensor characteristics and calibrations, or whether the trend is related to climate variation throughout the Alpine region.

5.2 Outcome

The three studies presented in the Chapters 2, 3 and 4 each focus on a specific aspect of floodplains. However, they can be considered complementary rather than strictly

independent of each other. By considering the different approaches as a whole, we can identify some points that emerge from these studies. In the following section, three discussions are therefore developed on the basis of the fusion and articulation of the three main chapters of the thesis. The first point concerns the methodology for extracting information from remote sensing products for river science. The second point concerns the impacts of flow alteration on plants. Finally, the third point opens a complex but important discussion on the impact of the results on the management of hydropower infrastructure.

5.2.1 Which features of airborne and spaceborne imagery allow a robust description of the riverine landscape and its dynamics?

We have seen in Chapter 2 that a robust estimation of river habitat dynamics based on high-resolution images is possible by focusing on the water-gravel interface. In parallel with these results, I have shown that the 3D information extracted considerably increases the accuracy of the classification. In this study, the recording of high-resolution multimodal images was successfully performed using mutual information metrics. In Chapter 3, we saw that standard statistical tools are not appropriate for comparing different systems. It was therefore necessary to adapt the statistical approach to allow a correct description of the river landscape. I applied t-tests on the average of the recovered plant characteristics to compare the different systems considered. Since the data along each section had a relatively high autocorrelation, I used the approach proposed by Griffith [180] to use an effective sample size. In Chapter 4, the quantities used to describe the river landscape are the NDVI index and the fractional coverage calculated from the spectral analysis of the mixtures. Both quantities have advantages and disadvantages, leading to a more robust description of the object of interest when used together. Overall, the chapters are based on different technologies and, as a result, the interest characteristics of the data acquired differ according to the approaches. This variety of approaches suggests that each technology used in this thesis has described another aspect of the river landscape and are complementary to each other. A common conclusion from the different chapters is found in the use of remote sensing to augment some specific information on the river system, at few locations in space and time, with more measurements, providing more robust estimations. The range of technology spanned in the dissertation highlights directly the advantages and capabilities of each system. The various works were successfully carried out, less by constraining the detection system than the object under study. A direct answer to the question posed as a section title would be that the specificity of land cover allows for a robust description of the river landscape, such as the spatio-temporal relationships between water, gravel and vegetation cover.

River channel dynamics were mapped by remote sensing using various approaches [330, 331, 332]. Although it is easier and faster than ever to map channel changes

with remote sensing products, very high quality maps have been produced in the past by ground survey, such as the famous Fisk map of the Mississippi Meander Belt. Monitoring of small-scale river dynamics has rarely been the subject of research studies. While the development of river habitat classification and monitoring has increased considerably in recent years [85, 333], the focus has almost never been on habitat dynamics. The emergence of the use of UAS for river science has been driven by the ability of these systems to describe geomorphological changes in floodplains [334, 335, 336]. Bertoldi et al. (2011) [47] have demonstrated early use of satellite remote sensing to monitor changes in riparian vegetation. More recently, bare movements have been monitored by high-resolution remote sensing [337]. River habitat studies allow a more integrated use of remote sensing for ecohydrological applications [338, 339, 340]. In the current state of use of remote sensing technology for river science, this thesis contributes particularly to the use of remote sensing for small rivers.

5.2.2 Which impact does an alteration of the water flow have on riparian vegetation?

Only few data are available on the ecological status of riparian ecosystems before and after dam construction. This is why many studies have focused on comparisons between the upstream and downstream sections of dams. The problem with this approach is that often, some alterations are found even further upstream, up to the limit of the vegetation in the mountains. In the case of this thesis, we considered two rivers located in the same region, with similar characteristics in terms of geology, flora and watershed, while a river has been affected by the presence of a dam and hydropower plant since 1954. The presence of these obstacles makes it possible to take into account two distinct river sections with different water and sediment regimes in Chapters 2 and 3, in comparison with a section representing the natural reference. To complement the observations made in these two studies, Chapter 4 discusses observations made along the Sense River and three other underwater rivers with large open gravel banks, two of which are also influenced by changes in water flow through hydropower production.

The studies presented here suggest that the processes that shape the plant characteristics of riparian vegetation operate over a relatively long period of time. Chapter 3 shows that the conditions encountered along the rivers considered seem to have an impact on willow resource allocation strategies, which should be a relatively stable status for the plant. However, it is not clear whether the difference between reaches is due to plastic changes in individuals or differences in community composition. In Chapter 2, we observed a greater dynamic between riparian vegetation and open gravel areas along the altered sections compared to the natural reference. This dynamic can be attributed to the growth of grasses and petasites in areas that are regularly submerged. These communities are only found in small quantities

along the natural stretch, suggesting that the change in flow regime also has an impact on the composition of riparian vegetation communities. In Chapter 4, satellite time series covering a total of 29 years are used. In these time series, we observe trends in overall land cover on floodplains, particularly along the sections affected by upstream hydropower production. Although the observations made here are not directly related to plant traits, other data sources and studies on the same objects reveal a shift from riparian areas to a forest ecosystem, resulting in a narrowing of the channel. Stream narrowing after dam implementation is a typical impact observed after dam implementation, although often observed very quickly [12]. The examination of hydropeaking impacts on riparian vegetation is consistent with our observations [341]: daily variations in water level create areas suitable for colonisation by ruderal plants supporting submerged conditions. This thesis contributes to this discussion by showing that the effect of flow alteration along the hydropeaking reach also modifies the characteristics of plants that are not directly affected by the change in water level, such as most willow stands examined in Chapter 3. The expansion of vegetation along the Maggia has already been described by previous studies considering the same section [253, 257]. The fact that a similar inference can be drawn from the Earth observation data archives suggests that taking into account river sections at different locations could be considered and controlled in the same way.

5.2.3 What characteristics of the water flow are necessary to support floodplains functioning?

To help answer this question, our results must be placed in a broader and applied research context. In the following paragraphs, the aim is therefore to give a clear and definitive answer to this question, but to add an element of discussion to it in the constantly increasing knowledge resource. Understanding the water flow characteristics necessary for the functioning of floodplains would lead to better management of the downstream ecosystem and hydropower resources. An important element of this understanding is the description of the interaction between water flow alteration and ecosystem change.

The extensive review of Poff published in 2009 [192], which reviews 165 studies to draw quantitative conclusions on the impact of water flow modification, showed only mixed conclusions in predicting flow characteristics on ecosystems. Although a clear link was established between the change in water flow, especially peak flow, and ecosystem change, no conclusion could have been drawn between the type of change and the type of subsequent change. This review, although ten years old, highlights the need and current state of our understanding of the links between water flow characteristics and riparian ecosystems.

Although understanding river processes is of paramount and necessary importance in the current development of our society, they are the subject of active research all over the world. Currently, water flow management focuses on the design and implementation of environmental flows. In 2017, the Brisbane Declaration on Environmental Flows was revised to become [342]:

> *"Environmental flows describe the quantity, timing, and quality of freshwater flows and levels necessary to sustain aquatic ecosystems which, in turn, support human cultures, economies, sustainable livelihoods, and well-being."*

The implementation of environmental flows is hampered on several fronts, including the transferability of guidelines, the availability of water resources for the required flow and an understanding of the impact of controlled flooding on ecosystems. The study of environmental flow needs is an active area of research and it is known that environmental flow recommendations are difficult to transfer from one region to another [343, 344], although the needs assessment method could be. Due to the difficulties of imitating the natural flow regime downstream of the dam, water management based on specific and targeted impacts, called *designer flows*, has attracted some interest in recent years [345]. Long-term monitoring of flow-controlled sections of rivers is still rare, but of primary interest. For example, long-term monitoring of the Spöl River in Switzerland shows that ecosystem conditions have improved by supporting the resilience of the system to significant disturbances [346]. Although this study presents positive of effect of control flooding, observations were only collected on the aquatic portion of riparian ecosystems. The study of environmental flows and the understanding of river processes is increasing day by day. However, as illustrated above (and also explicitly mentioned by the above definition of environmental flow), the focus is often on the aquatic part of the river ecosystem.

Only recently has the importance of including riparian areas in environmental flow planning been emphasised [347, 348]. This thesis contributes to the discussion on the flow characteristics required to maintain a natural state of riparian ecosystems. In Chapter 3, the summer drought stress period is an important component of riparian vegetation. In this context, a minimum residual flow with an environmental flow is not likely to restore drought dynamics in the river landscape. Droughts are natural phenomena that occur on undisturbed floodplains and can have positive consequences, although riparian vegetation is likely to decline in such cases [349, 348]. In Chapter 4, high flows are observed over the Maggia and Brenno rivers, although a steady extension of vegetation cover has been observed in recent decades. This observation is consistent with models showing that homogenisation of flow would degrade the structure of riparian vegetation [350]. In Chapter 2, a high dynamic at the gravel-water interface is observed along the natural river. This observation raises the question of the relevance of the sediment regime in natural systems and its interactions with riparian environments. In the discussion of environmental

flow, sediment flow is often considered less important than water flow [233]. Sediment flow management to restore ecosystem functioning is also an area of research actively studied in Switzerland [351]. Sediment flow can reveal important characteristics related to the riparian ecosystem, for example by increasing the erosivity of flow through the presence of sediments [352].

Without being the real focus of the thesis, the present results suggest that the impact of floods depends on the overall characteristics of the sequence rather than the magnitude of individual floods. Although it is now believed that riparian vegetation is mainly shaped by major floods that affect the river's landscape, more frequent, smaller events, which are generally the main drivers of sediment transport, could also have a significant impact on the riparian ecosystem. Such a sediment-laden flow would have a greater erosive power on riverbanks and their presence could explain the more frequent destruction of riparian areas along unmodified floodplains.

5.3 Conclusion

The basis for this research was the observation of river dynamics and riparian vegetation conditions using remote sensing techniques to support and complement ground-based observations. The research was conducted in an important societal context provided by Switzerland's National Research Project 70: Energy turnaround. While the overall research project aimed at contributing to ensuring a sustainable energy policy for the country, the work carried out in the frame of this dissertation focused on the ecological impact of hydropower production. The ultimate aim underlying the research carried out was the search for optimised water management between electricity production and support for riparian ecosystems. The research conducted is closely linked to the specific issues found along Swiss rivers, and this thesis presents an important methodological aspect on the use of information extraction methodology from remotely sensed data.

5.3.1 Contributions to the Research

Methodological approaches have been developed to carry out research and extract valuable information from remote sensing data. The most important methodological contributions include i) the recording of multimodal imagery of drones (Chapter 2), ii) the development of a spatially heterogeneous classification framework based on pixels and objects, adapted to the classification of river land cover (Chapter 2), iii) the mapping of relatively small woody debris with UAS (Chapter 2), iv) the mapping of CSR scores at the individual level (Chapter 3) and v) the use of average satellite imagery archives on sub-mountainous rivers (Chapter 4). Referring to Chapter 3, a note on the mapping of plant characteristics should be highlighted here: the absence of statistical links between plant characteristics and modelled spectral response or

laboratory measurements should not prevent scientists from mapping plant characteristics in the field. For example, it is very likely that the CSR scores of the maps produced in this thesis are based on a statistical relationship between spectroscopic data and variables external to the plant characteristics considered, including the spectral response of the background.

In addition to the methodological contribution to the field of remote sensing, applied ecological contributions have been made in this thesis. The previous Section 5.2 expands on the results of the main chapters to obtain meaningful outcomes. The new knowledge acquired through this thesis has found its place in current research on floodplains and riparian vegetation. In addition, recommendations for monitoring river habitat dynamics have been developed in Chapter 2. These recommendations can be easily put into practice and could serve as a unified means of monitoring and quantifying river habitat dynamics throughout Switzerland.

Although the approaches developed in each of the chapters were effective in the cases presented, multiple attempts to develop methods for similar or different tasks were attempted in the context of this thesis, but they were not presented because they did not achieve a satisfactory level of quality (e.g. predictive power or classification accuracy). The wide variation in land cover and vegetation types at different scales across the river landscape makes any type of airborne or spaceborne measurement complex. Moreover, not all the approaches presented in the main chapters of the thesis are easily transferable to any environment without adaptation. For example, the practical existence of willow stands found along all sections is highlighted in Chapter 3, which can make it difficult to transfer research to environments without appropriate vegetation to achieve the necessary data quality. In addition, the study in Chapter 4 is not fully reproducible for sections that do not have sufficient water discharge data. In conclusion, with regard to the methodological contributions of this thesis, the various studies undertaken indicate that remote sensing is informative on riparian environments, but cannot be carried out without substantial adaptations.

5.3.2 River Systems under a Changing Climate – Conflicts and Synergies

The title of this section is an allusion to the document "*Biodiversité et climat: conflits et synergies au niveau des mesures, Prise de position de l'Académie suisse des sciences naturelles (SCNAT)*" (Biodiversity and climate: conflicts and synergies in the measures, stance from the Swiss Academy of Sciences). The expected situation of the floodplains in Switzerland in the near future is well summarised in the summary of this report (translated from the French version):

> *"Except for the increase of the existing installation efficiency, an additional extension [of CO_2-free hydropower production] is virtually feasible only if the level of residual discharge, already low, is further lowered or if the river reaches still not equipped [with hydropower installations] are also exploited."*

Although the report was published in 2008, the conclusions are still valid today. The situation may even deteriorate, given the current economic instability affecting the hydropower sector. Since climate change can increase the frequency and magnitude of floods [353], its expected impact on the floodplain is not clearly predicted. Expected trends in the water cycle in Switzerland include a decrease in summer precipitation, an increase in the frequency of flooding in winter and spring and a decrease in snowfall. However, the direct impact of climate change is not expected to be significant for floodplain ecosystems, since anthropogenic impacts through dams, flood protection and bank stabilisation already contribute to the near total annihilation of natural floodplains. The pressure of climate change is therefore reflected in the continued adaptation of water management to hydropower production. The results of this thesis can only support the SCNAT's message from the above-mentioned report, namely not to further reduce the already low residual flow in most Swiss rivers.

The results of this thesis also suggest that other solutions, not directly related to water flow, should be explored. For example, since the effects of vegetation on the channel are now better understood, direct management of riparian vegetation may be possible, with hopefully other positive impacts on the aquatic portion of the river's ecosystems. To imagine one possible measure, clearcutting, which has a dramatic impact on forest ecosystems, could be positive if applied locally to a specific site in riparian areas where intrinsic and recurrent destruction of the established ecosystem is part of environmental processes. However, these disturbances have only been the subject of a few studies [354, 355] and the expected evolution of the river system is unknown. This reflection leads us to draw some conclusions about the possible continuation of the work undertaken throughout this thesis.

5.3.3 Outlook

The results of this thesis encourage the use of remote sensing for river system monitoring, both locally, using multispectral UAS data or airborne imaging spectroscopy technology to focus on a specific and controlled system, and on a large scale, using satellite remote sensing for long-term river system development. The knowledge acquired and methods developed in this thesis show that research on riparian habitat dynamics and vegetation still requires additional efforts on multiple levels.

I personally believe that good research is research that raises more questions than the number of answer it gives. I will therefore conclude this thesis with some questions opened by the research conducted here:

- To what extend does the CSR-score quantification defined by the Stratefy models confidently represent the variations occurring at the intra-species level?
- Is the current trend observed in vegetation indices along Alpine rivers (already) driven by a change in climate?

- To what extent is groundwater variation a key factor in supporting the presence of floodplain vegetation?
- What are the variations in the water table that cause water stress in riparian vegetation along natural reaches?
- Is water stress part of the environmental conditions that support natural floodplains?
- What is the potential of imaging spectroscopy to initiate physical modeling of river systems?
- Are the observed dynamics between gravel and water areas universal between braided rivers with natural dynamics and how can a universal dynamics indicator based on remote sensing products be extracted?

Bibliography

[1] R. Müller-Wenk, F. Huber, N. Kuhn, and A. Peter, "Riverine floodplain use and environmental damage," *Environmental Series No. 361: Nature and Landscape Life Cycle Assessments*, p. 76, 2004.

[2] B. L. Ilhardt, E. S. Verry, and B. J. Palik, "Defining riparian areas," *Forestry and the riparian zone, Orono, Maine*, pp. 7–14, 2000.

[3] S. J. Capon, L. E. Chambers, R. Mac Nally, R. J. Naiman, P. Davies, N. Marshall, J. Pittock, M. Reid, T. Capon, M. Douglas, *et al.*, "Riparian ecosystems in the 21st century: hotspots for climate change adaptation?," *Ecosystems*, vol. 16, no. 3, pp. 359–381, 2013.

[4] K. Tockner and J. A. Stanford, "Riverine flood plains: present state and future trends," *Environmental conservation*, vol. 29, no. 3, pp. 308–330, 2002.

[5] M. A. Palmer, H. L. Menninger, and E. Bernhardt, "River restoration, habitat heterogeneity and biodiversity: a failure of theory or practice?," *Freshwater biology*, vol. 55, pp. 205–222, 2010.

[6] F. K. Ligon, W. E. Dietrich, and W. J. Trush, "Downstream ecological effects of dams," *BioScience*, vol. 45, no. 3, pp. 183–192, 1995.

[7] G. E. Grant, J. C. Schmidt, and S. L. Lewis, "A geological framework for interpreting downstream effects of dams on rivers," *Water Science and Application*, vol. 7, pp. 209–225, 2003.

[8] J. C. Schmidt and P. R. Wilcock, "Metrics for assessing the downstream effects of dams," *Water Resources Research*, vol. 44, no. 4, 2008.

[9] J. E. O'Connor, J. J. Duda, and G. E. Grant, "1000 dams down and counting," *Science*, vol. 348, no. 6234, pp. 496–497, 2015.

[10] J. J. Major, A. E. East, J. E. O'Connor, G. E. Grant, A. C. Wilcox, C. S. Magirl, M. J. Collins, and D. D. Tullos, "Geomorphic responses to dam removal in the united states–a two-decade perspective," *Gravel-Bed Rivers*, vol. 10, no. 9781118971437, pp. 355–383, 2017.

[11] J. Bendix and J. Stella, "Riparian vegetation and the fluvial environment: A biogeographic perspective," in *Treatise on Geomorphology* (J. F. Shroder, ed.), pp. 53 – 74, San Diego: Academic Press, 2013.

[12] G. P. Williams and M. G. Wolman, "Downstream effects of dams on alluvial rivers," 1984.

[13] W. C. Johnson, R. L. Burgess, and W. R. Keammerer, "Forest overstory vegetation and environment on the missouri river floodplain in north dakota," *Ecological Monographs*, vol. 46, no. 1, pp. 59–84, 1976.

[14] W. Osterkamp, M. L. Scott, G. T. Auble, *et al.*, "Downstream effects of dams on channel geometry and bottomland vegetation: regional patterns in the great plains," *Wetlands*, vol. 18, no. 4, pp. 619–633, 1998.

[15] F. C. Aguiar, M. J. Martins, P. C. Silva, and M. R. Fernandes, "Riverscapes downstream of hydropower dams: Effects of altered flows and historical land-use change," *Landscape and Urban Planning*, vol. 153, pp. 83–98, 2016.

[16] A. Gurnell, "Plants as river system engineers," *Earth Surface Processes and Landforms*, vol. 39, no. 1, pp. 4–25, 2014.

[17] M. Tal and C. Paola, "Effects of vegetation on channel morphodynamics: results and insights from laboratory experiments," *Earth Surface Processes and Landforms*, vol. 35, no. 9, pp. 1014–1028, 2010.

[18] G. Vane, A. F. Goetz, and J. B. Wellman, "Airborne imaging spectrometer: A new tool for remote sensing," *IEEE Transactions on Geoscience and Remote Sensing*, no. 6, pp. 546–549, 1984.

[19] D. Feurer, J.-S. Bailly, C. Puech, Y. Le Coarer, and A. A. Viau, "Very-high-resolution mapping of river-immersed topography by remote sensing," *Progress in Physical Geography*, vol. 32, no. 4, pp. 403–419, 2008.

[20] C. J. Legleiter, D. A. Roberts, and R. L. Lawrence, "Spectrally based remote sensing of river bathymetry," *Earth Surface Processes and Landforms*, vol. 34, no. 8, pp. 1039–1059, 2009.

[21] R. C. Hilldale and D. Raff, "Assessing the ability of airborne lidar to map river bathymetry," *Earth Surface Processes and Landforms*, vol. 33, no. 5, pp. 773–783, 2008.

[22] D. Tonolla, V. Acuña, U. Uehlinger, T. Frank, and K. Tockner, "Thermal heterogeneity in river floodplains," *Ecosystems*, vol. 13, pp. 727–740, Aug 2010.

[23] S. J. Dugdale, "A practitioner's guide to thermal infrared remote sensing of rivers and streams: recent advances, precautions and considerations," *Wiley Interdisciplinary Reviews: Water*, vol. 3, no. 2, pp. 251–268, 2016.

[24] Z. Kugler and T. De Groeve, "The global flood detection system," *Office for Official Publications of the European Communities, Luxembourg*, 2007.

[25] K. K. Yilmaz, R. F. Adler, Y. Tian, Y. Hong, and H. F. Pierce, "Evaluation of a satellite-based global flood monitoring system," *International Journal of Remote Sensing*, vol. 31, no. 14, pp. 3763–3782, 2010.

[26] F. Thielen, A.-C. Cosandey, N. Perrottet, and C. Roulier, "Cartographie des zones alluviales - clés de photo-interprétation," 2003.

[27] S. Dufour, I. Bernez, J. Betbeder, S. Corgne, L. Hubert-Moy, J. Nabucet, S. Rapinel, J. Sawtschuk, and C. Trollé, "Monitoring restored riparian vegetation: how can recent developments in remote sensing sciences help?," *Knowledge and Management of Aquatic Ecosystems*, no. 410, p. 10, 2013.

[28] V. Klemas, "Remote sensing of riparian and wetland buffers: an overview," *Journal of Coastal Research*, vol. 30, no. 5, pp. 869–880, 2014.

[29] B. Fu and I. Burgher, "Riparian vegetation ndvi dynamics and its relationship with climate, surface water and groundwater," *Journal of Arid Environments*, vol. 113, pp. 59–68, 2015.

[30] G. F. Ricci, G. Romano, V. Leronni, and F. Gentile, "Effect of check dams on riparian vegetation cover: A multiscale approach based on field measurements and satellite images for leaf area index assessment," *Science of The Total Environment*, vol. 657, pp. 827–838, 2019.

[31] A. Michez, H. Piégay, L. Jonathan, H. Claessens, and P. Lejeune, "Mapping of riparian invasive species with supervised classification of unmanned aerial system (uas) imagery," *International journal of applied earth observation and geoinformation*, vol. 44, pp. 88–94, 2016.

[32] N. Bachiller-Jareno, M. Hutchins, M. Bowes, M. Charlton, and H. Orr, "A novel application of remote sensing for modelling impacts of tree shading on water quality," *Journal of environmental management*, vol. 230, pp. 33–42, 2019.

[33] P. Olofsson, G. M. Foody, S. V. Stehman, and C. E. Woodcock, "Making better use of accuracy data in land change studies: Estimating accuracy and area and quantifying uncertainty using stratified estimation," *Remote Sensing of Environment*, vol. 129, pp. 122–131, 2013.

[34] S. Diaz, J. Hodgson, K. Thompson, M. Cabido, J. . Cornelissen, A. Jalili, G. Montserrat-Marti, J. Grime, F. Zarrinkamar, Y. Asri, *et al.*, "The plant traits that drive ecosystems: evidence from three continents," *Journal of vegetation science*, vol. 15, no. 3, pp. 295–304, 2004.

[35] S. Pierce, D. Negreiros, B. E. Cerabolini, J. Kattge, S. Díaz, M. Kleyer, B. Shipley, S. J. Wright, N. A. Soudzilovskaia, V. G. Onipchenko, *et al.*, "A global method for calculating plant csr ecological strategies applied across biomes world-wide," *Functional Ecology*, vol. 31, no. 2, pp. 444–457, 2017.

[36] G. Milani, M. Volpi, D. Tonolla, M. Doering, C. Robinson, M. Kneubühler, and M. Schaepman, "Robust quantification of riverine land cover dynamics by high-resolution remote sensing," *Remote sensing of environment*, vol. 217, pp. 491–505, 2018.

[37] G. Milani, M. Kneubühler, D. Tonolla, M. Doering, and M. E. Schaepman, "Remotely sensing variation in ecological strategies and plant traits of willows in perialpine floodplains," *Journal of geophysical research: biogeosciences*, vol. 124, no. 7, pp. 2090–2106, 2019.

[38] G. Milani, M. Kneubühler, D. Tonolla, M. Doering, and M. E. Schaepman, "Characterizing flood impact on swiss floodplains using inter-annual time series of satellite imagery," *Manuscript submitted for publication*.

[39] S. Postel and S. Carpenter, "Freshwater ecosystem services," *Nature's services: Societal dependence on natural ecosystems*, vol. 195, 1997.

[40] E. Mosselman, G. Angela, R. Massimo, C. Wolter, S. Bizzi, M. O'Hare, N. Friberg, I. Cowx, R. Brouwer, D. Herings, J. Kail, and M. Bussettini, "Reform policy brief no.3 - a fresh look on effective river restoration: Key conclusions from the reform project," report, 2016.

[41] M. G. Turner, W. H. Romme, R. H. Gardner, R. V. O'Neill, and T. K. Kratz, "A revised concept of landscape equilibrium: disturbance and stability on scaled landscapes," *Landscape Ecology*, vol. 8, no. 3, pp. 213–227, 1993.

[42] P. Haase, D. Hering, S. Jähnig, A. Lorenz, and A. Sundermann, "The impact of hydromorphological restoration on river ecological status: a comparison of fish, benthic invertebrates, and macrophytes," *Hydrobiologia*, vol. 704, no. 1, pp. 475–488, 2013.

[43] M. A. Palmer, H. L. Menninger, and E. Bernhardt, "River restoration, habitat heterogeneity and biodiversity: a failure of theory or practice?," *Freshwater biology*, vol. 55, no. s1, pp. 205–222, 2010.

[44] D. B. Arscott, K. Tockner, D. van der Nat, and J. Ward, "Aquatic habitat dynamics along a braided alpine river ecosystem (tagliamento river, northeast italy)," *Ecosystems*, vol. 5, no. 8, pp. 0802–0814, 2002.

[45] J. J. Latterell, J. Scott Bechtold, T. C. O'KEEFE, R. Pelt, and R. J. Naiman, "Dynamic patch mosaics and channel movement in an unconfined river valley of the olympic mountains," *Freshwater Biology*, vol. 51, no. 3, pp. 523–544, 2006.

[46] N. Clerici, M. L. Paracchini, and J. Maes, "Land-cover change dynamics and insights into ecosystem services in european stream riparian zones," *Ecohydrology & Hydrobiology*, vol. 14, no. 2, pp. 107–120, 2014.

[47] W. Bertoldi, N. A. Drake, and A. M. Gurnell, "Interactions between river flows and colonizing vegetation on a braided river: exploring spatial and temporal dynamics in riparian vegetation cover using satellite data," *Earth Surface Processes and Landforms*, vol. 36, no. 11, pp. 1474–1486, 2011.

[48] T. Coulthard, D. Hicks, and M. J. Van De Wiel, "Cellular modelling of river catchments and reaches: advantages, limitations and prospects," *Geomorphology*, vol. 90, no. 3, pp. 192–207, 2007.

[49] A. Crosato and M. S. Saleh, "Numerical study on the effects of floodplain vegetation on river planform style," *Earth Surface Processes and Landforms*, vol. 36, no. 6, pp. 711–720, 2011.

[50] A. B. Murray and C. Paola, "Modelling the effect of vegetation on channel pattern in bedload rivers," *Earth Surface Processes and Landforms*, vol. 28, no. 2, pp. 131–143, 2003.

[51] E. Perucca, C. Camporeale, and L. Ridolfi, "Significance of the riparian vegetation dynamics on meandering river morphodynamics," *Water Resources Research*, vol. 43, no. 3, pp. n/a–n/a, 2007.

[52] L. Kooistra, W. Wamelink, G. Schaepman-Strub, M. Schaepman, H. van Dobben, U. Aduaka, and O. Batelaan, "Assessing and predicting biodiversity in a floodplain ecosystem: Assimilation of net primary production derived from imaging spectrometer data into a dynamic vegetation model," *Remote Sensing of Environment*, vol. 112, no. 5, pp. 2118–2130, 2008.

[53] S. V. Gregory, F. J. Swanson, W. A. McKee, and K. W. Cummins, "An ecosystem perspective of riparian zones," *BioScience*, vol. 41, no. 8, pp. 540–551, 1991.

[54] F. Eugenio, J. Marcello, and J. Martin, "High-resolution maps of bathymetry and benthic habitats in shallow-water environments using multispectral remote sensing imagery," *Geoscience and Remote Sensing, IEEE Transactions on*, vol. 53, no. 7, pp. 3539–3549, 2015.

[55] C. J. Legleiter and B. T. Overstreet, "Mapping gravel bed river bathymetry from space," *Journal of Geophysical Research: Earth Surface (2003–2012)*, vol. 117, no. F4, 2012.

[56] W. A. Marcus, C. J. Legleiter, R. J. Aspinall, J. W. Boardman, and R. L. Crabtree, "High spatial resolution hyperspectral mapping of in-stream habitats, depths, and woody debris in mountain streams," *Geomorphology*, vol. 55, no. 1, pp. 363–380, 2003.

[57] K. M. Smikrud and A. Prakash, "Monitoring large woody debris dynamics in the unuk river alaska, using digital aerial photography," *GIScience and Remote Sensing*, vol. 43, no. 2, pp. 142–154, 2006.

[58] Y. Hamada, D. A. Stow, L. L. Coulter, J. C. Jafolla, and L. W. Hendricks, "Detecting tamarisk species (tamarix spp.) in riparian habitats of southern california using high spatial resolution hyperspectral imagery," *Remote Sensing of Environment*, vol. 109, no. 2, pp. 237–248, 2007.

[59] R. G. Bryant and D. J. Gilvear, "Quantifying geomorphic and riparian land cover changes either side of a large flood event using airborne remote sensing: River tay, scotland," *Geomorphology*, vol. 29, no. 3, pp. 307–321, 1999.

[60] M. Schaepman, G. Wamelink, H. Van Dobben, M. Gloor, G. Schaepman-Strub, L. Kooistra, J. Clevers, A. Schmidt, and F. Berendse, "River floodplain vegetation scenario development using imaging spectroscopy derived products as input variables in a dynamic vegetation model," *Photogrammetric Engineering & Remote Sensing*, vol. 73, no. 10, pp. 1179–1188, 2007.

[61] L. Javernick, J. Brasington, and B. Caruso, "Modeling the topography of shallow braided rivers using structure-from-motion photogrammetry," *Geomorphology*, vol. 213, pp. 166–182, 2014.

[62] I. Güneralp, A. M. Filippi, and J. Randall, "Estimation of floodplain aboveground biomass using multispectral remote sensing and nonparametric modeling," *International Journal of Applied Earth Observation and Geoinformation*, vol. 33, pp. 119–126, 2014.

[63] C. J. Gleason and L. C. Smith, "Toward global mapping of river discharge using satellite images and at-many-stations hydraulic geometry," *Proceedings of the National Academy of Sciences*, vol. 111, no. 13, pp. 4788–4791, 2014.

[64] I. Colomina and P. Molina, "Unmanned aerial systems for photogrammetry and remote sensing: A review," *ISPRS Journal of Photogrammetry and Remote Sensing*, vol. 92, pp. 79–97, 2014.

[65] H. Torabzadeh, F. Morsdorf, and M. E. Schaepman, "Fusion of imaging spectroscopy and airborne laser scanning data for characterization of forest ecosystems – a review," *ISPRS Journal of Photogrammetry and Remote Sensing*, vol. 97, pp. 25–35, 2014.

[66] S. Siebert and J. Teizer, "Mobile 3d mapping for surveying earthwork projects using an unmanned aerial vehicle (uav) system," *Automation in Construction*, vol. 41, pp. 1–14, 2014.

[67] Q. Feng, J. Liu, and J. Gong, "Uav remote sensing for urban vegetation mapping using random forest and texture analysis," *Remote Sensing*, vol. 7, no. 1, pp. 1074–1094, 2015.

[68] D. Feurer, J.-S. Bailly, C. Puech, Y. Le Coarer, and A. A. Viau, "Very-high-resolution mapping of river-immersed topography by remote sensing," *Progress in Physical Geography*, vol. 32, no. 4, pp. 403–419, 2008.

[69] K. Flynn and S. Chapra, "Remote sensing of submerged aquatic vegetation in a shallow non-turbid river using an unmanned aerial vehicle," *Remote Sensing*, vol. 6, no. 12, p. 12815, 2014.

[70] A. Tamminga, B. Hugenholtz, M. Eaton, and Lapointe, "Hyperspatial remote sensing of channel reach morphology and hydraulic fish habitat using an unmanned aerial vehicle (uav): A first assessment in the context of river research and management," *River research and applications*, vol. 31, no. 3, pp. 379–391, 2015.

[71] J. Langhammer and T. Vacková, "Detection and mapping of the geomorphic effects of flooding using uav photogrammetry," *Pure and Applied Geophysics*, pp. 1–23, 2018.

[72] C. Cleve, M. Kelly, F. R. Kearns, and M. Moritz, "Classification of the wildland–urban interface: A comparison of pixel-and object-based classifications using high-resolution aerial photography," *Computers, Environment and Urban Systems*, vol. 32, no. 4, pp. 317–326, 2008.

[73] S. W. Myint, P. Gober, A. Brazel, S. Grossman-Clarke, and Q. Weng, "Per-pixel vs. object-based classification of urban land cover extraction using high spatial resolution imagery," *Remote sensing of environment*, vol. 115, no. 5, pp. 1145–1161, 2011.

[74] D. Tuia, F. Pacifici, M. Kanevski, and W. J. Emery, "Classification of very high spatial resolution imagery using mathematical morphology and support vector machines," *IEEE Transactions on Geoscience and Remote Sensing*, vol. 47, no. 11, pp. 3866–3879, 2009.

[75] M. Kim, T. A. Warner, M. Madden, and D. S. Atkinson, "Multi-scale geobia with very high spatial resolution digital aerial imagery: scale, texture and image objects," *International Journal of Remote Sensing*, vol. 32, no. 10, pp. 2825–2850, 2011.

[76] M. Herold, J. Scepan, and K. C. Clarke, "The use of remote sensing and landscape metrics to describe structures and changes in urban land uses," *Environment and Planning A*, vol. 34, no. 8, pp. 1443–1458, 2002.

[77] K. S. Willis, "Remote sensing change detection for ecological monitoring in united states protected areas," *Biological Conservation*, vol. 182, pp. 233–242, 2015.

[78] A. Butt, R. Shabbir, S. S. Ahmad, and N. Aziz, "Land use change mapping and analysis using remote sensing and gis: A case study of simly watershed, islamabad, pakistan," *The Egyptian Journal of Remote Sensing and Space Science*, vol. 18, no. 2, pp. 251–259, 2015.

[79] I. Güneralp, A. M. Filippi, and B. Hales, "Influence of river channel morphology and bank characteristics on water surface boundary delineation using high-resolution passive remote sensing and template matching," *Earth Surface Processes and Landforms*, vol. 39, no. 7, pp. 977–986, 2014.

[80] K. Johansen, N. C. Coops, S. E. Gergel, and Y. Stange, "Application of high spatial resolution satellite imagery for riparian and forest ecosystem classification," *Remote Sensing of Environment*, vol. 110, no. 1, pp. 29–44, 2007.

[81] L. Demarchi, S. Bizzi, and H. Piégay, "Hierarchical object-based mapping of riverscape units and in-stream mesohabitats using lidar and vhr imagery," *Remote Sensing*, vol. 8, no. 2, p. 97, 2016.

[82] K. Richards, J. Brasington, and F. Hughes, "Geomorphic dynamics of floodplains: ecological implications and a potential modelling strategy," *Freshwater Biology*, vol. 47, no. 4, pp. 559–579, 2002.

[83] D. Knighton, *Fluvial forms and processes: a new perspective*. Routledge, 2014.

[84] M. E. Harmon, J. F. Franklin, F. J. Swanson, P. Sollins, S. Gregory, J. Lattin, N. Anderson, S. Cline, N. G. Aumen, J. Sedell, *et al.*, "Ecology of coarse woody debris in temperate ecosystems," in *Advances in ecological research*, vol. 15, pp. 133–302, Elsevier, 1986.

[85] A. S. Woodget, R. Austrums, I. P. Maddock, and E. Habit, "Drones and digital photogrammetry: from classifications to continuums for monitoring river habitat and hydromorphology," *Wiley Interdisciplinary Reviews: Water*, vol. 4, no. 4, p. e1222, 2017.

[86] A. P. Tewkesbury, A. J. Comber, N. J. Tate, A. Lamb, and P. F. Fisher, "A critical synthesis of remotely sensed optical image change detection techniques," *Remote Sensing of Environment*, vol. 160, pp. 1–14, 2015.

[87] P. Serra, X. Pons, and D. Sauri, "Post-classification change detection with data from different sensors: some accuracy considerations," *International Journal of Remote Sensing*, vol. 24, no. 16, pp. 3311–3340, 2003.

[88] M. Hussain, D. Chen, A. Cheng, H. Wei, and D. Stanley, "Change detection from remotely sensed images: From pixel-based to object-based approaches," *ISPRS Journal of Photogrammetry and Remote Sensing*, vol. 80, pp. 91–106, 2013.

[89] P. Van Oort, "Improving land cover change estimates by accounting for classification errors," *International Journal of Remote Sensing*, vol. 26, no. 14, pp. 3009–3024, 2005.

[90] C. Manual, *Camera User Guide IXUS 125 HS*. Canon Inc., 2012.

[91] senseFly Manual, *multiSPEC 4C camera User Manual*. sensFly Ltd, 2014.

[92] S. Pix4D, *Pix4D mapper Software*. 1015 Lausanne, Switzerland, 2016.

[93] B. C. Lowekamp, D. T. Chen, L. Ibáñez, and D. Blezek, "The design of simpleitk," *Frontiers in neuroinformatics*, vol. 7, p. 45, 2013.

[94] D. Mattes, D. R. Haynor, H. Vesselle, T. K. Lewellen, and W. Eubank, "Nonrigid multimodality image registration," *Medical imaging*, vol. 4322, no. 1, pp. 1609–1620, 2001.

[95] R. G. Pontius Jr and M. Millones, "Death to kappa: birth of quantity disagreement and allocation disagreement for accuracy assessment," *International Journal of Remote Sensing*, vol. 32, no. 15, pp. 4407–4429, 2011.

[96] P. Olofsson, G. M. Foody, S. V. Stehman, and C. E. Woodcock, "Making better use of accuracy data in land change studies: Estimating accuracy and area and quantifying uncertainty using stratified estimation," *Remote Sensing of Environment*, vol. 129, pp. 122 – 131, 2013.

[97] D. H. Card, "Using known map category marginal frequencies improve estimates of thematic map accuracy," *Photogrammetric Engineering and Remote Sensing*, vol. 48, no. 3, pp. 431–439, 1982.

[98] L. Breiman, "Random forests," *Machine learning*, vol. 45, no. 1, pp. 5–32, 2001.

[99] A. Liaw, M. Wiener, *et al.*, "Classification and regression by randomforest," *R news*, vol. 2, no. 3, pp. 18–22, 2002.

[100] D. Tuia, M. Volpi, L. Copa, M. Kanevski, and J. Munoz-Mari, "A survey of active learning algorithms for supervised remote sensing image classification," *IEEE Journal of Selected Topics in Signal Processing*, vol. 5, no. 3, pp. 606–617, 2011.

[101] D. G. Leckie, E. Cloney, C. Jay, and D. Paradine, "Automated mapping of stream features with high-resolution multispectral imagery," *Photogrammetric Engineering & Remote Sensing*, vol. 71, no. 2, pp. 145–155, 2005.

[102] R. Dunford, K. Michel, M. Gagnage, H. Piégay, and M.-L. Trémelo, "Potential and constraints of unmanned aerial vehicle technology for the characterization of mediterranean riparian forest," *International Journal of Remote Sensing*, vol. 30, no. 19, pp. 4915–4935, 2009.

[103] G. Geerling, M. Labrador-Garcia, J. Clevers, A. Ragas, and A. Smits, "Classification of floodplain vegetation by data fusion of spectral (casi) and lidar data," *International Journal of Remote Sensing*, vol. 28, no. 19, pp. 4263–4284, 2007.

[104] L. Bruzzone and F. Bovolo, "A novel framework for the design of change-detection systems for very-high-resolution remote sensing images," *Proceedings of the IEEE*, vol. 101, no. 3, pp. 609–630, 2013.

[105] P. Olofsson, G. M. Foody, M. Herold, S. V. Stehman, C. E. Woodcock, and M. A. Wulder, "Good practices for estimating area and assessing accuracy of land change," *Remote Sensing of Environment*, vol. 148, pp. 42–57, 2014.

[106] Y. Ma, F. Chen, J. Liu, Y. He, J. Duan, and X. Li, "An automatic procedure for early disaster change mapping based on optical remote sensing," *Remote Sensing*, vol. 8, no. 4, p. 272, 2016.

[107] A. S. Laliberte, M. A. Goforth, C. M. Steele, and A. Rango, "Multispectral remote sensing from unmanned aircraft: Image processing workflows and applications for rangeland environments," *Remote Sensing*, vol. 3, no. 11, pp. 2529–2551, 2011.

[108] D. Tuia, G. Camps-Valls, G. Matasci, and M. Kanevski, "Learning relevant image features with multiple-kernel classification," *IEEE Transactions on Geoscience and Remote Sensing*, vol. 48, no. 10, pp. 3780–3791, 2010.

[109] R. Lawrence, A. Bunn, S. Powell, and M. Zambon, "Classification of remotely sensed imagery using stochastic gradient boosting as a refinement of classification tree analysis," *Remote sensing of environment*, vol. 90, no. 3, pp. 331–336, 2004.

[110] Q. Feng, J. Liu, and J. Gong, "Urban flood mapping based on unmanned aerial vehicle remote sensing and random forest classifier—a case of yuyao, china," *Water*, vol. 7, no. 4, pp. 1437–1455, 2015.

[111] C. Knoth, B. Klein, T. Prinz, and T. Kleinebecker, "Unmanned aerial vehicles as innovative remote sensing platforms for high-resolution infrared imagery to support restoration monitoring in cut-over bogs," *Applied Vegetation Science*, vol. 16, no. 3, pp. 509–517, 2013.

[112] A. Polyak and L. Wolf, "Channel-level acceleration of deep face representations," *IEEE Access*, vol. 3, pp. 2163–2175, 2015.

[113] Z. I. Petrou, T. Stathaki, I. Manakos, M. Adamo, C. Tarantino, and P. Blonda, "Land cover to habitat map conversion using remote sensing data: A supervised learning approach," in *Geoscience and Remote Sensing Symposium (IGARSS), 2014 IEEE International*, pp. 4683–4686, IEEE, 2014.

[114] R. M. Haralick, K. Shanmugam, *et al.*, "Textural features for image classification," *IEEE Transactions on systems, man, and cybernetics*, no. 6, pp. 610–621, 1973.

[115] C. Gevaert, C. Persello, R. Sliuzas, and G. Vosselman, "Informal settlement classification using point-cloud and image-based features from uav data," *ISPRS Journal of Photogrammetry and Remote Sensing*, vol. 125, pp. 225–236, 2017.

[116] G. J. Hay and G. Castilla, "Geographic object-based image analysis (geobia): A new name for a new discipline," *Object-based image analysis*, pp. 75–89, 2008.

[117] M. Roy, S. Ghosh, and A. Ghosh, "A novel approach for change detection of remotely sensed images using semi-supervised multiple classifier system," *Information Sciences*, vol. 269, pp. 35–47, 2014.

[118] D. Jiang, Y. Huang, D. Zhuang, Y. Zhu, X. Xu, and H. Ren, "A simple semi-automatic approach for land cover classification from multispectral remote sensing imagery," *PloS one*, vol. 7, no. 9, p. e45889, 2012.

[119] A. S. Laliberte and A. Rango, "Texture and scale in object-based analysis of subdecimeter resolution unmanned aerial vehicle (uav) imagery," *IEEE Transactions on Geoscience and Remote Sensing*, vol. 47, no. 3, pp. 761–770, 2009.

[120] R. Achanta, A. Shaji, K. Smith, A. Lucchi, P. Fua, and S. Süsstrunk, "Slic superpixels compared to state-of-the-art superpixel methods," *IEEE transactions on pattern analysis and machine intelligence*, vol. 34, no. 11, pp. 2274–2282, 2012.

[121] F. Pedregosa, G. Varoquaux, A. Gramfort, V. Michel, B. Thirion, O. Grisel, M. Blondel, P. Prettenhofer, R. Weiss, V. Dubourg, J. Vanderplas, A. Passos, D. Cournapeau, M. Brucher, M. Perrot, and E. Duchesnay, "Scikit-learn: Machine learning in Python," *Journal of Machine Learning Research*, vol. 12, pp. 2825–2830, 2011.

[122] G. M. Chaikin, "An algorithm for high-speed curve generation," *Computer graphics and image processing*, vol. 3, no. 4, pp. 346–349, 1974.

[123] GRASS Development Team, *Geographic Resources Analysis Support System (GRASS GIS) Software, Version 7.2*. Open Source Geospatial Foundation, 2017.

[124] D. Corenblit, E. Tabacchi, J. Steiger, and A. M. Gurnell, "Reciprocal interactions and adjustments between fluvial landforms and vegetation dynamics in river corridors: a review of complementary approaches," *Earth-Science Reviews*, vol. 84, no. 1-2, pp. 56–86, 2007.

[125] A. M. Gurnell, "Plants as river system engineers," *Earth Surface Processes and Landforms*, vol. 39, no. 1, pp. 4–25, 2014.

[126] M. O'Hare, J. Mountford, J. Maroto, and I. Gunn, "Plant traits relevant to fluvial geomorphology and hydrological interactions," *River Research and Applications*, vol. 32, no. 2, pp. 179–189, 2016.

[127] S. Lavorel and É. Garnier, "Predicting changes in community composition and ecosystem functioning from plant traits: revisiting the holy grail," *Functional ecology*, vol. 16, no. 5, pp. 545–556, 2002.

[128] G. Bornette, E. Tabacchi, C. Hupp, S. Puijalon, and J.-C. Rostan, "A model of plant strategies in fluvial hydrosystems," *Freshwater Biology*, vol. 53, no. 8, pp. 1692–1705, 2008.

[129] S. Xiong, C. Nilsson, M. E. Johansson, and R. Jansson, "Responses of riparian plants to accumulation of silt and plant litter: the importance of plant traits," *Journal of Vegetation Science*, vol. 12, no. 4, pp. 481–490, 2001.

[130] J. P. Grime, K. Thompson, R. Hunt, J. G. Hodgson, J. H. C. Cornelissen, I. H. Rorison, G. A. F. Hendry, T. W. Ashenden, A. P. Askew, S. R. Band, R. E. Booth, C. C. Bossard, B. D. Campbell, J. E. L. Cooper, A. W. Davison, P. L. Gupta, W. Hall, D. W. Hand, M. A. Hannah, S. H. Hillier, D. J. Hodkinson, A. Jalili, Z. Liu, J. M. L. Mackey, N. Matthews, M. A. Mowforth, A. M. Neal, R. J. Reader, K. Reiling, W. Ross-Fraser, R. E. Spencer, F. Sutton, D. E. Tasker, P. C. Thorpe, and J. Whitehouse, "Integrated screening validates primary axes of specialisation in plants," *Oikos*, vol. 79, no. 2, pp. 259–281, 1997.

[131] P. B. Reich, "The world-wide 'fast–slow' plant economics spectrum: a traits manifesto," *Journal of Ecology*, vol. 102, no. 2, pp. 275–301, 2014.

[132] J. Weiner, "Allocation, plasticity and allometry in plants," *Perspectives in Plant Ecology, Evolution and Systematics*, vol. 6, no. 4, pp. 207–215, 2004.

[133] B. J. Enquist and K. J. Niklas, "Global allocation rules for patterns of biomass partitioning in seed plants," *Science*, vol. 295, no. 5559, pp. 1517–1520, 2002.

[134] J. P. Grime, "Vegetation classification by reference to strategies," *Nature*, vol. 250, no. 5461, p. 26, 1974.

[135] J. P. Grime and S. Pierce, *The evolutionary strategies that shape ecosystems*. John Wiley & Sons, 2012.

[136] J. Hodgson, P. Wilson, R. Hunt, J. Grime, and K. Thompson, "Allocating csr plant functional types: a soft approach to a hard problem," *Oikos*, pp. 282–294, 1999.

[137] S. Pierce, G. Brusa, I. Vagge, and B. E. Cerabolini, "Allocating csr plant functional types: the use of leaf economics and size traits to classify woody and herbaceous vascular plants," *Functional Ecology*, vol. 27, no. 4, pp. 1002–1010, 2013.

[138] T. Kattenborn, F. E. Fassnacht, S. Pierce, J. Lopatin, J. P. Grime, and S. Schmidtlein, "Linking plant strategies and plant traits derived by radiative transfer modelling," *Journal of Vegetation Science*, vol. 28, no. 4, pp. 717–727, 2017.

[139] S. Schmidtlein, H. Feilhauer, and H. Bruelheide, "Mapping plant strategy types using remote sensing," *Journal of Vegetation Science*, vol. 23, no. 3, pp. 395–405, 2012.

[140] A. K. Schweiger, M. Schütz, A. C. Risch, M. Kneubühler, R. Haller, and M. E. Schaepman, "How to predict plant functional types using imaging spectroscopy: Linking vegetation community traits, plant functional types and spectral response," *Methods in Ecology and Evolution*, vol. 8, no. 1, pp. 86–95, 2017.

[141] A. Elosegi and S. Sabater, "Effects of hydromorphological impacts on river ecosystem functioning: a review and suggestions for assessing ecological impacts," *Hydrobiologia*, vol. 712, no. 1, pp. 129–143, 2013.

[142] C. R. Hupp, A. R. Pierce, and G. B. Noe, "Floodplain geomorphic processes and environmental impacts of human alteration along coastal plain rivers, usa," *Wetlands*, vol. 29, no. 2, pp. 413–429, 2009.

[143] E. Gonzalez, E. Muller, B. Gallardo, F. A. Comín, and M. González-Sanchis, "Factors controlling litter production in a large mediterranean river floodplain forest," *Canadian journal of forest research*, vol. 40, no. 9, pp. 1698–1709, 2010.

[144] A. Gurnell, W. Bertoldi, and D. Corenblit, "Changing river channels: The roles of hydrological processes, plants and pioneer fluvial landforms in humid temperate, mixed load, gravel bed rivers," *Earth-Science Reviews*, vol. 111, no. 1-2, pp. 129–141, 2012.

[145] C. Camporeale, E. Perucca, L. Ridolfi, and A. Gurnell, "Modeling the interactions between river morphodynamics and riparian vegetation," *Reviews of Geophysics*, vol. 51, no. 3, pp. 379–414, 2013.

[146] F. Ecke, S. Hellsten, J. Köhler, A. W. Lorenz, J. Rääpysjärvi, S. Scheunig, J. Segersten, and A. Baattrup-Pedersen, "The response of hydrophyte growth forms and plant strategies to river restoration," *Hydrobiologia*, vol. 769, pp. 41–54, Apr 2016.

[147] P. Modrak, S. Brunzel, and A. W. Lorenz, "Riparian plant species preferences indicate diversification of site conditions after river restoration," *Ecohydrology*, vol. 10, no. 5, pp. e1852–n/a, 2017. e1852 ECO-15-0208.R2.

[148] M. Sterk, G. Gort, H. De Lange, W. Ozinga, M. Sanders, K. Van Looy, and A. Van Teeffelen, "Plant trait composition as an indicator for the ecological memory of rehabilitated floodplains," *Basic and Applied Ecology*, vol. 17, no. 6, pp. 479–488, 2016.

[149] "Meteoswiss: Climate normals." `https://www.meteoswiss.admin.ch/home/climate/swiss-climate-in-detail/climate-normals/normal-values-per-measured-parameter.html`, 2018. Accessed: 2018-10-19.

[150] S. Karrenberg, P. Edwards, and J. Kollmann, "The life history of salicaceae living in the active zone of floodplains," *Freshwater Biology*, vol. 47, no. 4, pp. 733–748, 2002.

[151] J. A. Savage and J. Cavender-Bares, "Habitat specialization and the role of trait lability in structuring diverse willow (genus salix) communities," *Ecology*, vol. 93, no. sp8, 2012.

[152] J. D. Schade and D. B. Lewis, "Plasticity in resource allocation and nitrogen-use efficiency in riparian vegetation: Implications for nitrogen retention," *Ecosystems*, vol. 9, pp. 740–755, Aug 2006.

[153] P. N. Slater, "Radiometric considerations in remote sensing," *Proceedings of the IEEE*, vol. 73, no. 6, pp. 997–1011, 1985.

[154] T. Y. Lee and Y. J. Kaufman, "Non-lambertian effects on remote sensing of surface reflectance and vegetation index," *IEEE Transactions on Geoscience and Remote Sensing*, no. 5, pp. 699–708, 1986.

[155] M. E. Schaepman, M. Jehle, A. Hueni, P. D'Odorico, A. Damm, J. Weyermann, F. D. Schneider, V. Laurent, C. Popp, F. C. Seidel, *et al.*, "Advanced radiometry measurements and earth science applications with the airborne prism experiment (apex)," *Remote Sensing of Environment*, vol. 158, pp. 207–219, 2015.

[156] A. Hueni, K. Lenhard, A. Baumgartner, and M. E. Schaepman, "Airborne prism experiment calibration information system," *IEEE Transactions on Geoscience and Remote Sensing*, vol. 51, no. 11, pp. 5169–5180, 2013.

[157] A. Hueni, J. Biesemans, K. Meuleman, F. Dell'Endice, D. Schlapfer, D. Odermatt, M. Kneubuehler, S. Adriaensen, S. Kempenaers, J. Nieke, *et al.*, "Structure, components, and interfaces of the airborne prism experiment (apex) processing and archiving facility," *IEEE Transactions on Geoscience and Remote Sensing*, vol. 47, no. 1, pp. 29–43, 2009.

[158] R. Richter and D. Schläpfer, "Geo-atmospheric processing of airborne imaging spectrometry data. part 2: atmospheric/topographic correction," *International Journal of Remote Sensing*, vol. 23, no. 13, pp. 2631–2649, 2002.

[159] D. Schläpfer and R. Richter, "Geo-atmospheric processing of airborne imaging spectrometry data. part 1: parametric orthorectification," *International Journal of Remote Sensing*, vol. 23, no. 13, pp. 2609–2630, 2002.

[160] F. D. Schneider, F. Morsdorf, B. Schmid, O. L. Petchey, A. Hueni, D. S. Schimel, and M. E. Schaepman, "Mapping functional diversity from remotely sensed morphological and physiological forest traits," *Nature communications*, vol. 8, no. 1, p. 1441, 2017.

[161] A. Marcinkowska, B. Zagajewski, A. Ochtyra, A. Jarocińska, E. Raczko, L. Kupková, P. Stych, and K. Meuleman, "Mapping vegetation communities of the karkonosze national park using apex hyperspectral data and support vector machines," *Miscellanea Geographica*, vol. 18, no. 2, pp. 23–29, 2014.

[162] D. Braun, A. Damm, E. Paul-Limoges, A. Revill, N. Buchmann, O. L. Petchey, L. Hein, and M. E. Schaepman, "From instantaneous to continuous: Using imaging spectroscopy and in situ data to map two productivity-related ecosystem services," *Ecological Indicators*, vol. 82, pp. 409–419, 2017.

[163] J. Cornelissen, S. Lavorel, E. Garnier, S. Diaz, N. Buchmann, D. Gurvich, P. Reich, H. Ter Steege, H. Morgan, M. Van Der Heijden, *et al.*, "A handbook of protocols for standardised and easy measurement of plant functional traits worldwide," *Australian journal of Botany*, vol. 51, no. 4, pp. 335–380, 2003.

[164] R. Esteban, O. Barrutia, U. Artetxe, B. Fernández-Marín, A. Hernández, and J. I. García-Plazaola, "Internal and external factors affecting photosynthetic pigment composition in plants: a meta-analytical approach," *New Phytologist*, vol. 206, no. 1, pp. 268–280, 2015.

[165] L. Solari, M. Van Oorschot, B. Belletti, D. Hendriks, M. Rinaldi, and A. Vargas-Luna, "Advances on modelling riparian vegetation-hydromorphology interactions," *River Research and Applications*, vol. 32, no. 2, pp. 164–178, 2016.

[166] A. Al Mahmud, M. Hossain, M. S. Kadian, and M. A. Hoque, "Physiological and biochemical changes in potato under water stress condition," *Indian Journal of Plant Physiology*, vol. 20, no. 4, pp. 297–303, 2015.

[167] R. S. Alberte, J. P. Thornber, and E. L. Fiscus, "Water stress effects on the content and organization of chlorophyll in mesophyll and bundle sheath chloroplasts of maize," *Plant Physiology*, vol. 59, no. 3, pp. 351–353, 1977.

[168] H. Sircelj, F. Batic, and F. Stampar, "Effects of drought stress on pigment, ascorbic acid and free amino acids content in leaves of two apple tree cultivars," *PHYTON-HORN-*, vol. 39, no. 3, pp. 97–100, 1999.

[169] L. V. Junker, A. Kleiber, K. Jansen, H. Wildhagen, M. Hess, Z. Kayler, B. Kammerer, J.-P. Schnitzler, J. Kreuzwieser, A. Gessler, *et al.*, "Variation in short-term and long-term responses of photosynthesis and isoprenoid-mediated photoprotection to soil water availability in four douglas-fir provenances," *Scientific reports*, vol. 7, p. 40145, 2017.

[170] L. Hallik, T. Kazantsev, A. Kuusk, J. Galmés, M. Tomás, and Ü. Niinemets, "Generality of relationships between leaf pigment contents and spectral vegetation indices in mallorca (spain)," *Regional Environmental Change*, vol. 17, no. 7, pp. 2097–2109, 2017.

[171] J. A. Gamon, K. F. Huemmrich, C. Y. Wong, I. Ensminger, S. Garrity, D. Y. Hollinger, A. Noormets, and J. Peñuelas, "A remotely sensed pigment index reveals photosynthetic phenology in evergreen conifers," *Proceedings of the National Academy of Sciences*, vol. 113, no. 46, pp. 13087–13092, 2016.

[172] S. L. Ustin, A. A. Gitelson, S. Jacquemoud, M. Schaepman, G. P. Asner, J. A. Gamon, and P. Zarco-Tejada, "Retrieval of foliar information about plant pigment systems from high resolution spectroscopy," *Remote Sensing of Environment*, vol. 113, pp. S67–S77, 2009.

[173] F. Baret and S. Buis, "Estimating canopy characteristics from remote sensing observations: Review of methods and associated problems," in *Advances in land remote Sensing*, pp. 173–201, Springer, 2008.

[174] S. V. Ollinger, "Sources of variability in canopy reflectance and the convergent properties of plants," *New Phytologist*, vol. 189, no. 2, pp. 375–394, 2011.

[175] G. P. Asner, C. B. Anderson, R. E. Martin, R. Tupayachi, D. E. Knapp, and F. Sinca, "Landscape biogeochemistry reflected in shifting distributions of chemical traits in the amazon forest canopy," *Nature Geoscience*, vol. 8, no. 7, p. 567, 2015.

[176] D. M. Haaland and E. V. Thomas, "Partial least-squares methods for spectral analyses. 1. relation to other quantitative calibration methods and the extraction of qualitative information," *Analytical chemistry*, vol. 60, no. 11, pp. 1193–1202, 1988.

[177] W. A. Dorigo, R. Zurita-Milla, A. J. de Wit, J. Brazile, R. Singh, and M. E. Schaepman, "A review on reflective remote sensing and data assimilation techniques for enhanced agroecosystem modeling," *International journal of applied earth observation and geoinformation*, vol. 9, no. 2, pp. 165–193, 2007.

[178] F. Garfagnoli, G. Martelloni, A. Ciampalini, L. Innocenti, and S. Moretti, "Two guis-based analysis tool for spectroradiometer data pre-processing," *Earth Science Informatics*, vol. 6, pp. 227–240, Dec 2013.

[179] F. Pedregosa, G. Varoquaux, A. Gramfort, V. Michel, B. Thirion, O. Grisel, M. Blondel, P. Prettenhofer, R. Weiss, V. Dubourg, *et al.*, "Scikit-learn: Machine learning in python," *Journal of machine learning research*, vol. 12, no. Oct, pp. 2825–2830, 2011.

[180] D. A. Griffith, "Effective geographic sample size in the presence of spatial autocorrelation," *Annals of the Association of American Geographers*, vol. 95, no. 4, pp. 740–760, 2005.

[181] M. R. Dale and M.-J. Fortin, "Spatial autocorrelation and statistical tests in ecology," *Ecoscience*, vol. 9, no. 2, pp. 162–167, 2002.

[182] S. P. Serbin, A. Singh, B. E. McNeil, C. C. Kingdon, and P. A. Townsend, "Spectroscopic determination of leaf morphological and biochemical traits for northern temperate and boreal tree species," *Ecological Applications*, vol. 24, no. 7, pp. 1651–1669, 2014.

[183] A. Singh, S. P. Serbin, B. E. McNeil, C. C. Kingdon, and P. A. Townsend, "Imaging spectroscopy algorithms for mapping canopy foliar chemical and morphological traits and their uncertainties," *Ecological Applications*, vol. 25, no. 8, pp. 2180–2197, 2015.

[184] T. Kattenborn, F. E. Fassnacht, and S. Schmidtlein, "Differentiating plant functional types using reflectance: which traits make the difference?," *Remote Sensing in Ecology and Conservation*, 2018.

[185] S. Wold, J. Trygg, A. Berglund, and H. Antti, "Some recent developments in pls modeling," *Chemometrics and Intelligent Laboratory Systems*, vol. 58, no. 2, pp. 131 – 150, 2001. PLS Methods.

[186] M. M. Verstraete, B. Pinty, and R. B. Myneni, "Potential and limitations of information extraction on the terrestrial biosphere from satellite remote sensing," *Remote Sensing of Environment*, vol. 58, no. 2, pp. 201–214, 1996.

[187] E. Ögren and U. Sundin, "Photosynthetic responses to variable light: a comparison of species from contrasting habitats," *Oecologia*, vol. 106, no. 1, pp. 18–27, 1996.

[188] A. Takenaka, I. Washitani, N. Kuramoto, and K. Inoue, "Life history and demographic features of aster kantoensis, an endangered local endemic of floodplains," *Biological Conservation*, vol. 78, no. 3, pp. 345 – 352, 1996.

[189] N. L. Poff, J. D. Allan, M. B. Bain, J. R. Karr, K. L. Prestegaard, B. D. Richter, R. E. Sparks, and J. C. Stromberg, "The natural flow regime," *BioScience*, vol. 47, no. 11, pp. 769–784, 1997.

[190] J. Steiger, E. Tabacchi, S. Dufour, D. Corenblit, and J.-L. Peiry, "Hydrogeomorphic processes affecting riparian habitat within alluvial channel–floodplain river systems: a review for the temperate zone," *River Research and Applications*, vol. 21, no. 7, pp. 719–737, 2005.

[191] C. R. Hupp and W. Osterkamp, "Riparian vegetation and fluvial geomorphic processes," *Geomorphology*, vol. 14, no. 4, pp. 277 – 295, 1996. Fluvial Geomorphology and Vegetation.

[192] N. L. Poff and J. K. Zimmerman, "Ecological responses to altered flow regimes: a literature review to inform the science and management of environmental flows," *Freshwater Biology*, vol. 55, no. 1, pp. 194–205, 2010.

[193] P. B. Shafroth, J. C. Stromberg, and D. T. Patten, "Riparian vegetation response to altered disturbance and stress regimes," *Ecological Applications*, vol. 12, no. 1, pp. 107–123, 2002.

[194] J. C. Stromberg, S. J. Lite, R. Marler, C. Paradzick, P. B. Shafroth, D. Shorrock, J. M. White, and M. S. White, "Altered stream-flow regimes and invasive plant species: the tamarix case," *Global Ecology and Biogeography*, vol. 16, no. 3, pp. 381–393, 2007.

[195] J. Li, S. Dong, Z. Yang, M. Peng, S. Liu, and X. Li, "Effects of cascade hydropower dams on the structure and distribution of riparian and upland vegetation along the middle-lower lancang-mekong river," *Forest Ecology and Management*, vol. 284, pp. 251–259, 2012.

[196] C. E. Bradley and D. G. Smith, "Plains cottonwood recruitment and survival on a prairie meandering river floodplain, milk river, southern alberta and northern montana," *Canadian Journal of Botany*, vol. 64, no. 7, pp. 1433–1442, 1986.

[197] S. Karrenberg, S. Blaser, J. Kollmann, T. Speck, and P. Edwards, "Root anchorage of saplings and cuttings of woody pioneer species in a riparian environment," *Functional ecology*, vol. 17, no. 2, pp. 170–177, 2003.

[198] C. R. Hupp and M. Rinaldi, "Riparian vegetation patterns in relation to fluvial landforms and channel evolution along selected rivers of tuscany (central italy)," *Annals of the Association of American Geographers*, vol. 97, no. 1, pp. 12–30, 2007.

[199] F. Swanson, S. Gregory, J. Sedell, and A. Campbell in *Land-water interactions: the riparian zone*, Stroudsburg, Pa.: Hutchinson Ross Pub. Co.;[New York]: distributed worldwide by Academic Press, 1982.

[200] J. Bendix, C. R. Hupp, *et al.*, "Hydrological and geomorphological impacts on riparian plant communities," *Hydrological processes*, vol. 14, no. 16, pp. 2977–2990, 2000.

[201] E. González, B. Bourgeois, A. Masip, and A. Sher, "Trade-offs in seed dispersal strategies across riparian trees: The how matters as much as the when," *River Research and Applications*, vol. 32, no. 4, pp. 786–794, 2016.

[202] L. S. Barreto, "The reconciliation of the rk, and csr-models for life-history strategies," *Silva Lusitana*, vol. 16, no. 1, pp. 97–103, 2008.

[203] C. Roulier, *Typologie et dynamique de la végétation des zones alluviales de Suisse*. PhD thesis, Université de Neuchâtel, 1997.

[204] J. P. Grime, "Trait convergence and trait divergence in herbaceous plant communities: mechanisms and consequences," *Journal of Vegetation Science*, vol. 17, no. 2, pp. 255–260, 2006.

[205] J. H. Burns and S. Y. Strauss, "Effects of competition on phylogenetic signal and phenotypic plasticity in plant functional traits," *Ecology*, vol. 93, no. sp8, pp. S126–S137, 2012.

[206] M. Abakumova, K. Zobel, A. Lepik, and M. Semchenko, "Plasticity in plant functional traits is shaped by variability in neighbourhood species composition," *New Phytologist*, vol. 211, no. 2, pp. 455–463, 2016.

[207] B. J. Cardinale and M. A. Palmer, "Disturbance moderates biodiversity–ecosystem function relationships: experimental evidence from caddisflies in stream mesocosms," *Ecology*, vol. 83, no. 7, pp. 1915–1927, 2002.

[208] D. Thom and R. Seidl, "Natural disturbance impacts on ecosystem services and biodiversity in temperate and boreal forests," *Biological Reviews*, vol. 91, no. 3, pp. 760–781, 2016.

[209] R. E. Drenovsky, A. Khasanova, and J. J. James, "Trait convergence and plasticity among native and invasive species in resource-poor environments," *American Journal of Botany*, vol. 99, no. 4, pp. 629–639, 2012.

[210] B. Choat, S. Jansen, T. J. Brodribb, H. Cochard, S. Delzon, R. Bhaskar, S. J. Bucci, T. S. Feild, S. M. Gleason, U. G. Hacke, *et al.*, "Global convergence in the vulnerability of forests to drought," *Nature*, vol. 491, no. 7426, p. 752, 2012.

[211] E. Weiher, G. P. Clarke, and P. A. Keddy, "Community assembly rules, morphological dispersion, and the coexistence of plant species," *Oikos*, pp. 309–322, 1998.

[212] N. J. Kraft, P. B. Adler, O. Godoy, E. C. James, S. Fuller, and J. M. Levine, "Community assembly, coexistence and the environmental filtering metaphor," *Functional Ecology*, vol. 29, no. 5, pp. 592–599, 2015.

[213] P. B. Shafroth, J. C. Stromberg, and D. T. Patten, "Riparian vegetation response to altered disturbance and stress regimes," *Ecological Applications*, vol. 12, no. 1, pp. 107–123, 2002.

[214] N. M. Amlin *et al.*, *Influences of drought and flood stresses on riparian cottonwoods and willows*. PhD thesis, Lethbridge, Alta.: University of Lethbridge, Faculty of Arts and Science, 2000, 2000.

[215] I. V. Splunder, L. Voesenek, X. D. Vries, C. Blom, and H. Coops, "Morphological responses of seedlings of four species of salicaceae to drought," *Canadian Journal of Botany*, vol. 74, no. 12, pp. 1988–1995, 1996.

[216] M. Stoffel and D. J. Wilford, "Hydrogeomorphic processes and vegetation: disturbance, process histories, dependencies and interactions," *Earth Surface Processes and Landforms*, vol. 37, no. 1, pp. 9–22, 2012.

[217] R. Sato, H. Ito, and A. Tanaka, "Chlorophyll b degradation by chlorophyll b reductase under high-light conditions," *Photosynthesis research*, vol. 126, no. 2-3, pp. 249–259, 2015.

[218] B. Ke, *Photosynthesis photobiochemistry and photobiophysics*, vol. 10. Springer Science & Business Media, 2001.

[219] Y.-E. Chen, W.-J. Liu, Y.-Q. Su, J.-M. Cui, Z.-W. Zhang, M. Yuan, H.-Y. Zhang, and S. Yuan, "Different response of photosystem ii to short and long-term drought stress in arabidopsis thaliana," *Physiologia plantarum*, vol. 158, no. 2, pp. 225–235, 2016.

[220] E. M. Schwarz, S. Tietz, and J. E. Froehlich, "Photosystem i-lhcii megacomplexes respond to high light and aging in plants," *Photosynthesis research*, vol. 136, no. 1, pp. 107–124, 2018.

[221] V. K. Dalal and B. C. Tripathy, "Water-stress induced downsizing of light-harvesting antenna complex protects developing rice seedlings from photo-oxidative damage," *Scientific reports*, vol. 8, no. 1, p. 5955, 2018.

[222] B. Demmig-Adams, K. Winter, E. Winkelmann, A. Krüger, and F.-C. Czygan, "Photosynthetic characteristics and the ratios of chlorophyll, β-carotene, and the components of the xanthophyll cycle upon a sudden increase in growth light regime in several plant species," *Botanica Acta*, vol. 102, no. 4, pp. 319–325, 1989.

[223] N. Nisar, L. Li, S. Lu, N. C. Khin, and B. J. Pogson, "Carotenoid metabolism in plants," *Molecular plant*, vol. 8, no. 1, pp. 68–82, 2015.

[224] R. Sanchez, A. Hall, N. Trapani, and R. C. De Hunau, "Effects of water stress on the chlorophyll content, nitrogen level and photosynthesis of leaves of two maize genotypes," *Photosynthesis research*, vol. 4, no. 1, pp. 35–47, 1983.

[225] A. Mafakheri, A. Siosemardeh, B. Bahramnejad, P. Struik, Y. Sohrabi, *et al.*, "Effect of drought stress on yield, proline and chlorophyll contents in three chickpea cultivars," *Australian journal of crop science*, vol. 4, no. 8, p. 580, 2010.

[226] S. R. Carpenter, E. H. Stanley, and M. J. Vander Zanden, "State of the world's freshwater ecosystems: physical, chemical, and biological changes," *Annual review of Environment and Resources*, vol. 36, pp. 75–99, 2011.

[227] C. Zarfl, A. E. Lumsdon, J. Berlekamp, L. Tydecks, and K. Tockner, "A global boom in hydropower dam construction," *Aquatic Sciences*, vol. 77, no. 1, pp. 161–170, 2015.

[228] S. Tealdi, C. Camporeale, and L. Ridolfi, "Modeling the impact of river damming on riparian vegetation," *Journal of Hydrology*, vol. 396, no. 3-4, pp. 302–312, 2011.

[229] G. Bornette and C. Amoros, "Disturbance regimes and vegetation dynamics: role of floods in riverine wetlands," *Journal of vegetation Science*, vol. 7, no. 5, pp. 615–622, 1996.

[230] C. R. Hupp and W. Osterkamp, "Riparian vegetation and fluvial geomorphic processes," *Geomorphology*, vol. 14, no. 4, pp. 277–295, 1996.

[231] A. Gurnell, G. E. Petts, D. M. Hannah, B. P. Smith, P. J. Edwards, J. Kollmann, J. V. Ward, and K. Tockner, "Riparian vegetation and island formation along the gravel-bed fiume Tagliamento, Italy," *Earth Surface Processes and Landforms: The Journal of the British Geomorphological Research Group*, vol. 26, no. 1, pp. 31–62, 2001.

[232] C. Nilsson and K. Berggren, "Alterations of riparian ecosystems caused by river regulation: Dam operations have caused global-scale ecological changes in riparian ecosystems. how to protect river environments and human needs of rivers remains one of the most important questions of our time," *BioScience*, vol. 50, no. 9, pp. 783–792, 2000.

[233] E. Wohl, B. P. Bledsoe, R. B. Jacobson, N. L. Poff, S. L. Rathburn, D. M. Walters, and A. C. Wilcox, "The natural sediment regime in rivers: broadening the foundation for ecosystem management," *BioScience*, vol. 65, no. 4, pp. 358–371, 2015.

[234] R. Brigante, C. Cencetti, P. De Rosa, A. Fredduzzi, F. Radicioni, and A. Stoppini, "Use of aerial multispectral images for spatial analysis of flooded riverbed-alluvial plain systems: the case study of the paglia river (central italy)," *Geomatics, Natural Hazards and Risk*, vol. 8, no. 2, pp. 1126–1143, 2017.

[235] S. Lallias-Tacon, F. Liébault, and H. Piégay, "Use of airborne lidar and historical aerial photos for characterising the history of braided river floodplain morphology and vegetation responses," *Catena*, vol. 149, pp. 742–759, 2017.

[236] P. M. Rodríguez-González, A. Albuquerque, M. Martínez-Almarza, and R. Diaz-Delgado, "Long-term monitoring for conservation management: Lessons from a case study integrating remote sensing and field approaches in floodplain forests," *Journal of environmental management*, vol. 202, pp. 392–402, 2017.

[237] J. Girel, "Télédétection et cartographie à grande échelle de la végétation alluviale: exemple de la basse plaine de l'ain," *P. Ozenda, Documents de Cartographie Écologique*, vol. 29, pp. 45–74, 1986.

[238] D. C. Whited, M. S. Lorang, M. J. Harner, F. R. Hauer, J. S. Kimball, and J. A. Stanford, "Climate, hydrologic disturbance, and succession: drivers of floodplain pattern," *Ecology*, vol. 88, no. 4, pp. 940–953, 2007.

[239] J. Lejot, H. Piégay, P. D. Hunter, B. Moulin, and M. Gagnage, "Utilisation de la télédétection pour la caractérisation des corridors fluviaux: Exemples d'applications et enjeux actuels," *Géomorphologie: relief, processus, environnement*, vol. 17, no. 2, pp. 157–172, 2011.

[240] I. Nitze and G. Grosse, "Detection of landscape dynamics in the arctic lena delta with temporally dense landsat time-series stacks," *Remote sensing of environment*, vol. 181, pp. 27–41, 2016.

[241] P. Carbonneau and H. Piégay, *Fluvial remote sensing for science and management*. John Wiley & Sons, 2012.

[242] S. Bizzi, L. Demarchi, R. C. Grabowski, C. J. Weissteiner, and W. Van de Bund, "The use of remote sensing to characterise hydromorphological properties of european rivers," *Aquatic Sciences*, vol. 78, no. 1, pp. 57–70, 2016.

[243] M. Laba, R. Downs, S. Smith, S. Welsh, C. Neider, S. White, M. Richmond, W. Philpot, and P. Baveye, "Mapping invasive wetland plants in the hudson river national estuarine research reserve using quickbird satellite imagery," *Remote sensing of Environment*, vol. 112, no. 1, pp. 286–300, 2008.

[244] R. J. Strick, P. J. Ashworth, G. H. Sambrook Smith, A. P. Nicholas, J. L. Best, S. N. Lane, D. R. Parsons, C. J. Simpson, C. A. Unsworth, and J. Dale, "Quantification of bedform dynamics and bedload sediment flux in sandy braided rivers from airborne and satellite imagery," *Earth Surface Processes and Landforms*, 2018.

[245] M. Onderka and P. Pekárová, "Retrieval of suspended particulate matter concentrations in the danube river from landsat etm data," *Science of the Total Environment*, vol. 397, no. 1-3, pp. 238–243, 2008.

[246] J.-M. Martinez, J.-L. Guyot, N. Filizola, and F. Sondag, "Increase in suspended sediment discharge of the amazon river assessed by monitoring network and satellite data," *Catena*, vol. 79, no. 3, pp. 257–264, 2009.

[247] N. Kayastha, V. Thomas, J. Galbraith, and A. Banskota, "Monitoring wetland change using inter-annual landsat time-series data," *Wetlands*, vol. 32, no. 6, pp. 1149–1162, 2012.

[248] K. C. Fickas, W. B. Cohen, and Z. Yang, "Landsat-based monitoring of annual wetland change in the willamette valley of oregon, usa from 1972 to 2012," *Wetlands ecology and management*, vol. 24, no. 1, pp. 73–92, 2016.

[249] I. Van Splunder, H. Coops, L. Voesenek, and C. Blom, "Establishment of alluvial forest species in floodplains: the role of dispersal timing, germination characteristics and water level fluctuations," *Acta Botanica Neerlandica*, vol. 44, no. 3, pp. 269–278, 1995.

[250] I. Pattison, S. N. Lane, R. J. Hardy, and S. M. Reaney, "The role of tributary relative timing and sequencing in controlling large floods," *Water Resources Research*, vol. 50, no. 7, pp. 5444–5458, 2014.

[251] B. Belletti, S. Dufour, and H. Piégay, "Regional assessment of the multi-decadal changes in braided riverscapes following large floods (example of 12 reaches in south east of france)," *Advances in Geosciences*, vol. 37, pp. 57–71, 2014.

[252] E. Politti, W. Bertoldi, A. Gurnell, and A. Henshaw, "Feedbacks between the riparian salicaceae and hydrogeomorphic processes: A quantitative review," *Earth-Science Reviews*, vol. 176, pp. 147–165, 2018.

[253] P. Perona, P. Molnar, M. Savina, and P. Burlando, "An observation-based stochastic model for sediment and vegetation dynamics in the floodplain of an alpine braided river," *Water Resources Research*, vol. 45, no. 9, 2009.

[254] C. P. Henry and C. Amoros, "Are the banks a source of recolonization after disturbance: an experiment on aquatic vegetation in a former channel of the rhône river," *Hydrobiologia*, vol. 330, no. 2, pp. 151–162, 1996.

[255] B. Loučková, "Vegetation–landform assemblages along selected rivers in the czech republic, a decade after a 500-year flood event," *River Research and Applications*, vol. 28, no. 8, pp. 1275–1288, 2012.

[256] W. Gostner, M. Alp, A. J. Schleiss, and C. T. Robinson, "The hydro-morphological index of diversity: a tool for describing habitat heterogeneity in river engineering projects," *Hydrobiologia*, vol. 712, no. 1, pp. 43–60, 2013.

[257] S. Rohde, F. Kienast, and M. Bürgi, "Assessing the restoration success of river widenings: a landscape approach," *Environmental management*, vol. 34, no. 4, pp. 574–589, 2004.

[258] M. Döring, D. Tonolla, C. T. Robinson, A. Schleiss, S. Stähly, C. Gufler, M. Geilhausen, and N. Di Cugno, "Künstliches hochwasser an der saane-eine massnahme zum nachhaltigen auenmanagement," *Wasser Energie Luft*, vol. 110, pp. 119–127, 2018.

[259] R. G. Receanu, *Modélisation hydrologique des précipitations et des crues extrêmes dans les bassins versants alpin*. PhD thesis, Université de Lausanne, Faculté des géosciences et de l'environnement, 2013.

[260] D. N. Collins, "Variability of runoff from alpine basins," *IAHS publication*, vol. 308, p. 466, 2006.

[261] P. Molnar, V. Favre, P. Perona, P. Burlando, C. Randin, and W. Ruf, "Floodplain forest dynamics in a hydrologically altered mountain river," *Peckiana*, vol. 5, pp. 17–24, 2008.

[262] M. Brunke, "Floodplains of a regulated southern alpine river (brenno, switzerland): ecological assessment and conservation options," *Aquatic Conservation: Marine and Freshwater Ecosystems*, vol. 12, no. 6, pp. 583–599, 2002.

[263] A. Tillack, A. Clasen, B. Kleinschmit, and M. Förster, "Estimation of the seasonal leaf area index in an alluvial forest using high-resolution satellite-based vegetation indices," *Remote Sensing of Environment*, vol. 141, pp. 52–63, 2014.

[264] "Landsat surface reflectance data," Report 2015-3034, U.S. Geological Survey, Reston, VA, 2015.

[265] G. Chander, B. L. Markham, and D. L. Helder, "Summary of current radiometric calibration coefficients for landsat mss, tm, etm+, and eo-1 ali sensors," *Remote sensing of environment*, vol. 113, no. 5, pp. 893–903, 2009.

[266] B. L. Markham and D. L. Helder, "Forty-year calibrated record of earth-reflected radiance from landsat: A review," *Remote Sensing of Environment*, vol. 122, pp. 30–40, 2012.

[267] B. L. Markham, J. C. Storey, D. L. Williams, and J. R. Irons, "Landsat sensor performance: history and current status," *IEEE Transactions on Geoscience and Remote Sensing*, vol. 42, no. 12, pp. 2691–2694, 2004.

[268] J. Masek, E. Vermote, N. Saleous, R. Wolfe, F. Hall, K. Huemmrich, F. Gao, J. Kutler, and T. Lim, "Ledaps landsat calibration, reflectance, atmospheric correction preprocessing code," *ORNL DAAC*, 2012.

[269] J. Ju, D. P. Roy, E. Vermote, J. Masek, and V. Kovalskyy, "Continental-scale validation of modis-based and ledaps landsat etm+ atmospheric correction methods," *Remote Sensing of Environment*, vol. 122, pp. 175–184, 2012.

[270] T. R. Loveland and J. R. Irons, "Landsat 8: The plans, the reality, and the legacy," *Remote Sensing of Environment*, vol. 185, pp. 1–6, 2016.

[271] J. R. Schott, A. Gerace, C. E. Woodcock, S. Wang, Z. Zhu, R. H. Wynne, and C. E. Blinn, "The impact of improved signal-to-noise ratios on algorithm performance: Case studies for landsat class instruments," *Remote Sensing of Environment*, vol. 185, pp. 37–45, 2016.

[272] E. Vermote, C. Justice, M. Claverie, and B. Franch, "Preliminary analysis of the performance of the landsat 8/oli land surface reflectance product," *Remote Sensing of Environment*, vol. 185, pp. 46–56, 2016.

[273] J. W. Rouse Jr, R. H. Haas, J. Schell, and D. Deering, "Monitoring the vernal advancement and retrogradation (green wave effect) of natural vegetation," tech. rep., Texas A&M Univ.; Remote Sensing Center., College Station, TX, United States, 1973.

[274] D. P. Turner, W. B. Cohen, R. E. Kennedy, K. S. Fassnacht, and J. M. Briggs, "Relationships between leaf area index and landsat tm spectral vegetation indices across three temperate zone sites," *Remote sensing of environment*, vol. 70, no. 1, pp. 52–68, 1999.

[275] H. Davi, K. Soudani, T. Deckx, E. Dufrene, V. Le Dantec, and C. Francois, "Estimation of forest leaf area index from spot imagery using ndvi distribution over forest stands," *International Journal of Remote Sensing*, vol. 27, no. 05, pp. 885–902, 2006.

[276] T. Bellone, P. Boccardo, and F. Perez, "Investigation of vegetation dynamics using long-term normalized difference vegetation index time-series," *American Journal of Environmental Sciences*, vol. 5, no. 4, p. 461, 2009.

[277] N. Pettorelli, J. O. Vik, A. Mysterud, J.-M. Gaillard, C. J. Tucker, and N. C. Stenseth, "Using the satellite-derived ndvi to assess ecological responses to environmental change," *Trends in ecology & evolution*, vol. 20, no. 9, pp. 503–510, 2005.

[278] A. J. Peters, E. A. Walter-Shea, L. Ji, A. Vina, M. Hayes, and M. D. Svoboda, "Drought monitoring with ndvi-based standardized vegetation index," *Photogrammetric engineering and remote sensing*, vol. 68, no. 1, pp. 71–75, 2002.

[279] M. Forkel, N. Carvalhais, J. Verbesselt, M. D. Mahecha, C. S. Neigh, and M. Reichstein, "Trend change detection in ndvi time series: Effects of inter-annual variability and methodology," *Remote Sensing*, vol. 5, no. 5, pp. 2113–2144, 2013.

[280] J. W. Boardman, "Geometric mixture analysis of imaging spectrometry data," in *Proceedings of IGARSS'94-1994 IEEE International Geoscience and Remote Sensing Symposium*, vol. 4, pp. 2369–2371, IEEE, 1994.

[281] C. Small, "Estimation of urban vegetation abundance by spectral mixture analysis," *International journal of remote sensing*, vol. 22, no. 7, pp. 1305–1334, 2001.

[282] N. Keshava and J. F. Mustard, "Spectral unmixing," *IEEE signal processing magazine*, vol. 19, no. 1, pp. 44–57, 2002.

[283] Z. Mitraka, F. Del Frate, and F. Carbone, "Nonlinear spectral unmixing of landsat imagery for urban surface cover mapping," *IEEE Journal of Selected Topics in Applied Earth Observations and Remote Sensing*, vol. 9, no. 7, pp. 3340–3350, 2016.

[284] A. Baldridge, S. Hook, C. Grove, and G. Rivera, "The aster spectral library version 2.0," *Remote Sensing of Environment*, vol. 113, no. 4, pp. 711–715, 2009.

[285] L. W. Mays, *Water resources engineering*. John Wiley & Sons, 2010.

[286] A. Te Linde, J. Aerts, A. Bakker, and J. Kwadijk, "Simulating low-probability peak discharges for the rhine basin using resampled climate modeling data," *Water Resources Research*, vol. 46, no. 3, 2010.

[287] G. Villarini, J. A. Smith, F. Serinaldi, and A. A. Ntelekos, "Analyses of seasonal and annual maximum daily discharge records for central europe," *Journal of Hydrology*, vol. 399, no. 3-4, pp. 299–312, 2011.

[288] W. Mauser, T. Marke, and S. Stoeber, "Climate change and water resources: scenarios of low-flow conditions in the upper danube river basin," in *IOP Conference Series: Earth and Environmental Science*, vol. 4, p. 012027, IOP Publishing, 2008.

[289] D. Meissner, B. Klein, and M. Ionita, "Development of a monthly to seasonal forecast framework tailored to inland waterway transport in central europe," *Hydrology and Earth System Sciences*, vol. 21, pp. 6401–6423, 2017.

[290] B. Somers, G. P. Asner, L. Tits, and P. Coppin, "Endmember variability in spectral mixture analysis: A review," *Remote Sensing of Environment*, vol. 115, no. 7, pp. 1603–1616, 2011.

[291] A. J. Elmore, J. F. Mustard, S. J. Manning, and D. B. Lobell, "Quantifying vegetation change in semiarid environments: precision and accuracy of spectral mixture analysis and the normalized difference vegetation index," *Remote sensing of environment*, vol. 73, no. 1, pp. 87–102, 2000.

[292] R. Sonnenschein, T. Kuemmerle, T. Udelhoven, M. Stellmes, and P. Hostert, "Differences in landsat-based trend analyses in drylands due to the choice of vegetation estimate," *Remote sensing of environment*, vol. 115, no. 6, pp. 1408–1420, 2011.

[293] M. Halabisky, L. M. Moskal, A. Gillespie, and M. Hannam, "Reconstructing semi-arid wetland surface water dynamics through spectral mixture analysis of a time series of landsat satellite images (1984–2011)," *Remote sensing of environment*, vol. 177, pp. 171–183, 2016.

[294] K. Tockner, M. S. Lorang, and J. A. Stanford, "River flood plains are model ecosystems to test general hydrogeomorphic and ecological concepts," *River research and applications*, vol. 26, no. 1, pp. 76–86, 2010.

[295] L. Harrison, C. Legleiter, M. Wydzga, and T. Dunne, "Channel dynamics and habitat development in a meandering, gravel bed river," *Water Resources Research*, vol. 47, no. 4, 2011.

[296] F. J. Magilligan, E. Buraas, and C. Renshaw, "The efficacy of stream power and flow duration on geomorphic responses to catastrophic flooding," *Geomorphology*, vol. 228, pp. 175–188, 2015.

[297] C. Ilg, F. Dziock, F. Foeckler, K. Follner, M. Gerisch, J. Glaeser, A. Rink, A. Schanowski, M. Scholz, and O. Deichner, "Long-term reactions of plants and macroinvertebrates to extreme floods in floodplain grasslands," *Ecology*, vol. 89, no. 9, pp. 2392–2398, 2008.

[298] V. Garófano-Gómez, F. Martínez-Capel, W. Bertoldi, A. Gurnell, J. Estornell, and F. Segura-Beltrán, "Six decades of changes in the riparian corridor of a mediterranean river: a synthetic analysis based on historical data sources," *Ecohydrology*, vol. 6, no. 4, pp. 536–553, 2013.

[299] D. B. Arscott, K. Tockner, D. van der Nat, and J. Ward, "Aquatic habitat dynamics along a braided alpine river ecosystem (Tagliamento River, Northeast Italy)," *Ecosystems*, vol. 5, no. 8, pp. 0802–0814, 2002.

[300] D. M. Merritt, M. L. Scott, N. LeRoy Poff, G. T. Auble, and D. A. Lytle, "Theory, methods and tools for determining environmental flows for riparian vegetation: riparian vegetation-flow response guilds," *Freshwater Biology*, vol. 55, no. 1, pp. 206–225, 2010.

[301] C. A. Bateson, G. P. Asner, and C. A. Wessman, "Endmember bundles: A new approach to incorporating endmember variability into spectral mixture analysis," *IEEE transactions on geoscience and remote sensing*, vol. 38, no. 2, pp. 1083–1094, 2000.

[302] R. Receanu, J.-A. Hertig, J.-M. Fallot, and T. E. Man, "Determination of extreme floods using a distributed hydrological model," *Bulletin of the Polytehnica University of Timisoara (Romania), Transactions on Hydrotechnics*, vol. 56, no. 1, pp. 33–36, 2011.

[303] J. C. Stromberg and D. T. Patten, "Early recovery of an eastern sierra nevada riparian system after 40 years of stream diversion," in *Proceedings of the California Riparian Systems Conference: protection, management, and restoration for the 1990s*, vol. 110, pp. 399–404, 1989.

[304] D. H. Kim, H. Choi, and J. G. Kim, "Occupational strategy of persicaria thunbergii in riparian area: rapid recovery after harsh flooding disturbance," *Journal of Plant Biology*, vol. 55, no. 3, pp. 226–232, 2012.

[305] C. Nilsson and M. Svedmark, "Basic principles and ecological consequences of changing water regimes: riparian plant communities," *Environmental management*, vol. 30, no. 4, pp. 468–480, 2002.

[306] N. C. Sims and M. J. Colloff, "Remote sensing of vegetation responses to flooding of a semi-arid floodplain: implications for monitoring ecological effects of environmental flows," *Ecological Indicators*, vol. 18, pp. 387–391, 2012.

[307] K. Tockner, F. Malard, and J. Ward, "An extension of the flood pulse concept," *Hydrological processes*, vol. 14, no. 16-17, pp. 2861–2883, 2000.

[308] J. Steiger and A. M. Gurnell, "Spatial hydrogeomorphological influences on sediment and nutrient deposition in riparian zones: observations from the garonne river, france," *Geomorphology*, vol. 49, no. 1-2, pp. 1–23, 2003.

[309] D. Walling, Q. He, and W. Blake, "River flood plains as phosphorus sinks," *IAHS Publication(International Association of Hydrological Sciences)*, no. 263, pp. 211–218, 2000.

[310] N. E. Pettit and R. J. Naiman, "Flood-deposited wood creates regeneration niches for riparian vegetation on a semi-arid south african river," *Journal of Vegetation Science*, vol. 17, no. 5, pp. 615–624, 2006.

[311] E. González, E. Muller, F. A. Comín, and M. González-Sanchis, "Leaf nutrient concentration as an indicator of populus and tamarix response to flooding," *Perspectives in Plant Ecology, Evolution and Systematics*, vol. 12, no. 4, pp. 257–266, 2010.

[312] D. Hering, M. Gerhard, R. Manderbach, and M. Reich, "Impact of a 100-year flood on vegetation, benthic invertebrates, riparian fauna and large woody debris standing stock in an alpine floodplain," *River Research and Applications*, vol. 20, no. 4, pp. 445–457, 2004.

[313] P. W. Bogaart and R. T. Van Balen, "Numerical modeling of the response of alluvial rivers to quaternary climate change," *Global and Planetary Change*, vol. 27, no. 1-4, pp. 147–163, 2000.

[314] J. C. Knox, "Sensitivity of modern and holocene floods to climate change," *Quaternary Science Reviews*, vol. 19, no. 1-5, pp. 439–457, 2000.

[315] L. Ström, R. Jansson, and C. Nilsson, "Projected changes in plant species richness and extent of riparian vegetation belts as a result of climate-driven hydrological change along the vindel river in sweden," *Freshwater Biology*, vol. 57, no. 1, pp. 49–60, 2012.

[316] R. Rivaes, P. M. Rodríguez-González, A. Albuquerque, A. N. Pinheiro, G. Egger, and M. T. Ferreira, "Riparian vegetation responses to altered flow regimes driven by climate change in mediterranean rivers," *Ecohydrology*, vol. 6, no. 3, pp. 413–424, 2013.

[317] J. A. Catford, R. J. Naiman, L. E. Chambers, J. Roberts, M. Douglas, and P. Davies, "Predicting novel riparian ecosystems in a changing climate," *Ecosystems*, vol. 16, no. 3, pp. 382–400, 2013.

[318] D. Sulla-Menashe, M. A. Friedl, and C. E. Woodcock, "Sources of bias and variability in long-term landsat time series over canadian boreal forests," *Remote sensing of environment*, vol. 177, pp. 206–219, 2016.

[319] C. E. Holden and C. E. Woodcock, "An analysis of landsat 7 and landsat 8 underflight data and the implications for time series investigations," *Remote Sensing of Environment*, vol. 185, pp. 16–36, 2016.

[320] D. Helder, B. Markham, R. Morfitt, J. Storey, J. Barsi, F. Gascon, S. Clerc, B. LaFrance, J. Masek, D. Roy, *et al.*, "Observations and recommendations for the calibration of landsat 8 oli and sentinel 2 msi for improved data interoperability," *Remote Sensing*, vol. 10, no. 9, p. 1340, 2018.

[321] F. Caponi, A. Koch, W. Bertoldi, D. F. Vetsch, and A. Siviglia, "When does vegetation establish on gravel bars? observations and modelling in the alpine rhine river," *Frontiers in Environmental Science*, vol. 7, p. 124, 2019.

[322] P. Humphries and D. S. Baldwin, "Drought and aquatic ecosystems: an introduction," *Freshwater Biology*, vol. 48, no. 7, pp. 1141–1146, 2003.

[323] P. B. Shafroth, J. C. Stromberg, and D. T. Patten, "Woody riparian vegetation response to different alluvial water table regimes," *Western North American Naturalist*, vol. 60, no. 1, p. 6, 2000.

[324] N. M. Amlin and S. B. Rood, "Drought stress and recovery of riparian cottonwoods due to water table alteration along willow creek, alberta," *Trees*, vol. 17, no. 4, pp. 351–358, 2003.

[325] S. B. Rood, J. H. Braatne, and F. M. Hughes, "Ecophysiology of riparian cottonwoods: stream flow dependency, water relations and restoration," *Tree Physiology*, vol. 23, no. 16, pp. 1113–1124, 2003.

[326] A. Karnieli, N. Agam, R. T. Pinker, M. Anderson, M. L. Imhoff, G. G. Gutman, N. Panov, and A. Goldberg, "Use of ndvi and land surface temperature for drought assessment: Merits and limitations," *Journal of climate*, vol. 23, no. 3, pp. 618–633, 2010.

[327] A. AghaKouchak, A. Farahmand, F. Melton, J. Teixeira, M. Anderson, B. D. Wardlow, and C. Hain, "Remote sensing of drought: Progress, challenges and opportunities," *Reviews of Geophysics*, vol. 53, no. 2, pp. 452–480, 2015.

[328] K. Tockner, M. Push, D. Borchardt, and M. S. Lorang, "Multiple stressors in coupled river–floodplain ecosystems," *Freshwater Biology*, vol. 55, no. s1, pp. 135–151, 2010.

[329] M. Waskom, O. Botvinnik, D. O'Kane, P. Hobson, S. Lukauskas, D. C. Gemperline, T. Augspurger, Y. Halchenko, J. B. Cole, J. Warmenhoven, J. de Ruiter, C. Pye, S. Hoyer, J. Vanderplas, S. Villalba, G. Kunter, E. Quintero, P. Bachant, M. Martin, K. Meyer, A. Miles, Y. Ram, T. Yarkoni, M. L. Williams, C. Evans, C. Fitzgerald, Brian, C. Fonnesbeck, A. Lee, and A. Qalieh, "mwaskom/seaborn: v0.8.1 (september 2017)," Sept. 2017.

[330] J. McKean, D. Nagel, D. Tonina, P. Bailey, C. W. Wright, C. Bohn, and A. Nayegandhi, "Remote sensing of channels and riparian zones with a narrow-beam aquatic-terrestrial lidar," *Remote Sensing*, vol. 1, no. 4, pp. 1065–1096, 2009.

[331] J.-M. Martinez and T. Le Toan, "Mapping of flood dynamics and spatial distribution of vegetation in the amazon floodplain using multitemporal sar data," *Remote sensing of Environment*, vol. 108, no. 3, pp. 209–223, 2007.

[332] X. Yang, M. C. Damen, and R. A. Van Zuidam, "Satellite remote sensing and gis for the analysis of channel migration changes in the active yellow river delta, china," *International Journal of Applied Earth Observation and Geoinformation*, vol. 1, no. 2, pp. 146–157, 1999.

[333] M. Rusnák, J. Sládek, A. Kidová, and M. Lehotskỳ, "Template for high-resolution river landscape mapping using uav technology," *Measurement*, vol. 115, pp. 139–151, 2018.

[334] S. Lane, "The measurement of river channel morphology using digital photogrammetry," *The Photogrammetric Record*, vol. 16, no. 96, pp. 937–961, 2000.

[335] S. Hemmelder, W. Marra, H. Markies, and S. M. De Jong, "Monitoring river morphology & bank erosion using uav imagery–a case study of the river buëch, hautes-alpes, france," *International Journal of Applied Earth Observation and Geoinformation*, vol. 73, pp. 428–437, 2018.

[336] M. J. Westoby, J. Brasington, N. F. Glasser, M. J. Hambrey, and J. Reynolds, "'structure-from-motion'photogrammetry: A low-cost, effective tool for geoscience applications," *Geomorphology*, vol. 179, pp. 300–314, 2012.

[337] R. J. Strick, P. J. Ashworth, G. H. Sambrook Smith, A. P. Nicholas, J. L. Best, S. N. Lane, D. R. Parsons, C. J. Simpson, C. A. Unsworth, and J. Dale, "Quantification of bedform dynamics and bedload sediment flux in sandy braided rivers from airborne and satellite imagery," *Earth Surface Processes and Landforms*, 2019.

[338] J. Mouw, J. Chaffin, D. Whited, F. Hauer, P. Matson, and J. Stanford, "Recruitment and successional dynamics diversify the shifting habitat mosaic of an alaskan floodplain," *River Research and Applications*, vol. 29, no. 6, pp. 671–685, 2013.

[339] D. C. Whited, J. S. Kimball, M. Lorang, and J. A. Stanford, "Estimation of juvenile salmon habitat in pacific rim rivers using multiscalar remote sensing and geospatial analysis," *River Research and Applications*, vol. 29, no. 2, pp. 135–148, 2013.

[340] O. Stefankiv, T. J. Beechie, J. E. Hall, G. R. Pess, and B. Timpane-Padgham, "Influences of valley form and land use on large river and floodplain habitats in puget sound," *River Research and Applications*, vol. 35, no. 2, pp. 133–145, 2019.

[341] M. D. Bejarano, R. Jansson, and C. Nilsson, "The effects of hydropeaking on riverine plants: a review," *Biological Reviews*, vol. 93, no. 1, pp. 658–673, 2018.

[342] A. H. Arthington, A. Bhaduri, S. E. Bunn, S. E. Jackson, R. E. Tharme, D. Tickner, B. Young, M. Acreman, N. Baker, S. Capon, *et al.*, "The brisbane declaration and global action agenda on environmental flows (2018)," *Frontiers in Environmental Science*, vol. 6, 2018.

[343] A. H. Arthington, S. E. Bunn, N. L. Poff, and R. J. Naiman, "The challenge of providing environmental flow rules to sustain river ecosystems," *Ecological applications*, vol. 16, no. 4, pp. 1311–1318, 2006.

[344] N. L. Poff, B. D. Richter, A. H. Arthington, S. E. Bunn, R. J. Naiman, E. Kendy, M. Acreman, C. Apse, B. P. Bledsoe, M. C. Freeman, *et al.*, "The ecological limits of hydrologic alteration (eloha): a new framework for developing regional environmental flow standards," *Freshwater Biology*, vol. 55, no. 1, pp. 147–170, 2010.

[345] W. Chen and J. D. Olden, "Designing flows to resolve human and environmental water needs in a dam-regulated river," *Nature communications*, vol. 8, no. 1, p. 2158, 2017.

[346] C. T. Robinson, A. R. Siebers, and J. Ortlepp, "Long-term ecological responses of the river spöl to experimental floods," *Freshwater Science*, vol. 37, no. 3, pp. 433–447, 2018.

[347] R. Rivaes, P. M. Rodríguez-González, A. Albuquerque, A. N. Pinheiro, G. Egger, and M. T. Ferreira, "Reducing river regulation effects on riparian vegetation using flushing flow regimes," *Ecological Engineering*, vol. 81, pp. 428–438, 2015.

[348] D. S. Hayes, J. M. Brändle, C. Seliger, B. Zeiringer, T. Ferreira, and S. Schmutz, "Advancing towards functional environmental flows for temperate floodplain rivers," *Science of the Total Environment*, vol. 633, pp. 1089–1104, 2018.

[349] P. Reich and P. Lake, "Extreme hydrological events and the ecological restoration of flowing waters," *Freshwater Biology*, vol. 60, no. 12, pp. 2639–2652, 2015.

[350] J. D. Tonkin, D. M. Merritt, J. D. Olden, L. V. Reynolds, and D. A. Lytle, "Flow regime alteration degrades ecological networks in riparian ecosystems," *Nature ecology & evolution*, vol. 2, no. 1, p. 86, 2018.

[351] E. J. Martín, M. Doering, and C. T. Robinson, "Ecological assessment of a sediment by-pass tunnel on a receiving stream in switzerland," *River research and applications*, vol. 33, no. 6, pp. 925–936, 2017.

[352] T. Sunamura, "A fundamental equation for describing the rate of bedrock erosion by sediment-laden fluid flows in fluvial, coastal, and aeolian environments," *Earth Surface Processes and Landforms*, vol. 43, no. 15, pp. 3022–3041, 2018.

[353] T. Cui, T. Yang, C.-Y. Xu, Q. Shao, X. Wang, and Z. Li, "Assessment of the impact of climate change on flow regime at multiple temporal scales and potential ecological implications in an alpine river," *Stochastic environmental research and risk assessment*, pp. 1–18, 2018.

[354] F. Guillemette, A. P. Plamondon, M. Prévost, and D. Lévesque, "Rainfall generated stormflow response to clearcutting a boreal forest: peak flow comparison with 50 world-wide basin studies," *Journal of hydrology*, vol. 302, no. 1-4, pp. 137–153, 2005.

[355] L. Schwendenmann, "Soil properties of boreal riparian plant communities in relation to natural succession and clear-cutting, peace river lowlands, wood buffalo national park, canada," *Water, air, and soil pollution*, vol. 122, no. 3-4, pp. 449–467, 2000.

Acknowledgements

I suppose it is difficult to grasp the invaluable value of a supervisor's support until the last point on the last page has been written. Dear Mathias, I owe you a lot and I thank you very much for the patience you have shown over the years! I would like to start by thanking the rest of the team that was present at my side throughout the PhD

I thank Michael Schaepman, who has always had the right words at the right time, including the right questions (which means a lot to me). My sincere thanks go to Michael Doering and Diego Tonolla, who amazingly contributed to my research from beginning to end. I hope that our paths will cross again in the future! I would also like to give a warm thank you to Guido Wiesenberg and Michael Hilf, who supported me over too many hours in the laboratory environment.

Many thanks to my colleagues and friends of the RSL and the Geography Department who helped me build this research and made my days worth living during these four years. I remember the Chinese pots, the big sola run teams, the too few hikes in the Alps, the climbing in the fog, but also the Christmas kicker tournaments, the movie nights and all those moments shared with you and the (seriously...) too long coffee breaks. I have no doubt that you will all recognise each other and know how much you mean to me, whether you live in Zurich, the East, the West or even in the Netherlands.

I would like to extend special thanks to the Scouts of Courrendlin, Libellule, Touraco, Choucas, Renard and Luis, who helped to collect soil samples along the Sanne and Sense rivers. Also, I would like to apologise to my friends from the Jura, the ASJ and the EPFL for my almost total absence from your gatherings over the years. I hope to see you more often in the future! Finally, I would like to thank my parents and the rest of my family for being there when I don't need it, because they are only the ones doing it, which is sometimes very precious!

A big thanks to Adrian, Alex, Ali, Andy, Beni, Bernhard, Bruno, Carla, Christian, Christoph, Daniel H., Daniel K., Daniela, David, Davis, Diego, Elias, Emiliano, Ewa, Fabian, Fanny, Felix, Giulia, Hanneke, Hendrik, Hossein, Irene, Jing, Joan, Johan, Jonas, Julian, Liv, Marta, Oli, Parviz, Peter, Philip, Reik, Rifat, Rita, Rogier, Sandra, Sanne, Shivangi, Simon, Vladimir, Xiu and Zhaoju.

Gillian Milani

Curriculum Vitae

Rue Gustave-Amweg 6
2900 Porrentruy, Switzerland
☎ +41 78 757 15 12
✉ gillian.milani@gmail.com

Education

2015–Present **PhD Student**, *Remote Sensing Laboratories, Zürich University*, Zürich.
Plasticity of resource allocation strategies of plants related to riverine dynamics observed by imaging spectrometry

2012–2014 **Master of Engineering in Environment**, *Ecole Polytechnique Fédérale de Lausanne*, Lausanne, *GPA – 5.34 (6 best, 1 worst)*.
Specialization : Monitoring and modeling of the environment

2009–2012 **Bachelor of Engineering in Environment**, *Ecole Polytechnique Fédérale de Lausanne*, Lausanne, *GPA – 5.45*.
2 semesters in exchange program at the IIT Kanpur, India (N°271 QS-WU ranking 2016)

PhD Thesis – Ongoing

Title *Impacts of flow alteration on Swiss floodplains observed by remote sensing*

Supervisors Dr. Mathias Kneubühler & Pr. Michael E. Schaepman

Description UAS, imaging spectroscopy and satellite time series of images were used to describe and understand the interaction between the water flow, the riverine habitat dynamics and the riparian vegetation, particularly linked to alteration due to dams and hydropower production

Masters Thesis

Title *Pic2Map : Integration de photographies dans QGIS*

Supervisors Dr. Timothée Produit & Pr. François Golay

Description Creation of a plugin for QGIS, a Geographic Information System software, for the integration oblique images and the corresponding interactions between the projected and orthographic plans, including pose estimation. Graded 5.5

Experience

2017–present **Technical Chief - Co-Funder**, ExoLabs GmbH, Zürich.
Development of software services based on GIS and remote sensing technologies

2014–2015 **Junior Developer**, Camptocamp SA, Lausanne.
Development of a QGIS plugin for excavation planning in Swiss cities, development of web-mapping solutions, implementation of web print services

Summer 2012 **Internship**, Esri Schweiz SA, Nyon.
Creation of exercices for EPFL students with Esri GIS, ARCGIS.

Graduate Course

Promitionseminar I (Autumn 2015) & II (March 2017)

Graduate school retreat, presence in 2015, 2016 and 2017

Scientific Writing, followed in January and February 2017

voice training and presentations skills, followed in March 207

Teaching

Small group teaching, Fall semester 2015

Teaching assistant and exercice management for Geo 113, Geo 233 and Geo 442

External examinator for master thesis (two times)

Divers works (representation at scientifica, exam supervision, visit of students coordinated by the Science Lab)

Introduction to python programming, OOP and versioning tools, master and PhD students

Introduction to QGIS plugin development, PhD students

Coordination of the movie-project for the Ecosystem Services Workshop, 2017

Miscellaneous

2010–2014 **Teaching Assistant**, *EPFL*, Lausanne.
I have been involved in many courses for junior students. I have repeatedly worked as TA for Physics I (mechanics) and Physics II (thermodynamics). I have also worked as TA for the courses Distributed Intelligent System and Introduction to GIS.

Awards

2014 Master Thesis : Price of "Association Ingénieurs Géomètres de Suisse Occidentale"

Scientific Contributions

Peer-reviewed articles

Milani, G., Tonolla, D., Doering, M., Kneubühler, M., & Schaepman, M. (2018). Remotely sensing variation in ecological strategies and plant traits of willows in perialpine floodplains. Journal of geophysical research : biogeosciences, 124(7), 2090-2106.

Milani, G., Volpi, M., Tonolla, D., Doering, M., Robinson, C., Kneubühler, M., & Schaepman, M. (2018). Robust quantification of riverine land cover dynamics by high-resolution remote sensing. Remote sensing of environment, 217, 491-505.

Conferences Contributions

Milani, G., Tonolla, D., Robinson, C., Kneubühler, M., Doering, M., & Schaepman, M. (2016). Comparison of riverine habitat dynamic cycles conditioned by hydrological regimes under different anthropogenic pressure. Presentation at the Swiss Geoscience Meeting, Geneva, CH.

Milani, G., Kneubühler, M., Doering, M., & Schaepman, M. (2017). On the Utility of Deformable Transformations Based on Mutual Information : Application in Imaging Spectrometry and High-Resolution Imagery of Riverine Landscape. Poster at the EARSeL SIG Imaging Spectroscopy Workshop, Zürich, CH.

Milani, G., Kneubühler, M., Doering, M., & Schaepman, M. (2019). Correction of Spatial Autocorrelation for Comparison of Regional Statistics : a Case Study on Alluvial Vegetation. Presentation at the EARSeL SIG Imaging Spectroscopy Workshop, Brno, CZ.

Leuenberger, M., Meyer, A., **Milani, G.**, & Facchinetti, C. (2019). ADELE : Overview of a deep learning application for land use and landcover classification in Switzerland of Riverine Landscape. Presentation at the EGU General Assembly 2019, Vienna, AT.

Other publications

Produit, T., Ingensand, J., & **Milani, G.** (2016). QGIS plugin or web app ? Lessons learned in the development of a 3D georeferencer (No. e2243v2). PeerJ Preprints.